

# Folding DNA to create nanoscale shapes and patterns

## Supplementary Notes 1–11

Paul W. K. Rothermund

Computation and Neural Systems, and Computer Science, California Institute of Technology, Pasadena, California, United States of America

### Supplementary Note S1: Design of DNA origami

The program used for designing DNA origami, `multishapes.m`, may be downloaded from:

<http://www.dna.caltech.edu/SupplementaryMaterial/>

Below is a description of how design proceeds using this program. It is not meant to be a manual but rather to show the level of abstraction at which the origami are designed, and to show the various types of diagrams that the program can draw to aid in design. If scaffolded DNA origami becomes widely used, a better CAD design tool will have to be written. Given a desired shape (for example the red outline in Fig. 1a) design of a DNA origami to approximate it proceeds in five phases (two manual design steps and three passes of the program):

1. **Generation of a block diagram.** By hand, a rough geometric model is generated. It is comprised of rectangular blocks in which each block is taken to be one turn of DNA wide and one DNA helix plus the inter-helix gap in height. (Such a block diagram sloppily overestimates the height of a structure by one inter-helix gap.) An example block diagram is in Supplementary Fig. S1 step 1.

This step is performed with an eye towards the next step (generation of a folding path), in some cases the block diagram is conceived almost simultaneously with the folding path. The phase of the underlying periodic crossover lattice is chosen as well; generally this phasing is chosen so that seams and long edges of the shape align with columns of periodic crossovers. For blocks on the edge of the diagram, it is useful to keep track of the relationship of such blocks to the underlying crossover lattice. For an origami with 1.5-turn spacing between crossovers there are 3 possible offsets that an edge may have with respect to the underlying lattice—call them 0, +1 and -1 (Origami with 2.5 turn spacing have 5 possible offsets). For designs with a central seam, blocks on edges of offset 0 are colored red and blocks on edges of offset +1 and -1 are colored yellow and orange, depending on whether they occur to the left or right of the central seam. At this point the placement of seams may already be apparent; if so, half-blocks are used along seams. Adjacent half-blocks involved in the same scaffold crossover are colored the same (one of either green or purple) but adjacent half-blocks that participate in different crossovers are given different colors.

2. **Generation of a folding path,** by raster fill, through the block diagram. For a given shape there are many compatible raster fill patterns; currently the raster fill pattern must be hand-designed. For any helical domain in which the scaffold is to start and end on the same side of the helix (top or bottom), an integral number of turns (blocks) is traversed. For any helical domain in which the scaffold starts and ends on opposite sides of the helix, the scaffold traverses an odd number of half-turns (half-blocks). An example folding path is in Supplementary Fig. S1 step 2.
3. **Generation of a first pass design** based on the block diagram and folding path. The lengths of various helical domains, in units of DNA turns, are implied by the block diagram and folding paths; these are what is input to the computer program. For every design with seams presented here *except* the 3-hole disk, a single vertical seam was used in the design and so a simple matrix representation of the domain lengths could be used. Supplementary Fig. S1 step 3 shows a matrix (`design_turns`) of these domain lengths that is input to the program. (The equilateral and sharp triangle have a single seam *in each domain* that could be similarly specified by a single matrix. For the 3-hole disk, the position of seams was entered as a separate matrix and the routing of the scaffold between these seams as a matrix slightly more complicated than the `design_turns` matrix.) Column C0 gives the total number of turns in a particular row of the design. Column C1 and C4 give the total number of turns to the left and right of the seam, respectively. (Column C0, the sum of C1 and C4, was thus redundant and was used for checking the design.) Columns C2 and C3, unused for this design, give the offset (in number of turns) from the seam of the left and right helical domains, respectively; this feature is not used for the house design here, but is used for the bottom “legs” of the star design. The program converts lengths given (by the user) in turns to numbers of bases (matrix `design_lengths`) and outputs a first-pass design.

The first pass design can be output either as a line diagram (as in Supplementary Fig. S1 step 3) or as a detailed diagram showing the sequence of the scaffold laid out along the folding path, and the sequence of the staples where they appear in the final folded structure (Supplementary Fig. S2). In the detailed design diagram staple strands are indexed by  $xy$  position of the adjacent crossover and the designation ‘a’ or ‘b’ depending on whether the staple falls to the left or right of the crossover, respectively. Here names are of the form  $sXtYP$  where X is the  $x$  position, Y is the  $y$  position, and P the position with respect to the adjacent crossover.

4. **Refinement of the helical domain lengths** to minimize strain in the design. In a third sort of diagram (Supplementary Fig. S3), the computer program displays the predicted twist at each base position as a color (assuming the spacing of crossovers represents an exact number of half turns). Red indicates that the base at a particular position is pointing up, blue that it is pointing down. At crossover points, strand backbone positions should fall at the tangent point between helices; thus bases from the helix above a crossover should be blue and those from the helix below a crossover should be red. (More specifically, the color of bases at the crossover should be spaced equally clockwise and counterclockwise of the colors blue and red, that themselves should occur exactly at the tangent point.) All of the crossovers internal to the design are spaced 16 bases apart and related by a glide symmetry that should balance strain. This can be observed for the two types of crossovers ('+', major-groove up and '-' major-groove down) that occur internally in a shape, shown in both the boxed regions and at the lower left of Supplementary Fig. S3. (A naive view is that the bases of the crossover will actually be centered around the tangent point between helices. In reality, twist strain might be relieved by distortion of the crossover but the idea is that if so, such a distortion will be balanced by that of neighboring symmetrically-placed crossovers.)

Ideally, at all other crossovers in the design, the orientation of bases would be similar to that desired for the balanced internal crossovers. However, because of the non-integral number of bases in a single turn, and the major-minor groove angle, it is not possible to put all crossovers in this optimal orientation. Crossovers along the edges of the shape, in particular, must be adjusted to minimize strain. The program computes a “strain energy” along the edges of the design, and so positions of predicted high strain can be identified. (For a given strand passing through a crossover, the computed strain energy is just the sum of the squared angular deviation from the tangent point for the base before and the base after the crossover.)

By hand, helical domain lengths are changed by single bases until the strain energy is minimized. The map of twists aids in this process. For example, high twist strain occurs in a couple scaffold crossovers in the first pass design (marked by ‘s’ labels inside ovals in Supplementary Fig. S3). These crossovers were initially designed to be 5 bases away from the nearest internal crossover (a ‘-’ crossover). At bottom right, the situation for one such crossover may be compared to that which would occur if the distance to the nearest internal crossover were changed to 6 bases, as well as the ‘ideal’ situation for this type of crossover, that of a ‘+’ type crossover. The 6-base distance creates the least strain.

Once the appropriate adjustments are decided, a matrix of adjustments is input to the design program, with the original design (Supplementary Fig. S4, `design{ADJUSTMENTS}`, top). The matrix gives adjustments for the left and right edges of each helical domain in the design, columns C1 and C2 for domains to the left of the seam and columns C3 and C4 for columns to the right of the seam. The program updates `design_lengths` (Supplementary Fig. S4, bottom) accordingly and a second pass diagram is generated (Supplementary Fig. S5).

5. **Breaking and merging of strands.** The merging of strands is specified by giving a pairwise list of the names to be merged (i.e. `s-2t9b` and `s-1t8a`) along with the name of the new strand (i.e. `s-1t8e`). The program checks to see that all strands to be merged have adjacent 3' and 5' bases. The position of strands to be broken is specified by the name of a strand and the position along its length at which it is to be broken. The pattern of merges is not unique. Supplementary Fig. S6, Supplementary Fig. S8, and Supplementary Fig. S10 show three different diagrams (full sequence, line drawing, and crossover map) of a design that features bridging staple strands across the seam. Supplementary Fig. S7, Supplementary Fig. S9, and Supplementary Fig. S11 show three different diagrams (full sequence, line drawing, and crossover map) of a design that has no bridging staples. Diagrams are interleaved to allow comparison of the differences between these two designs. Using a PDF viewer, flip back and forth between two diagrams of the same type to see the effect of different merge patterns. Particularly interesting are the crossover maps, Supplementary Fig. S10 and Supplementary Fig. S11. The addition of bridging staples creates a characteristic pattern of “bars” down the center of the design which is observed in experiments that use bridging staples (and not observed in experiments that don’t use bridging staples.) Supplementary Fig. S12 highlights the basic type of grid underlying each merge pattern and the implications for applying pixels to the pattern.

The design method given here is a generalization of that developed by Nadrian Seeman for creating rigid molecules out of parallel helical domains (here helices are technically ‘antiparallel’ in the standard terminology), which was first elaborated for the creation of double-crossover molecules (molecules with two parallel helices, ref. 16) and later extended to triple crossover molecules (molecules with three parallel helices,<sup>24</sup>). The main principle used in these works is that **crossovers may be used to hold helices rigidly in a parallel orientation**. More specifically, wherever the twist of two parallel helices bring the backbones of the two helices sufficiently close, reciprocal strand exchange can be used to incorporate a crossover. Further, an amazing aspect of the principle is that such a crossover does not disturb base pairing in either helix; the crossover appears to contain only single phosphate from each strand. The basic principle can be extended to many general schemes with a variety of crossover spacings and crossover types (parallel or antiparallel), as was mentioned in ref. 16. Here I explore a scheme that uses a regular grid of antiparallel crossovers (spaced an odd number of half-turns apart) in the bulk of a shape but on the edges and seams of a shape admits the placement of a crossovers with arbitrary offsets (in integral numbers of turns) from the underlying crossover grid.

The composition of double crossovers into periodic two dimensional crystals<sup>25</sup> showed that, through the use of sticky-end interactions, arbitrary numbers of helices could be held in a parallel arrangement by crossovers. Because the natural equilibrium length for a single turn of DNA appears to be close to 10.5 base pairs<sup>26, 27</sup>, and because DNA backbones are not symmetrically spaced around the helix (there is a major and minor groove), designs of such two dimensional DNA nanostructures (which must use integral numbers of DNA bases) invariably incorporate features that should cause strain. That is, the design assumes a DNA geometry slightly different than that of a single isolated helix with 10.5 bases per turn with ‘normal’ major/minor groove angles. This difficulty appears to have manifested itself experimentally. A number of 2D DNA nanostructures form tubes rather than sheets<sup>15,22</sup>.

The solution to this problem was first articulated to me by Erik Winfree, and was implicit in the design of DAO-E double crossover lattices<sup>25</sup>: **crossovers (and nicks) in extended structures of parallel helices should be placed so that they have symmetries which balance strain**. This principle is described at length in ref. 15 and its supplemental materials; it is also often described as ‘corrugation’<sup>22</sup>. The principle has demonstrably inhibited tube formation in at least one system<sup>22</sup>.

For DNA origami this criterion was used in the placement of crossovers; after merging it does not hold true for nicks in some designs. The use of 16 bases to represent 1.5 turns of DNA (in the 1.5-turn crossover spacing structures) or 26 bases to represent 2.5 turns of DNA (in the 2.5-turn crossover spacing structures) means that the helical domains between crossovers are slightly overtwisted or undertwisted, respectively. To balance this strain, alternating columns of staple crossovers are related by a glide symmetry—the local configuration of crossovers in one column is identical to that of crossovers in the next column over after a translation and a ‘flip’ (a rotation about one of the crossovers in-plane axes). Cross-section 1 of Fig. 1d shows the presumed orientation of backbones through one column of crossovers in the lattice, and the top two helices of cross-section 2, the presumed orientation of crossovers in an adjacent column 1.5 turns away (alternatively the diagrams for ‘+’ and ‘-’ crossovers in Supplementary Fig. S3). This symmetry should tend to balance strain in the origami and cause them to be, on average, flat. (So far, no experimental evidence has demonstrated that the origami are flat, however).

The use of a glide symmetry means that large regions of a DNA origami should have balanced strain. However, at **seams and edges this is not necessarily true, even where a seam or edge lines up with the underlying crossover lattice**. At **seams or edges, because DNA has a major and minor groove, a crossover involving staple strands is in tension with an adjacent crossover involving the scaffold strand**. Such a configuration of crossovers in tension has never before been used in DNA nanostructures. For example, in Fig. 1d the cross-section through a seam (cross-section 2) has been drawn so that the staple crossover is relaxed (top two helices of three) and the scaffold crossover (bottom two helices of three) is highly strained. Perhaps both crossovers assume some intermediate conformation.

**How the strain is actually relieved is unknown, the final base pairs of each helix may be distorted. Strain at seams or edges does not appear to cause any gross defects in the origami; bases at the end of the helices are highly available for stacking against other DNA origami which suggests that the last base pair does form and assumes a planar configuration. If, in the future, strain associated defects should be detected at edges, then one or two scaffold bases could be left unpaired and allowed to form a hairpin that should relax the crossover.**

Another place that the design of scaffolded DNA origami currently breaks with normal DNA nanotechnology is in its use of a wide range of sequences for its antiparallel crossovers. Customarily, crossover sequences are drawn from one of a few sequences that both form an immobile branched junction<sup>28</sup> and have well-characterized geometry. Such junctions have been designed with minimal symmetry so that the junction cannot branch migrate back and forth. Because the crossover sequences in the DNA origami demonstrated here are determined by the M13mp18 DNA sequence, and hundreds of them are used, a few probably have symmetries that would allow them to branch migrate a few bases; the crossover sequences have not been inspected for such properties. Further, different crossover sequences show a varying tendency to assume one of two different stacked-X conformers<sup>29, 30</sup>, one of which is incompatible with

the DNA origami's intended structure at every crossover.

It is hoped that the juxtaposition of multiple crossovers in DNA origami inhibits both branch migrations and conformer isomerizations; isomerization or migration to an undesired form at one junction would tend to increase strain between adjacent junctions. A study of a pair of symmetric antiparallel junctions juxtaposed with an asymmetric antiparallel junction has shown that the asymmetric junction can prevent the adjacent symmetric junctions from branch migrating<sup>31</sup>. But the same study showed that two symmetric antiparallel junctions juxtaposed next to each other *can* branch migrate. Thus it seems possible that several symmetric junctions near each other might conspire and migrate. Indeed it seems likely that some local rearrangements of junctions in origami happen; since they are likely to be smaller than a few nanometers, they cannot be observed by AFM. Eventually higher resolution structural information on DNA origami will determine if such isomerizations occur. Importantly, I note that there is no reason why better characterized, well-behaved junction sequences should not be incorporated into DNA origami designs if it helps to create more precise structure. The incorporation of specific crossover sequences will require the use of a synthetic scaffold rather than a natural one, a practical inconvenience for very long scaffolds.

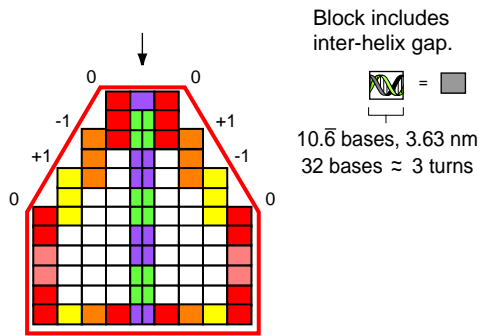
A note on seams: while most seams presented here are vertically aligned (for simplicity and convenience in design), and this necessitates the use of bridges to strengthen seams, it is possible to create staggered seams (as E. Winfree has suggested) so that staple strands naturally cross and bridge the seam vertically (between two adjacent helices) and no creation of horizontal bridges would be required. In these cases the addition of horizontal bridges across some parts of the seam might still add additional strength. A small instance of staggered seams occurs in the smiley face design. Above the right hand eye a small 2-helix seam appears that, because it is not aligned with other seams would not necessarily need bridges. An experiment in which the staples at this position were rearranged to remove horizontal bridging gave smileys of (not surprisingly) similar quality.

A note on folding paths and arbitrary shapes: there may be additional constraints on DNA origami that limit the family of shapes that can be approximated a little. In particular, shapes with lots of long thin projections or thin "waists" connecting two different parts of the shape may not form very well. As presented here, the minimum allowable width of a vertically oriented structure (such as a tall thin rectangle), if the scaffold rasters progresses in one direction vertically, is 1.5 turns, or about 5.4 nm wide. I have not tested the formation of such a narrow structure. The narrowest equivalent structure occurs at the jaw hinge of the smiley, 4.5 turns wide, about 16 nm wide. While most smileys are well formed, a significant number have dislocations along these 4.5 turn waists and it appears to be a weak spot.

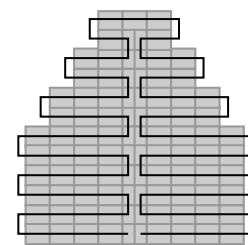
In some shapes it is desired that a strand pass both back and forth through a narrow waist so that it may access different portions of the shape. For example, consider a vertically oriented hourglass shape. If it is desired that a circular scaffold be used, then the scaffold must pass both up and down the narrow waist of the hourglass. As presented here, the minimal allowable width of the waist, which would accommodate the scaffold going up and down, would be 3 turns or about 11 nm. This width is the width of the top 4 helices of the star and because they do not image well, it seems that such a narrow waist may be floppy (in isolation). Clearly the analogous waist down the center of the smiley, which is 6 turns or 22 nm wide forms well and is mechanically stable in the context of the larger structure. Note that it is asymmetric and composed of 1.5 turn and 4.5 turn wide vertical rasters.

Similarly, consider a horizontally oriented hourglass. For a circular scaffold to pass both left and right through the waist of the hourglass would require two helices, and so in principle the waist could be about 5 nm wide. However, I am unsure how well such a skinny waist would form. Again the smiley gives the best example of the smallest such waist so far. Below each eye is a four helix waist, about 11 nm wide which forms well and is stable.

## 1. Block diagram



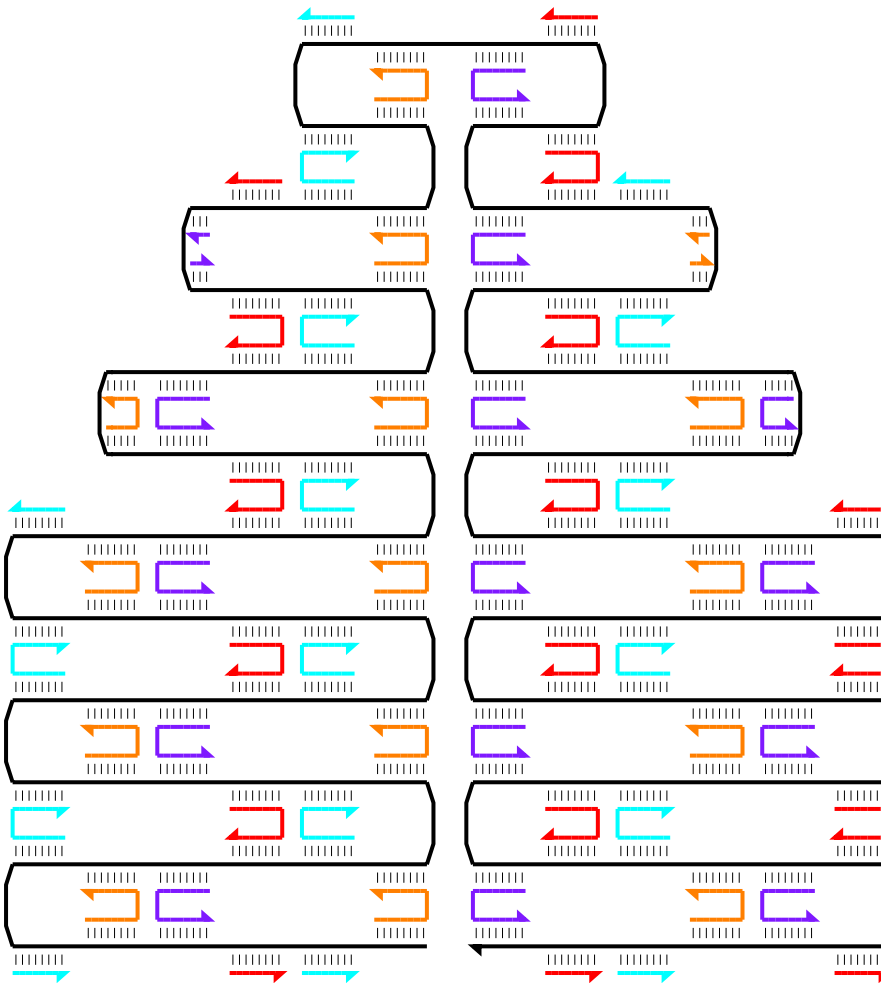
## 2. Folding path



## 3. First pass design

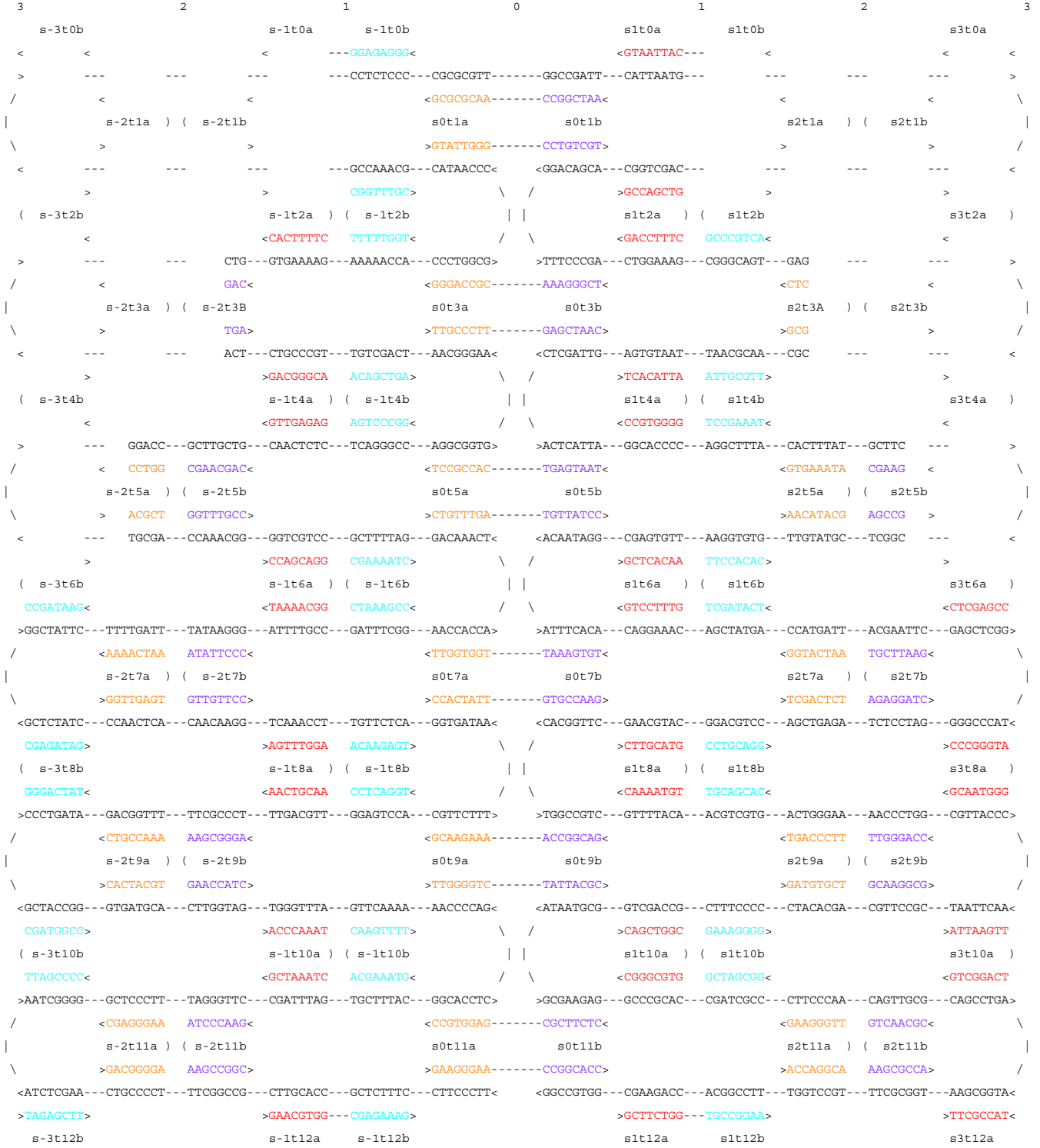
```
% C0 C1 C2 C3 C4
design_turns = [
    [3 1.5 0 0 1.5]; %H1
    [3 1.5 0 0 1.5]; %H2
    [5 2.5 0 0 2.5]; %H3
    [5 2.5 0 0 2.5]; %H4
    [7 3.5 0 0 3.5]; %H5
    [7 3.5 0 0 3.5]; %H6
    [9 4.5 0 0 4.5]; %H7
    [9 4.5 0 0 4.5]; %H8
    [9 4.5 0 0 4.5]; %H9
    [9 4.5 0 0 4.5]; %H10
    [9 4.5 0 0 4.5]; %H11
    [9 4.5 0 0 4.5]; %H12
];
```

Program outputs first pass design:



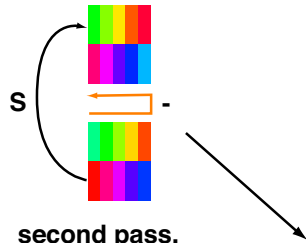
```
design_lengths = 
C0   C1   C2   C3   C4
32   16   0    0    16  %H1
32   16   0    0    16  %H2
54   27   0    0    27  %H3
54   27   0    0    27  %H4
74   37   0    0    37  %H5
74   37   0    0    37  %H6
96   48   0    0    48  %H7
96   48   0    0    48  %H8
96   48   0    0    48  %H9
96   48   0    0    48  %H10
96   48   0    0    48  %H11
96   48   0    0    48  %H12
```

Supplementary Figure S1: First three steps of origami design.

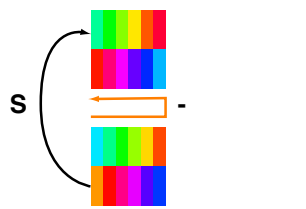


Supplementary Figure S2: First pass diagram, staple strands with *xy* labels and explicit bases.

first pass,  
5 bases from crossover,  
program reports high strain  
in scaffold crossovers  
(s, ovals). Consider left side.

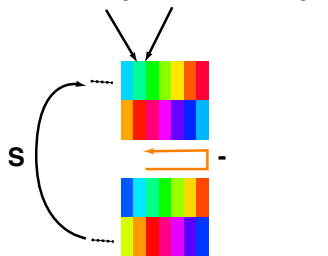


second pass,  
switch to 6 bases,  
Is strain lowered?

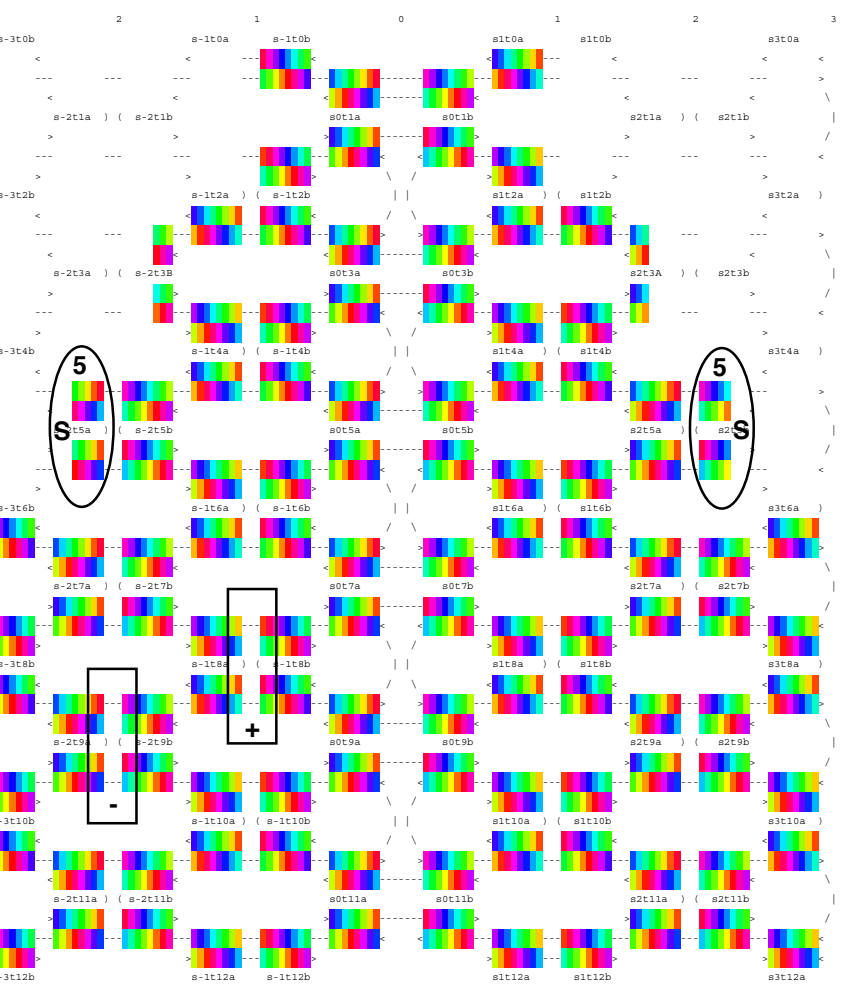
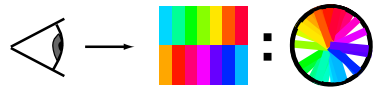


Inspect crossovers for  
situation with N+1 bases, and  
compare calculated strain.

6-7 boundary 5-6 boundary



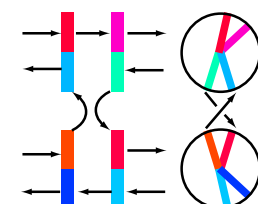
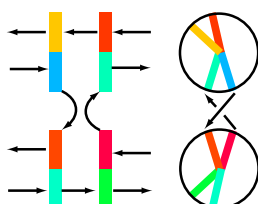
Map of twist at every base in origami.  
Cross sections viewed from left.  
Color indicates twist of each base.



Compare with balanced crossovers,  
placed every 1.5 turns

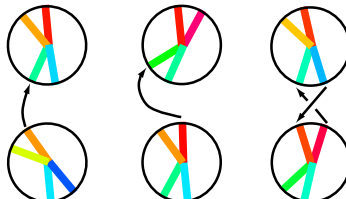
major groove up (+)

minor groove up (-)



6 bases minimize strain.  
here, only scaffold crosses.

6 bases 5 bases + is ideal



Colors (and hence twists) of exchanging strands are  
the same but colors of non-exchanging strands indicate  
positions of major and minor grooves.

Supplementary Figure S3: First pass diagram, twists displayed as colors for examination of strain.

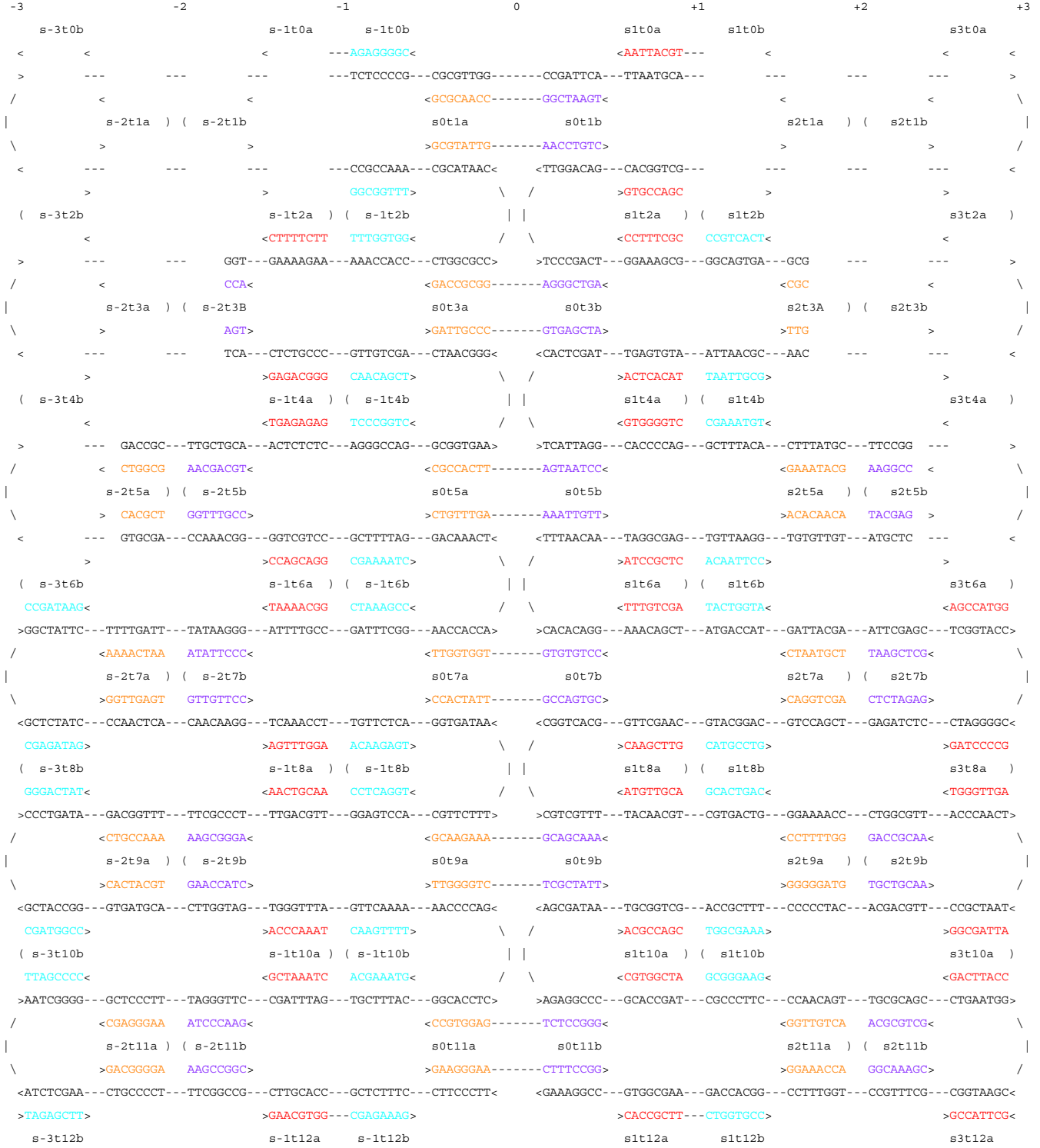
**In the second pass a matrix of adjustments (in nucleotides) is defined:**

```
%      C1   C2   C3   C4
design{ADJUSTMENTS} = [
    [0   0   0   0];      % H1
    [0   0   0   0];      % H2
    [0   0   0   0];      % H3
    [0   0   0   0];      % H4
→   [1   0   0   1];      % H5
→   [1   0   0   1];      % H6
    [0   0   0   0];      % H7
    [0   0   0   0];      % H8
    [0   0   0   0];      % H9
    [0   0   0   0];      % H10
    [0  0   0   0];      % H11
    [0  0   0   0];      % H12
];
```

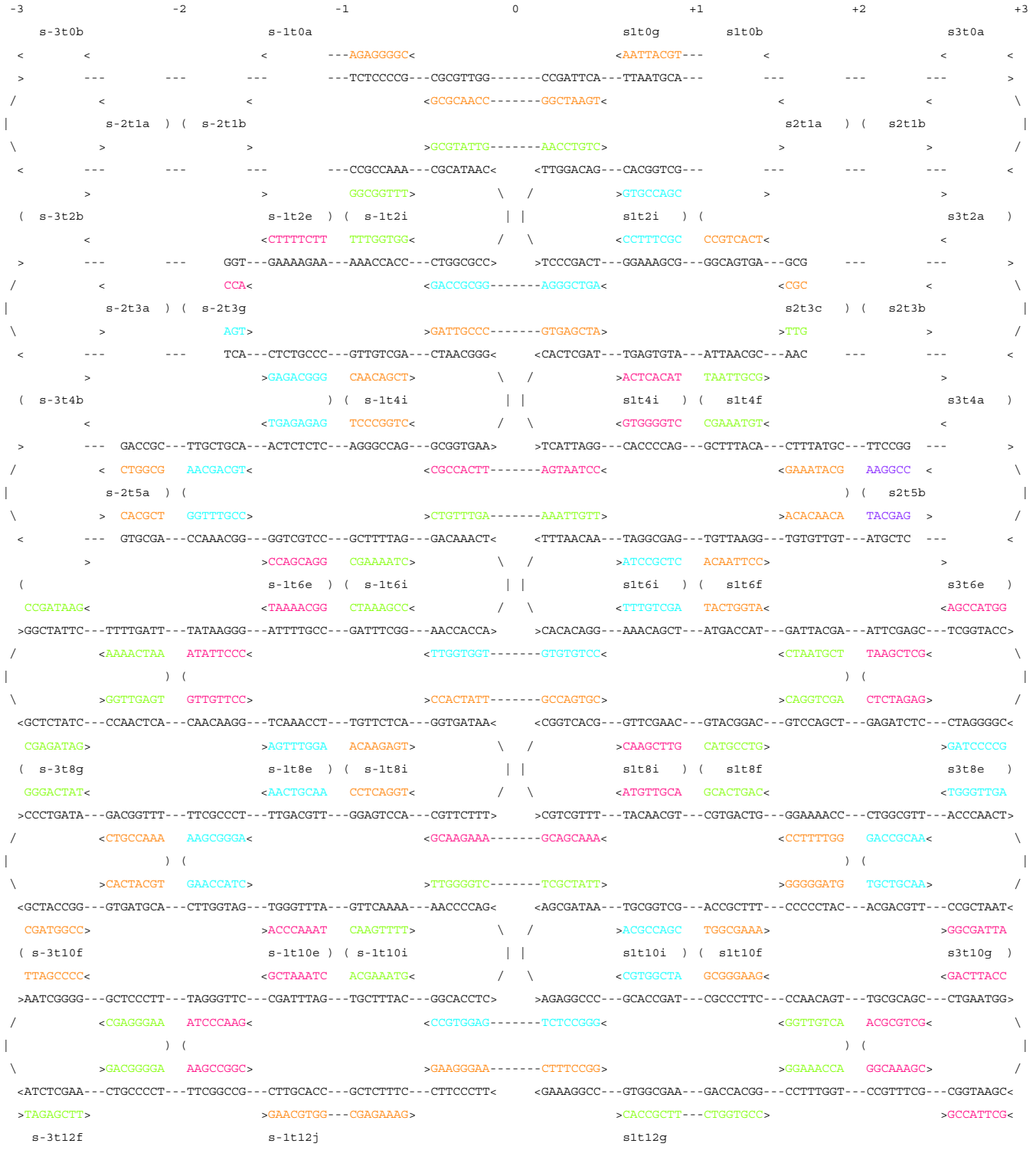
**And the design lengths are updated accordingly.**

```
design_lengths =
C0      C1      C2      C3      C4
32      16      0       0       16
32      16      0       0       16
54      27      0       0       27
54      27      0       0       27
→   76      38      0       0       38
→   76      38      0       0       38
96      48      0       0       48
96      48      0       0       48
96      48      0       0       48
96      48      0       0       48
96      48      0       0       48
```

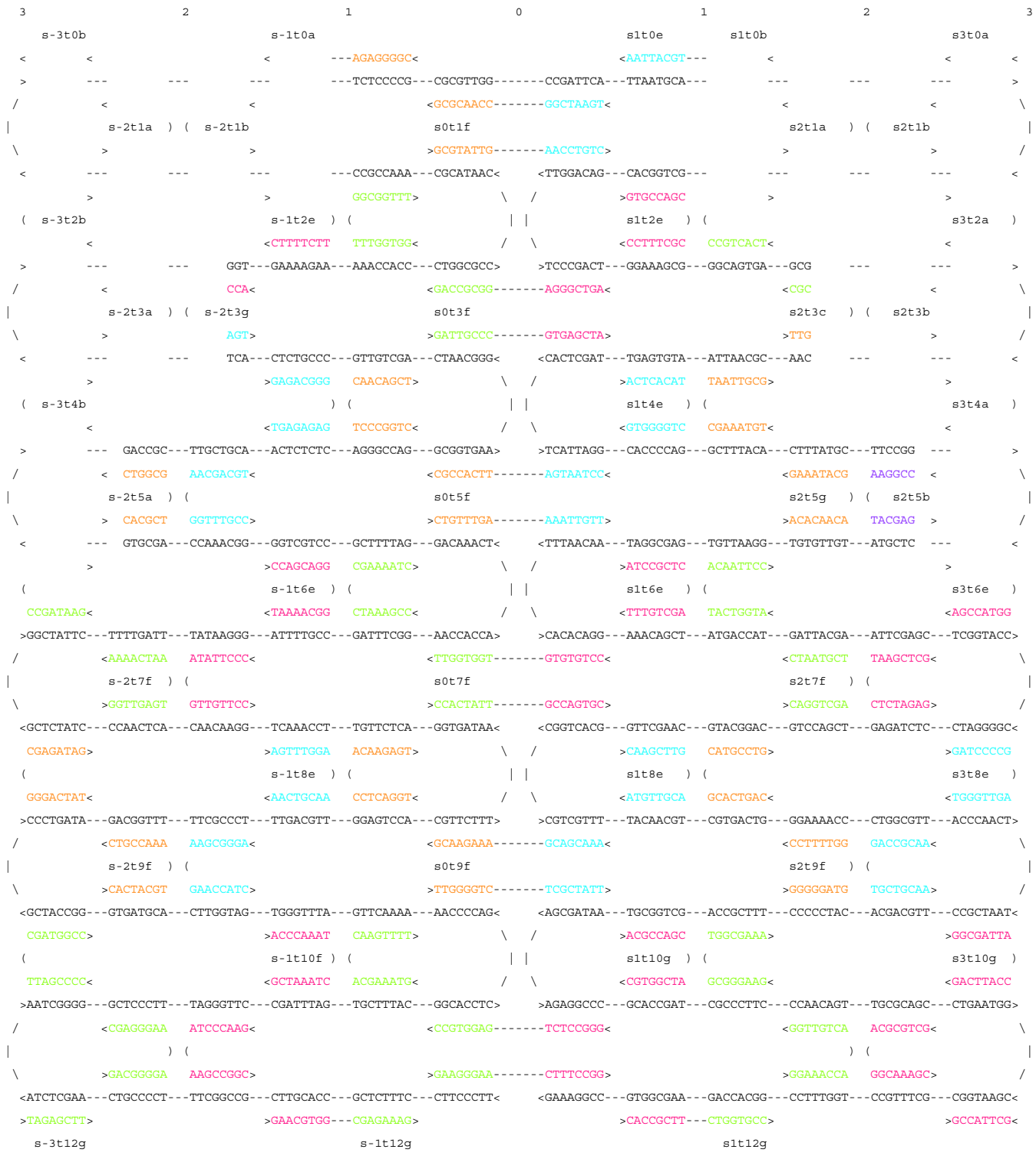
Supplementary Figure S4: Adjustments to applied during the second pass.



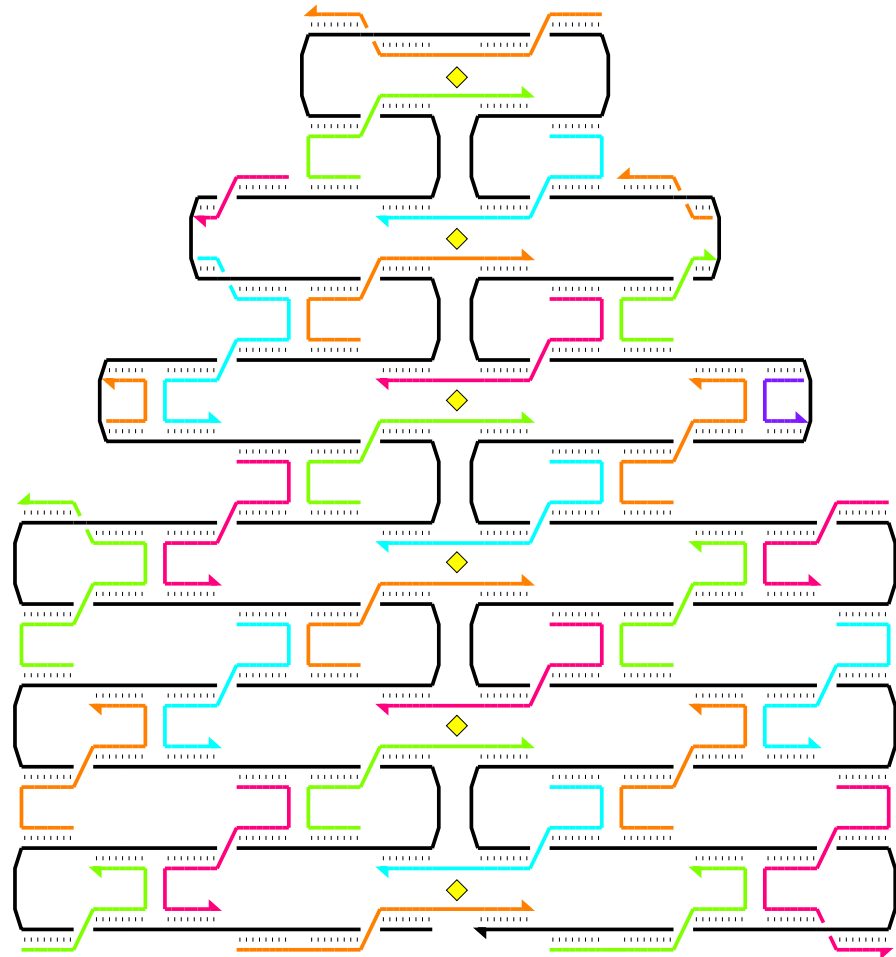
Supplementary Figure S5: Second pass diagram with staple strands before merge.



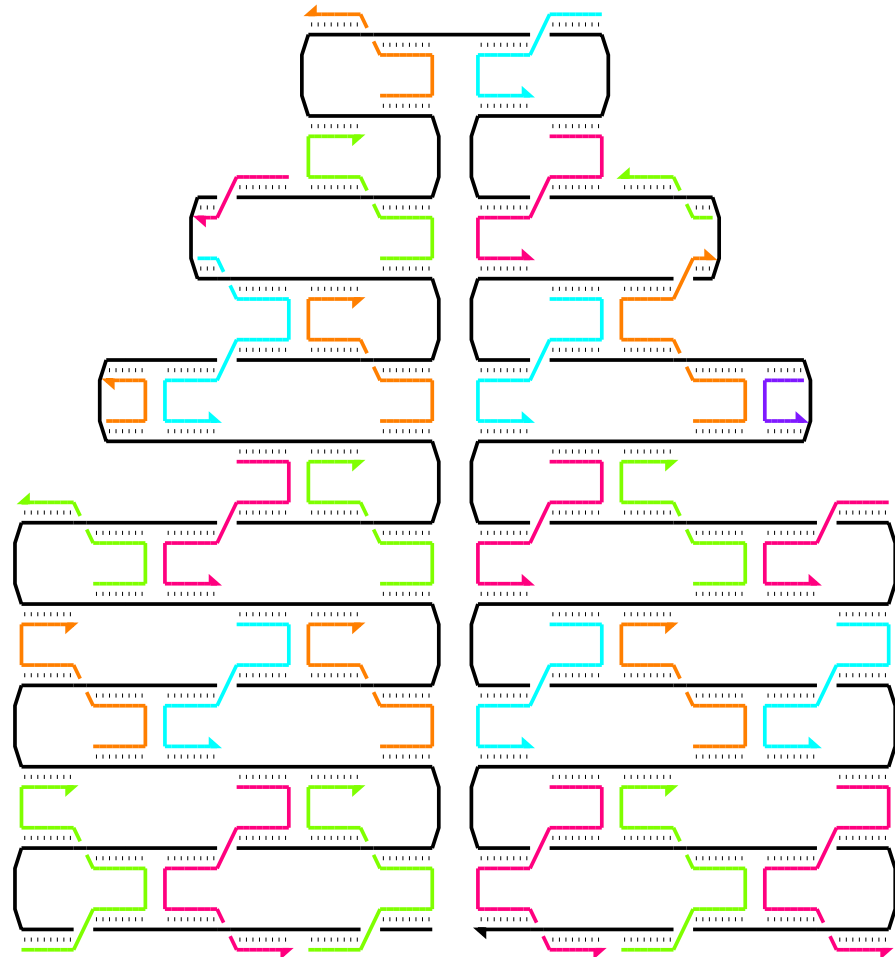
Supplementary Figure S6: Third pass diagram with staple strands after merge (bridged seam).



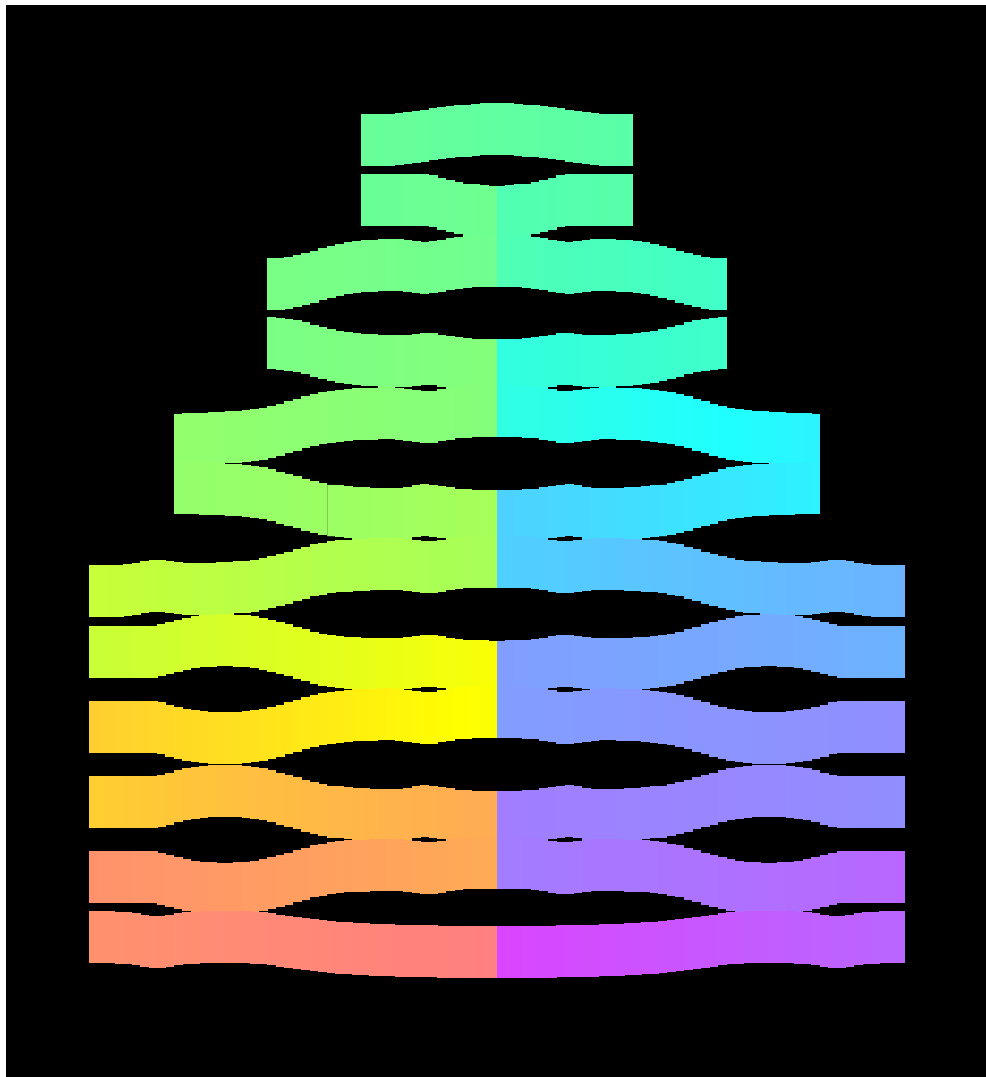
Supplementary Figure S7: Third pass diagram with staple strands after merge (unbridged seam).



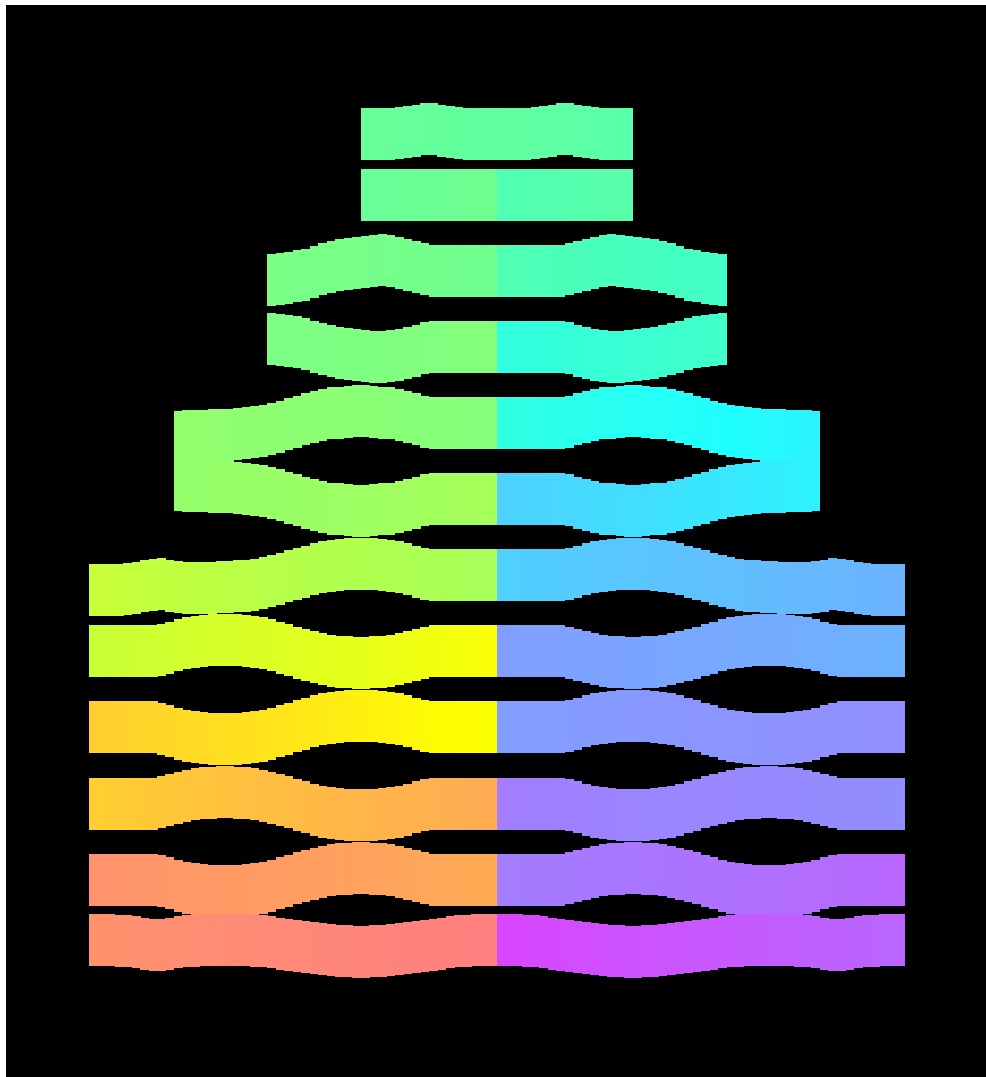
Supplementary Figure S8: Third pass diagram with staple strands after staggered merge.



Supplementary Figure S9: Third pass diagram with staple strands after rectilinear merge.



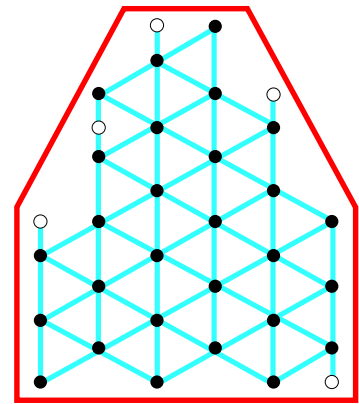
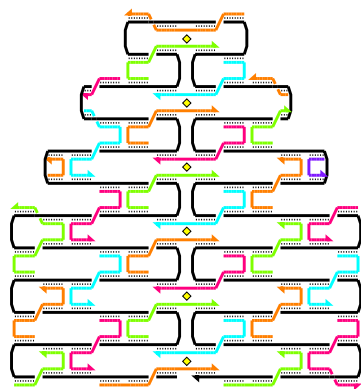
Supplementary Figure S10: Crossover diagram of bridged design.



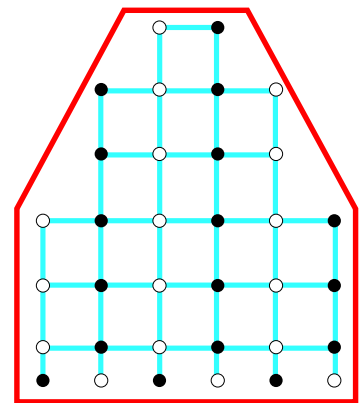
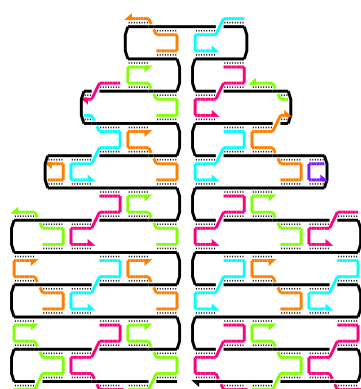
Supplementary Figure S11: Crossover diagram of unbridged design.

**a**

Staggered merge pattern

**b**

Rectilinear merge pattern



Supplementary Figure S12: Different patterns of merges yield different types of grids for any pixel pattern. Black dots indicate merges made on the top face of the structure, white dots indicate merges made on the bottom face. To create a ‘1’ pixel a hairpin is added at the position of one of the merges. Special cases on the edge of the shape are not normally used for pixels. **a** A staggered pattern of merges. In this case all modifications made to the middle of a staple strand fall on the same face of the lattice. **b** A rectilinear pattern of merges. In this case a modifications made to the middle of a staple strand fall on alternating faces of the lattice, depending on the column in which they occur. While the structure in **a** has a bridged seam, and the structure in **b** has an unbridged seam, the basic pattern of merges is independent of whether or not the seam is bridged.

## Supplementary Note S2: Effects of inter-helix gaps and DNA bending on the length and width of DNA nanostructures

When the first planar DNA nanostructures based on parallel double helical domains were made (DNA tile lattices based on double-crossover molecules<sup>25</sup>) a few assumptions were made about their structure. It was assumed (1) that the helices would be lie close-packed and (2) that the helices would be without bends. Implicit in these assumptions were two more: (3) the length of DNA nanostructures with parallel helices (measured perpendicular to the helices) was assumed to be given by  $2h$  nanometers where  $h$  is the number of helices and (4) the width was assumed to be  $.34n$  nanometers where  $n$  was the number of nucleotides in the structure. Here I review what has been learned about these assumptions. (1) turns out to be incorrect, at least for structures imaged by AFM on mica under buffer. Because of this, (2) appears to be incorrect and (3) is not a good approximation for the length (top to bottom) of a DNA nanostructure. While (4) is probably inexact it turns out to remain a useful approximation for the width of a DNA nanostructure.

When a DNA nanostructure with parallel helices bound together by crossovers is imaged by AFM, the result does not model a series of close-packed cylinders. Instead, AFM seems to reveal gaps between helices, typically 1-2 nm wide, whose position and length follow the pattern of crossovers in the underlying structure. Wherever two helices have a crossover, no gap is observed; a few nanometers away from a crossover, an inter-helix gap is observed.

The source of the inter-helix gap is unknown, it may be electrostatic repulsion between helices (as first, to my knowledge, suggested by Rizal Hariadi), or detailed geometry of the crossovers (free crossovers, when not constrained by adjacent crossovers in a multi-crossover molecule, assume an angle of approximately 60 degrees<sup>32, 33</sup>). It remains for the gap to be measured on different substrates, or in solution, or by a different imaging technique such as TEM, or for it to be measured as a function of salt concentration which might be expected to change the gap by changing the screening of electrostatic interactions.

Whatever the source, the width of the gap appears to depend on the spacing of crossovers: here origami with 16 nt spacing (about 1.5 turns) between crossovers have a ~1 nm gap, origami with 26 nt spacing (about 2.5 turns) appear to have a ~1.5 nm gap. I note that the relationship between crossover spacing and gap width is not yet proven. Here, all structures with 2.5-turn spacing have one pattern of nicks—that of Fig. 1c—that yields staples that connect only 2 helical domains; on the other hand, all structures with 1.5 turn spacing have a pattern of nicks—that of Fig. 1e that connect 3 helical domains. Thus it is possible that 2.5-turn spacing structure with a nick pattern like that of Fig. 1e might have a different spacing than the 2.5-turn structures explored here. To test whether the pattern of nicks has an effect one could re-render the 2.5-turn spacing square with 3-helix spanning staple strands as in Fig. 1e.

Because the interhelix gap appears to set the aspect ratio of DNA nanostructures constructed from parallel helices, we can use it to attempt to engineer the length and width of DNA origami. With an estimate of the gap in hand, it is simple to design DNA origami with a desired *length* (if a roughly periodic pattern of crossovers is used): the length of the structure should be  $2h + (h - 1)g$  nm where  $h$  is the number of 2 nm wide helices and  $g$  is the inter-helix gap. Lengths measured by AFM are typically within 5% of the predicted length by this formula; it assumed that this error is caused by AFM drift or miscalibration. Note that the formula predicts lengths roughly 50% and 75% greater than those that would be predicted assuming close-packed helices.

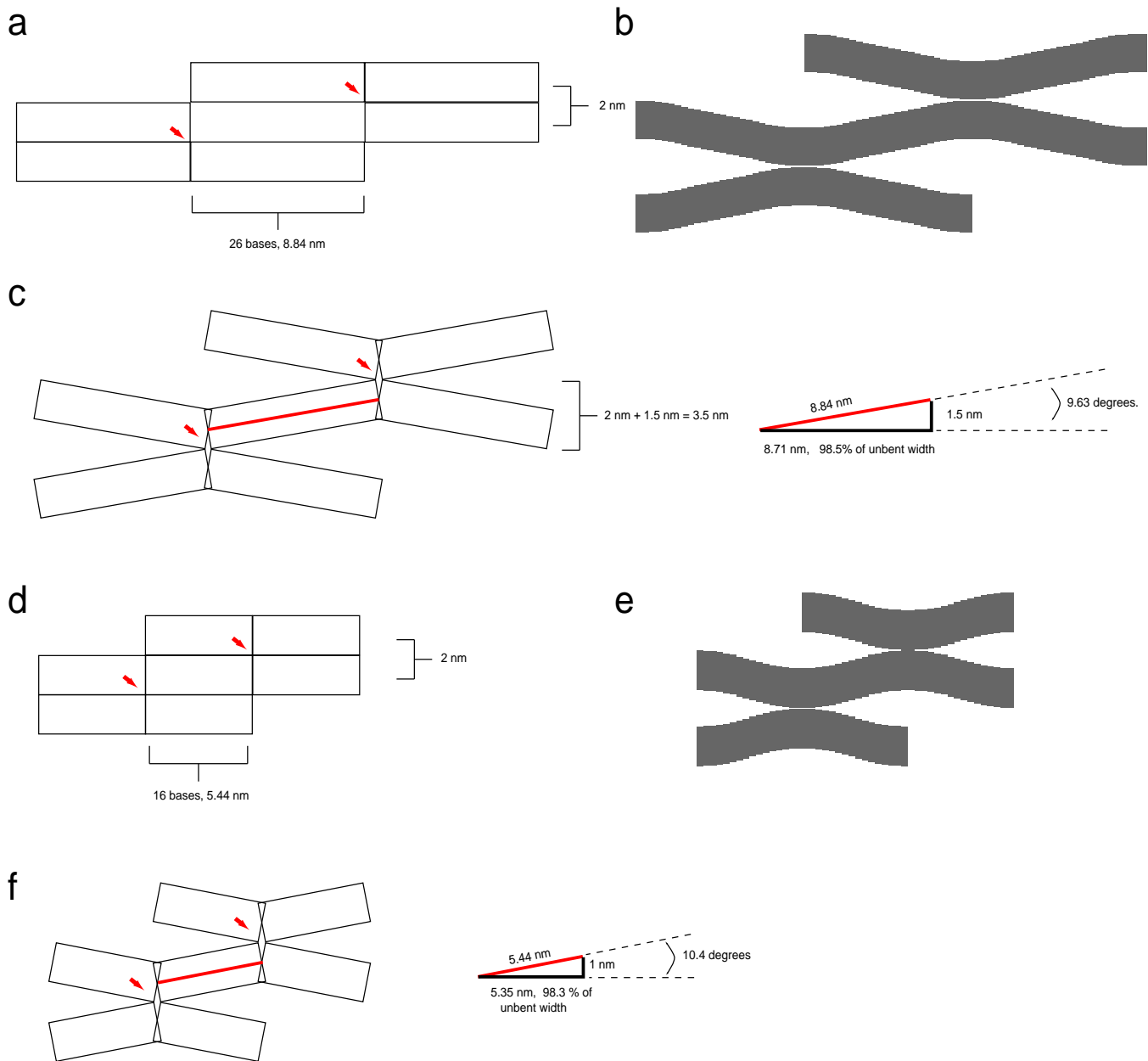
Given an estimate of the inter-helix gap, it would seem *a priori* more difficult to estimate or design the *width* of a DNA origami. To create the inter-helix gap it appears the DNA helices must bend back and forth between the crossovers in which they participate. If one assumes that the contour length of a helix of DNA does not change as it bends and follows a curve, then the end to end distance of a DNA helix following such a curve must be shorter than the end to end distance of a straight helix of the same number of nucleotides. That is, to get a correct estimate for the width of an origami, one must take the bend into account.

However, very little is known about the nature of the bending. So far, few AFM images of DNA have a resolution high enough for the contour of the helix to be traced explicitly and so it seems there is not enough data to model it accurately. Exactly what curve is followed by the helix is probably affected by electrostatic repulsion between the DNA backbones, mechanics of DNA bending, the amount of supercoiling between crossovers, and detailed geometry of the junctions. In the schematic drawing of DNA origami (row 2, Fig. 2) I give a cartoon version of the bending that seeks to reproduce structures seen in AFM images based on the pattern of crossovers in the design. Zooms of the curve used, (based on the sums of exponentials that decay away from crossovers) are giving in Supplementary Fig. S13b and e. There is no reason to believe that these curves are physically accurate.

As a very rough estimate of the change in width due to helix bending, close-packed versions of the 2.5 turn spacing and 1.5 turn spacing lattices (Supplementary Fig. S13 a and d) were deformed by bending the helical domains between crossovers an amount appropriate to create the inter-helix gap ( $\approx 10$  degrees). The projection of these bent domains on the x-axis was then calculated and taken as the new width between crossover. The width between crossovers

changed less than -2% in both cases (Supplementary Fig. S13 c and f), because of the small angles involved. I note that because I use 32 nt to cover 3 helical turns in the 1.5 turn spacing designs, the DNA in most designs is overtwisted (relative to 10.5 bases/turn) by 1.5%. Thus it is possible that relaxation of supercoiling might have a compensatory effect (relative to the effect of bending) on the width of DNA origami. (On the other hand, 52 bases are used to cover 5 turns in the 2.5 turn spacing designs and they are 1% undertwisted with respect to 10.5 bases/turn.)

Finally, the experimental widths of DNA origami are typically within 10% of that predicted using the  $.34n$  nanometers approximation. Thus while helix bending appears to happen to accomodate the inter-helix gap, the width of structures is predicted by the formula  $.34n$  nanometers to within AFM error.



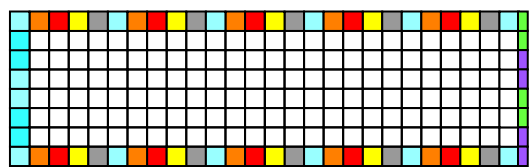
Supplementary Figure S13: A figure that suggests that the effect of helix bending between crossovers contributes little to the width of a DNA origami.

### **Supplementary Note S3: Designs and sequences**

In this note, for all large designs I include: (1) a block diagram and reproduction of the folding path (2) an enlargement of the schematics used to diagram the effects of crossover position on helix bending as in Fig. 2, row 2 and (3) the list of sequences used. A few comments:

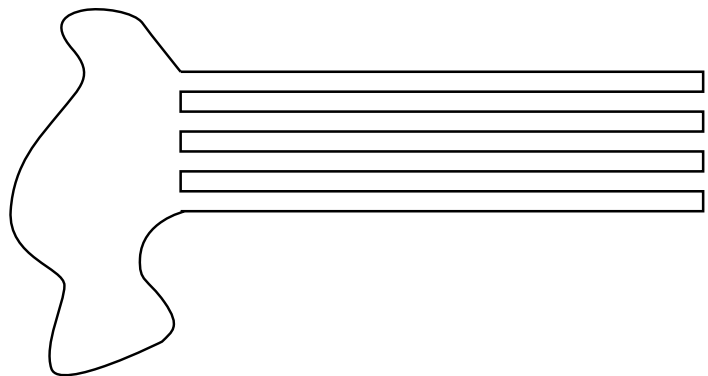
1. Because they are very large and do not print well, the full designs with staple and scaffold sequences explicitly written out appear in a separate file as Supplementary Note 12, not here.
2. For the 1/3 square, the crossover diagram is not included but is similar to that for the full square.
3. For the smiley and star I include high-resolution AFM that correponds well to the crossover models for comparison. For the smiley I inlude a model of how smileys can maximize stacking interactions.
4. For the tall rectangle, two different crossover diagrams are given, one for a bridged seam, and one for the unbridged seam (as used in Fig. 3e-i).
5. At the end of this note the full sequence of the New England Biolabs clone of M13mp18 used in this paper is included (Supplementary Fig. S39). The sequence is unpublished and appears to be available only from the NEB web site.

**a**



26.5 turns wide at 10.4 bases/turn -> 276 bases  
8 helices tall

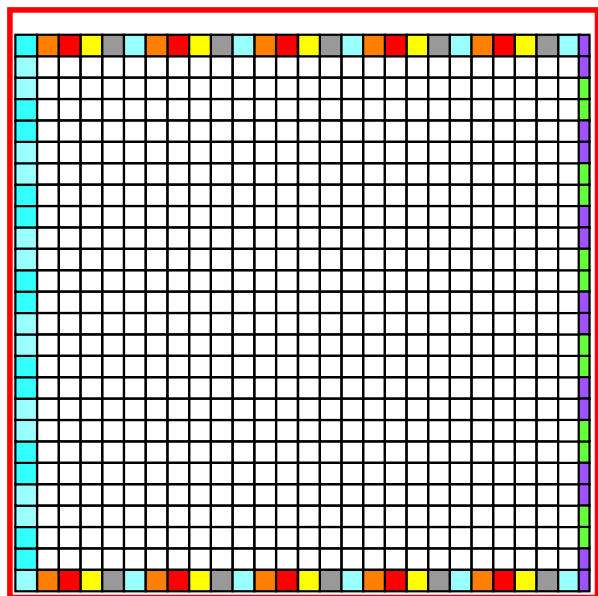
**b**



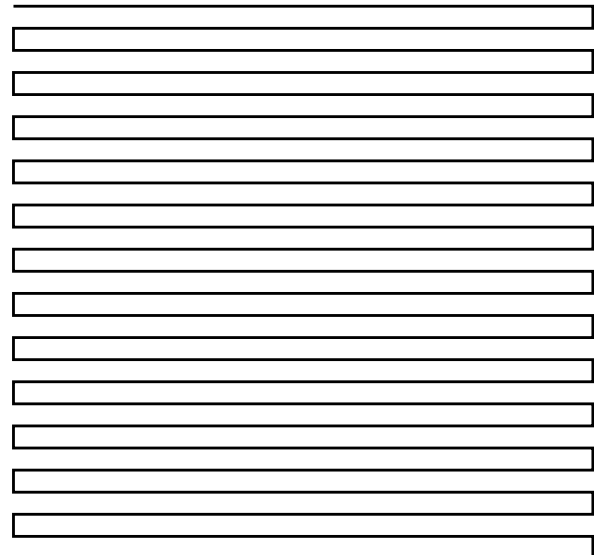
Supplementary Figure S14: Schematics for  $\sim 1/3$  of the square (8 helices) in Fig. 2a used in the first origami experiments (Supplemental Note S5.3). **a** Block diagram. Designed for 2.5-turn spacing blocks have 5 different offsets with respect to the underlying lattice of crossovers, hence the 5 different hues of blocks in different columns. As in other block diagrams, orange block/red block boundaries have an offset of 0 turns with respect to the underlying lattice of crossovers. **b** Folding path. A circular scaffold is used.

1y\_1C; GAGCCCCCGATTTAGAGCTTGACGGG  
 x3y\_1C; CAAGTTTTTGGGGTCAGGTGCGCGT  
 x5y\_1C; CGAAAAACCGTCTATCAGGGCGATGG  
 x7y\_1C; AGTTTGGAACAAAGACTCCACTATTAA  
 x9y\_1C; AATCGGCAAATCCTTATAAATCAAAGAATAG  
  
 x0y0A; CTGGGGTGCTTAATGAGTGAGCGTGGCGAGAAAGGAAGGGAA  
 x0y0B; GAAAGCCGGGAACACTAACCTCACATTA  
 x2y0A; CCAGTCGGAAACGGAAACCCCTAAAGG  
 x2y0B; AAAGCACTAAATCCCTGCGTGCAGC  
 x4y0A; GGGAGAGCGGTTCCATACCCCAAAT  
 x4y0B; CCCACTACGTGAATCGTATTGGCG  
 x6y0A; GAGACGGCAACACAACGTCAAAGGG  
 x6y0B; AGAACGTGGACTCGCTGATTGCCCT  
 x8y0A; GCAAGCGGTCACAGTGTGTTCC  
 x8y0B; CCCGAGATAGGGTGTGTTGCC  
  
 x1y1A; ATTGCGTTGCGCTCTCACAAATTCCAC  
 x1y1B; AAAATTGTTATCCGCATGCCCCGTTT  
 x3y1A; TGCATTAAATGAATCTGAATTCTGTAA  
 x3y1B; CCCGGGTACCGAGCGGCCAACGGCG  
 x5y1A; CCAGGGTGGTTTGCAGCTTCAAG  
 x5y1B; AAACGACGGCAGCTTACCCAGT  
 x7y1A; CACCGCTTGGCCGTTGGTAACGCC  
 x7y1B; GCAAGCGGATAATAGAGAGATTTGCA  
 x9y1A; AGCAGGCGAAAATTCTCGCTATTAC  
 x9y1B; GAAAGGGCGATCGGTGGGGCCCTGTTGATGGTGGTCCGA  
  
 x0y2A; CGCGTCTGGCTTCTCTGTAGCGGAAGCATAAAGTGTAAAGC  
 x0y2B; ACAACATACGAGCCAGCTTCATCAA  
 x2y2A; GTCGGATTCTCCGTGTTCTCTGTG  
 x2y2B; TCAATGTCATAGCTGGACAAACGG  
 x4y2A; CTTTGTGTAGATACTCTAGAGGATC  
 x4y2B; TGCCCTGCAGGTGGGGCGCATCGTAA  
 x6y2A; GACGACAGTATCGTACAGCAGTTGA  
 x6y2B; AGGGTTTCCCAGGCCAGAAAGAT  
 x8y2A; GCTTCTGSGTCCAGGGGGATGTCT  
 x8y2B; GCCAGCTGGCGAAGAAACCAGGAAA  
  
 x1y3A; CATTAAATGTGAGTAAATCAGCTCAT  
 x1y3B; ATTAATTTTGTGAGTAACAACCC  
 x3y3A; CGGATTGACCCGTATATTAAATTGTA  
 x3y3B; TTGTATAAGCAAATGGATAGGTCA  
 x5y3A; CGGTGCATCTGCCCGGGCGTTGATAA  
 x5y3B; TCAATCATATGTAAGTTTGAGGGAC  
 x7y3A; CGCACTCCAGCAACAAAGAGATCGA  
 x7y3B; GAGTCGGAGCAAGCTTCCGGCAC  
 x9y3A; GCGCCATTGCCATTGAGAGATCT  
 x9y3B; AATGCGGAGAGGGTAGCTATTCAAGGCTGCGCAACTGTTG  
  
 x0y4A; CAATAAATCATACAGCGAAGGGGAACGCCATAAAAAATT  
 x0y4B; TTTTTAACCAATACAAAGAATTAGCA  
 x2y4A; TAAAGCTAAATCTGTGTTAAATTGCG  
 x2y4B; AACGTTAAATTTGTGTTGACCAAAAA  
 x4y4A; GGAGAAGCCTTTAAAAAACAGGAAGA  
 x4y4B; TCAAAAGGCCCTTCAACCGCAAGG  
 x6y4A; TTTAAATGCAATTAAACACTAGCATG  
 x6y4B; TGAACGTTAATCGGCTGAGTAATGT  
 x8y4A; AAGGCCGGAGACAGGTATTGCGCT  
 x8y4B; ACAAAAGCTATCAGTCAAATCACCAT  
  
 x1y5A; AAAATAAGCAATAGCTGAAAAGGTTG  
 x1y5B; ATTTGGGGCGGAAAGGCCATCAGAGCA  
 x3y5A; CATTATGACCCGTGATTGCAATGG  
 x3y5B; GACCATTTGAGATACTAATACTTTGCG  
 x5y5A; ATA AAAAATTTTACAGTTGATTCCA  
 x5y5B; TCATTCCATATAAGAACCTCATATA  
 x7y5A; GTAGGTTAAAGATTGTTAAATATG  
 x7y5B; CTGTTAGCTCAACACAAAGGGTGAGA  
 x9y5A; CAATATGATAATTCTTGTGGGATGCG  
 x9y5B; CTCTTTGATAAGGGTCATAACCGTTCTAGCTGATAAATT  
  
 x0y6A; ATGTTTAGACTGGATAGGTCAATAGTAGCTGATTAACATC  
 x0y6B; CATCAATTCTACTCAACTGCGGAA  
 x2y6A; CTCAAATGCTTATAGCTTATTTTC  
 x2y6B; TCAATAACCTGTTAACAGTTGAGAAA  
 x4y6A; AGGTCCTTACCCCTGTAGATTAGTT  
 x4y6B; ATTCCTGGAAACGAGACTATTATAGTC  
 x6y6A; GATTAAGAGGAAGGTGCTGGAAAGTT  
 x6y6B; CAACTAAAGTACGCCGAAAGACTTC  
 x8y6A; AAACCGAAACCAAGAGCTGAATATAATG  
 x8y6B; TTAGAGCTTAATTCCGGAAGCAAACT  
  
 x1y7C; TCGTCATAAAATATTCTATTGAATCCCC  
 x3y7C; ACGAGAAATGACCATAAATCAAATC  
 x5y7C; AGAAAGCAAACCGGATTCGATCAA  
 x7y7C; AAATATCGGCTTTAATTGAGCTTC  
 x9y7C; CCAACAGGTCAAGGATTAGAGAGTACCTTTAATTG

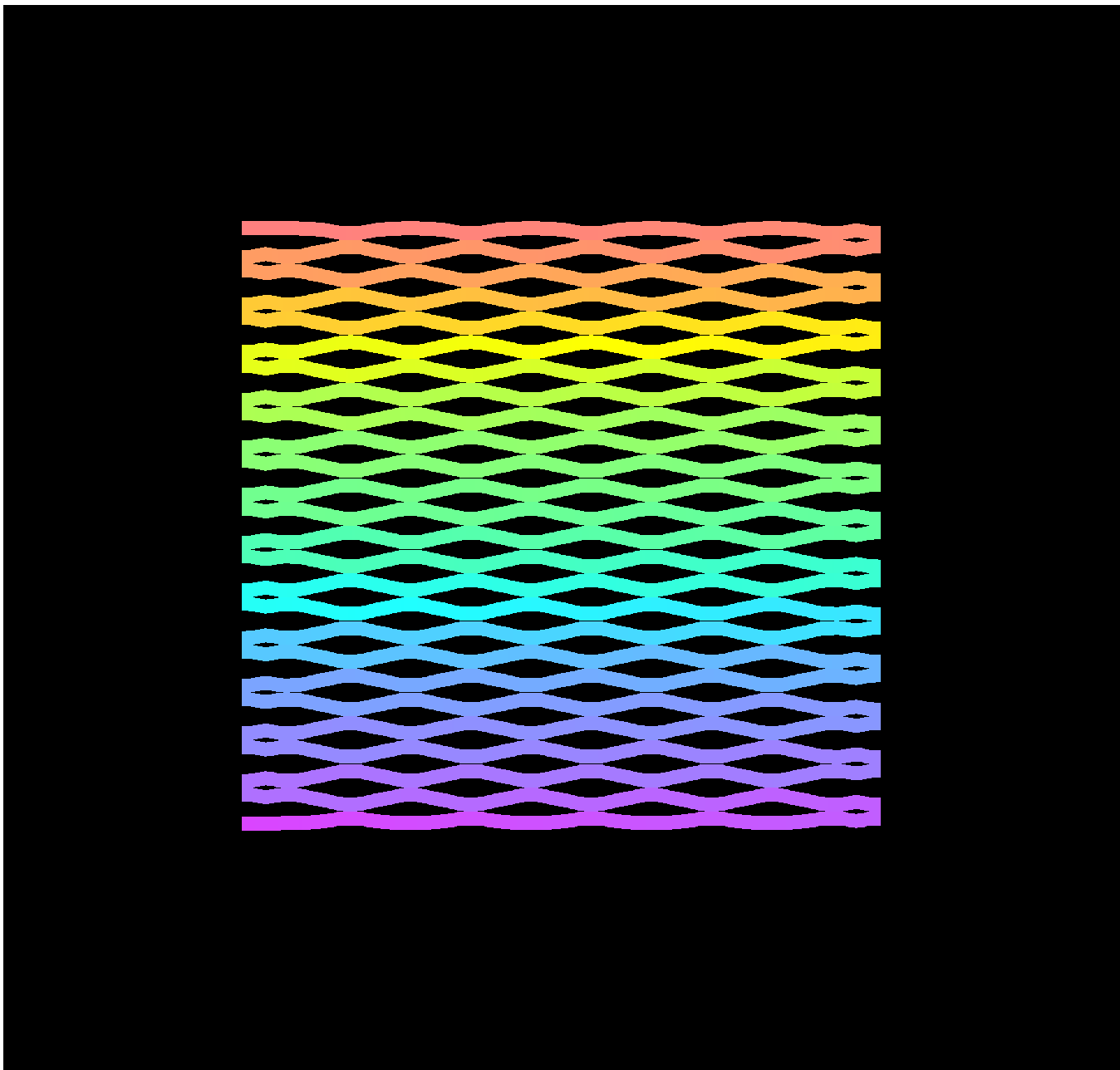
Supplementary Figure S15: Strands used to create  $\sim 1/3$  of a square.

**a**

26.5 turns wide at 10.4 bases/turn -> 276 bases  
26 helices tall

**b**

Supplementary Figure S16: Schematics for the square in Fig. 2a. **a** Block diagram. Designed for 2.5-turn spacing, blocks have 5 different offsets with respect to the underlying lattice of crossovers, hence the five different hues of blocks in different columns. As in other block diagrams, orange block/red block boundaries have an offset of 0 turns with respect to the underlying lattice of crossovers. The red square highlights our prediction for how well the design is expected to approximate a square. **b** Folding path.

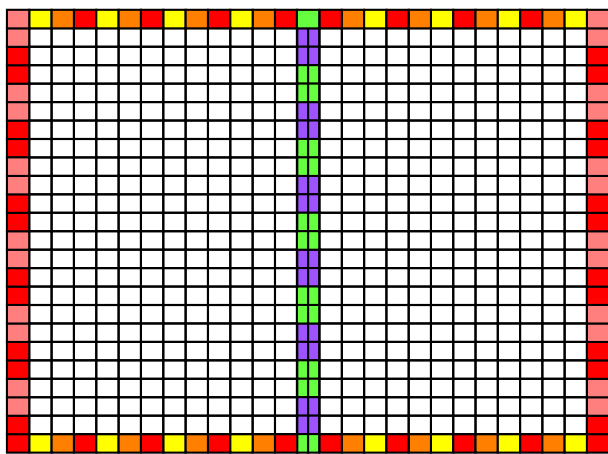


Supplementary Figure S17: Crossover induced structure of square.

x1y\_1C; GAGCCCCCGATTTAGGCTTGACGG  
 x3y\_1C; CAAGTTTTTGTGATTCGGTGCCTG  
 x5y\_1C; CGAAAAGCCGTATCAGGGCATGG  
 x7y\_1C; AGTTGGAACAGAGTCCACTATTA  
 x9y\_1C; AATCGGCAAATTCCTTATAAATCAAAAGATAG  
 x0y\_0A; CTGGGGTGCCTAATGGTGAGCTGGCGGAGAAAGGAAGGGAA  
 x0y\_0B; GAAAGCCGGCGAACTAATCACATTA  
 x2y\_0A; CCAGTCGGAAACCGGAAACCTAAAGG  
 x2y\_0B; AAAGCCTAAATCTCTGCTGCCAGC  
 x4y\_0A; GGGAGAGGGCGGTCTCATCACCAGAAT  
 x4y\_0B; CCCACTACGTGAGCTGGTATGGGGC  
 x6y\_0A; GAGACGGCGAACGGGAAACGG  
 x6y\_0B; GAACCTGGACTCTGGTATGCCCTT  
 x8y\_0A; GCAAGCGGTGACTGGTGTGTCTCC  
 x8y\_0B; CCGAGAGATGGTGTCTGGCCCC  
 x1y\_1A; ATGGGTTGGGCTTCAAACTTCCC  
 x1y\_1B; AAATTGTTATCCGCACTGCCCTT  
 x3y\_1A; TGCAATTAAATGCTGGTAACTCG  
 x3y\_1B; CCGGGTACCGGGGAAACGGG  
 x5y\_1A; CCAGGGTACCGGGAAACGGTCTTCA  
 x5y\_1B; AAACGCGGCCAGCTTCAACAG  
 x7y\_1A; CACCCGCTTACGGGAAACGG  
 x7y\_1B; GCAAGCGGAAATCTTCCGCTTAA  
 x9y\_1A; AGACGGCGAACGGTGTCTTCA  
 x9y\_1B; GAAGGGATGGCTGGGGGCTCTTGTGATGGGGTTC  
 x0y\_2A; CGGCTCTGGCTTCTGTGAGCTGGAGCATAAGTGTAAAGC  
 x0y\_2B; ACACATACGAGGCCAGCTTCA  
 x2y\_2A; GTGGATTCTGGCTGGTGTCTGGT  
 x2y\_2B; TCATGGTACAGGGAAACAAAGG  
 x4y\_2A; CGTGGTGTAGTACTGGAGGATC  
 x4y\_2B; TGGCTCAGGTGGCTGGCTGATCTTA  
 x6y\_2A; GACGACAGTGTGCACTGGAGCTT  
 x6y\_2B; AGGGTTTCCCAGGGCTCAGGAGAT  
 x8y\_2A; GCTTCTGGCCAGGGGGATGTGCT  
 x8y\_2B; GCAAGCGGAGAGGAAACGGCAA  
 x1y\_3A; CATTAAATGTGAGTAAATCAGCTCAT  
 x1y\_3B; ATTTAAATTGTCAGGAAACAA  
 x3y\_3A; GGAGTTGACCCATTATTTGAGGTT  
 x3y\_3B; TTGATAAAGCAGGATGGTAGCT  
 x5y\_3A; CCGGATCATGGGGGGGGGGGGT  
 x5y\_3B; TCAATCATATGTAAGTGGGGAC  
 x7y\_3A; CGAACCTGGCAACAGGAAAGTGA  
 x7y\_3B; GAGTCAGGACAGCTTCCGGCACC  
 x9y\_3A; GCGCCATTCCGATTGGAGGATCT  
 x9y\_3B; AATGCCGGAGAGGGTACTTACGGCTG  
 x0y\_4A; CAATAATCATACGCCAGGGGACGCCAT  
 x0y\_4B; TTTTAACCAATAAAGAAATAGCA  
 x2y\_4A; TAAAGCTAAATGCTGTTAACTTCC  
 x2y\_4B; AACGTTAATTTTGTGACCAAA  
 x4y\_4A; GGAGAAGCCTTAAACAGGAGA  
 x4y\_4B; TCAAGAAAGCCCCCTTCAACCAAGG  
 x6y\_4A; TTAAATGAGGAAATTTAACAGTGT  
 x6y\_4B; TGACCGTAACTGGCTGAGTATGT  
 x8y\_4A; AAGCCGGAGACAGGTCACTCCG  
 x8y\_4B; ACAAGGCTATCAGTAAATCCCAT  
 x1y\_5A; AAATTAAAGCAATAGCTGAAAGGTG  
 x1y\_5B; ATTGGGGCCGAAACGGCTTCAAG  
 x3y\_5A; CATTATGACCCGTATTGGCAAATGG  
 x3y\_5B; GACATTGATAGTACTATTTGGC  
 x5y\_5A; ATAAAATTTACGTTGATCCCA  
 x5y\_5B; TCATTCATATAGAACCCCTCATATA  
 x7y\_5A; GTAGGTTAAGATTGTTTAAATGT  
 x7y\_5B; CTGAGCTTACACACAAAGGGTGAG  
 x9y\_5A; CAATATGATTTCTGAGGATG  
 x9y\_5B; CTCTTTAGAGGCTATAACCGTTACGGTATAAAT  
 x0y\_6A; ATGTTTGGACTGATGGCTCAATAGTAGCTGATTAACATC  
 x0y\_6B; CATCAATTCTACTAACTACTCGGA  
 x2y\_6A; CTCAAACTGTTAATGCTTATTTC  
 x2y\_6B; CTCATAACCTGTTAACAGTCA  
 x4y\_6A; AGGTTTACCCCTGAGTATTAGTT  
 x4y\_6B; ATTCTGGGACAGGACTTATATAGTC  
 x6y\_6A; GATTAGAGGAGGTGCTGGAGTT  
 x6y\_6B; CAACTAAAGTGGCGGAGAACCTC  
 x8y\_6A; AAAGCAGGAGAGCTGAAATTAATG  
 x8y\_6B; TTAGAGCTTAACTCCGAGGAAACT  
 x1y\_7A; TCTCTATTAATATGAGGCTTTGG  
 x1y\_7B; AAAACAAAATAGTCAGGATCTCCC  
 x3y\_7A; ACAGAAATGACCAAGAACACTATCA  
 x3y\_7B; GAGGCATAGTGAAGTAAACAAATC  
 x5y\_7A; AGAGCAAGGCGATTGCTAAATGC  
 x5y\_7B; TTAGGAATACACCATGGCTAA  
 x7y\_7A; AAATATCGCTTACACATTATTC  
 x7y\_7B; ACAGAACTAACGGATAATTGAGGCTC  
 x9y\_7A; CCACAGGTAGGGCACTGAGACGT  
 x9y\_7B; TTTAAGAACTGGCTCATATAATTAGAGAGTACCTTAA  
 x0y\_8A; CGGGAACGAGGCGAGACGGTGCAGAGGGGGTAAAGTAAA  
 x0y\_8B; CAAAGAAGTTTCACTCATAAAGGGA  
 x2y\_8A; ACAGATGAGCAGGAGGATATA  
 x2y\_8B; TAACCTCTGTTAGTACAGGACAG  
 x4y\_8A; AGTAATCTTGTACACAAAGGAATTAC  
 x4y\_8B; AGATACATAAACCGGAAACGGGATATT  
 x6y\_8A; TGCTCATTTGCTGATCAGTGGAGAT  
 x6y\_8B; AGGTAGAAAGATAATTAAGGCTTGC  
 x8y\_8A; TAAATTGGGCTTGTGACTGTAAATAAA  
 x8y\_8B; TGGGAGAAAATAGATGGTTAA  
 x1y\_9A; ACCGAACTGACCGCTGTATAATTG  
 x1y\_9B; GATTGGTATCATCTGGTAAAGGAG  
 x3y\_9A; GCATGGCTGCTCCAGGATTATA  
 x3y\_9B; CTACATCTGGCAGGCTTCACTAAC  
 x5y\_9A; CATACCCAACTAACCACTAAAGGA  
 x5y\_9B; ACTACGAAAGCACACCTAACAAAGC  
 x7y\_9A; CTGAGGAAACATGAGGAAAGTTC  
 x7y\_9B; AAAGACTTTTCACAGAACAGTAG  
 x9y\_9A; TCACCTTAACTACGGAGAAT  
 x9y\_9B; TCAGCAGGAAACAGCATCTGGTAA  
 x1y\_10A; AACCTTCAACGTTCTGGGACCTCTCCATGTTACTTAG  
 x0y\_10B; TGTGCAATTCCGGTGAATGAAAG  
 x2y\_10A; ATAAATTCTTCAACAGAAC  
 x2y\_10B; CCAAGGGGAAACGGTAAATCTC  
 x4y\_10A; TAATTGTTGGCTTAACTAAC  
 x4y\_10B; AAGGGCAAAGATTATCAGCTG  
 x6y\_10A; GATACCGATAGTTGCTGATG  
 x6y\_10B; ATTAACGGTAAAGCCGGCA  
 x8y\_10A; ATATTGGCTGAGGACT  
 x8y\_10B; CAACGGCTACAGACTGGCT  
 x1y\_11A; AGGACAACTAAATTCTAAC  
 x1y\_11B; AAAGTTTACGGGAACTTCA  
 x3y\_11A; AAAAAAAGGCTTCACTCACAGACA  
 x3y\_11B; ACACGCTGTAAGCAGGAGGCTT  
 x5y\_11A; TTGGGGTGAATTCAGTGT  
 x5y\_11B; CCCAACTGGACCTTCAACAGCTT  
 x7y\_11A; CAACACCATGTCAGGAGG  
 x7y\_11B; CCTCAAGGGCCCCAAC  
 x9y\_11A; GGAGTTAACGGGACTCAGGG  
 x9y\_11B; CCGGATAGGTGATCTGGCT  
 x1y\_12A; GGGAAAGCAGTCTCTGAAATTG  
 x0y\_12B; GTTAAATGCTGGGATTCTGGCT  
 x2y\_12A; CAGGAGTGTACTGGCTG  
 x2y\_12B; GCGCTTCACTAGTGAATTA  
 x4y\_12A; GCGCTATAAACACAGTCA  
 x4y\_12B; ACTGAGTTCTGGTAACTGG  
 x6y\_12A; AACATGAAAGTACGGAGG  
 x6y\_12B; CCACCCCTATTGAGGCTG  
 x8y\_12A; CGGGGTTTGGCTGAGG  
 x8y\_12B; AGTACGGCCACCCAGTAC  
 x1y\_13A; AGCGCTATACATTTGGCTT  
 x1y\_13B; CGAGGTGAGCAGGCTTGG  
 x3y\_13A; ACAGGGTCACTGGCCACAGG  
 x3y\_13B; CGCCACAGAACCTTCA  
 x5y\_13A; GCGCTATTGGAGAACGG  
 x5y\_13B; CTGAGGCGAACCTT  
 x7y\_13A; CTCTCTAAGGAAAAAA  
 x7y\_13B; TCTTTCAATGGTAGGAG  
 x9y\_13A; TAAGTGGCTGAGCAGGCTT  
 x9y\_13B; CAGACTGTGGGGCTT  
 x1y\_14A; TTATTTGTCACATCA  
 x0y\_14B; TCACAAAATTTACATATG  
 x2y\_14A; GACATTCAACGGACAGG  
 x2y\_14B; CGCCGAGCTTGTGAGGAG  
 x4y\_14A; TAAAGGTGAATTGAGG  
 x4y\_14B; ACCCTCTGAGCCTTCA  
 x6y\_14A; GCGAAATCAGGAGG  
 x6y\_14B; CCAGGCCCCACTAG  
 x8y\_14A; TGAACACCTGAGGTT  
 x8y\_14B; CATAGGCCCCAACGG  
 x1y\_15A; TTACCAAGGGCAAAAGGG  
 x1y\_15B; AAAATACATACAA  
 x3y\_15A; GGTAAATTTGACATTAGCT  
 x3y\_15B; AGAGCTCTGGAAATTATC  
 x5y\_15A; CTGAGCTTGAAGGAG  
 x5y\_15B; ACAAAAGTACGGGA  
 x7y\_15A; ATTAGCAAGGGCTACGG  
 x7y\_15B; GCAATAGCTTGTGAG  
 x9y\_15A; TCAAGTGGACAGG  
 x9y\_15B; GAGAGATAACCC  
 x1y\_16A; ATTCAGGCTTCTGG  
 x0y\_16B; TATAAGGAAAGCTC  
 x2y\_16A; ATACCGCAGTCTGG  
 x2y\_16B; ATTACCGCAGTATG  
 x4y\_16A; ATTATTTCACCA  
 x4y\_16B; AAAGCCTAATAAC  
 x6y\_16A; GAAAGTACGG  
 x6y\_16B; TTAAAGAAA  
 x8y\_16A; GACGGGAGA  
 x8y\_16B; TAATAAGAG  
 x1y\_17A; ATTATTCTGGTGT  
 x1y\_17B; TTCTAAGAAGCCG  
 x3y\_17A; TTGCGAGT  
 x3y\_17B; TCAATTACCGG  
 x5y\_17A; AGCATTTTGT  
 x5y\_17B; AGTACGGC  
 x7y\_17A; TACATTA  
 x7y\_17B; AATCAATATCG  
 x9y\_17A; AACAAAGT  
 x9y\_17B; TAGAGTACT  
 x1y\_18A; AATAAGAATAAC  
 x0y\_18B; AACCTCCG  
 x2y\_18A; TATAAAATCT  
 x2y\_18B; ATACGAT  
 x4y\_18A; AGAATGG  
 x4y\_18B; AGCCGTTT  
 x6y\_18A; GAGGCGAGT  
 x6y\_18B; TCAATT  
 x8y\_18A; CAGAGC  
 x8y\_18B; TCTTA  
 x1y\_19A; AAAAGC  
 x1y\_19B; TCAATTCTT  
 x3y\_19A; CAAGGCT  
 x3y\_19B; ATCCG  
 x5y\_19A; CATGTA  
 x5y\_19B; CTC  
 x7y\_19A; ACCG  
 x7y\_19B; AGCT  
 x9y\_19A; TCACTG  
 x9y\_19B; TTAATT  
 x1y\_20A; TTAAACG  
 x0y\_20B; TTGAAT  
 x2y\_20A; TTCCG  
 x2y\_20B; CTT  
 x4y\_20A; TTCTTCA  
 x4y\_20B; TATATG  
 x6y\_20A; CAAA  
 x6y\_20B; TAGG  
 x8y\_20A; CAGT  
 x8y\_20B; ATAGCT  
 x1y\_21A; TTACATCG  
 x1y\_21B; TACCT  
 x3y\_21A; TTACAA  
 x3y\_21B; TATAAT  
 x5y\_21A; AGATG  
 x5y\_21B; GOAGC  
 x7y\_21A; ATT  
 x7y\_21B; TTAAAG  
 x9y\_21A; GAA  
 x9y\_21B; ATTAG  
 x1y\_22A; ATACCG  
 x0y\_22B; AACAG  
 x2y\_22A; CGCT  
 x2y\_22B; TTCT  
 x4y\_22A; TACACTT  
 x4y\_22B; ATTAC  
 x6y\_22A; GCAAA  
 x6y\_22B; TTTC  
 x8y\_22A; AGC  
 x8y\_22B; AAATC  
 x1y\_23A; GAGGT  
 x1y\_23B; TTG  
 x3y\_23A; CAGC  
 x3y\_23B; AGAT  
 x5y\_23A; ACC  
 x5y\_23B; CGAC  
 x7y\_23A; GGA  
 x7y\_23B; GGA  
 x9y\_23A; CGT  
 x9y\_23B; CTG  
 x1y\_24A; GCG  
 x0y\_24B; CGC  
 x2y\_24B; CGT  
 x2y\_24B; GTC  
 x4y\_24A; ATT  
 x4y\_24B; AATA  
 x6y\_24A; TA  
 x6y\_24B; TGG  
 x8y\_24A; AATA  
 x8y\_24B; GCA  
 x1y\_25C; GTG  
 x3y\_25C; AGCT  
 x5y\_25C; ATCC  
 x7y\_25C; COAT  
 x9y\_25C; CACT

Supplementary Figure S18: Sequences for the square.

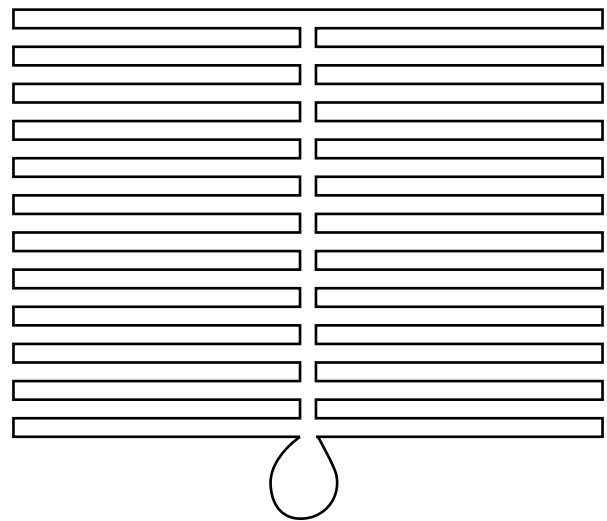
**a**



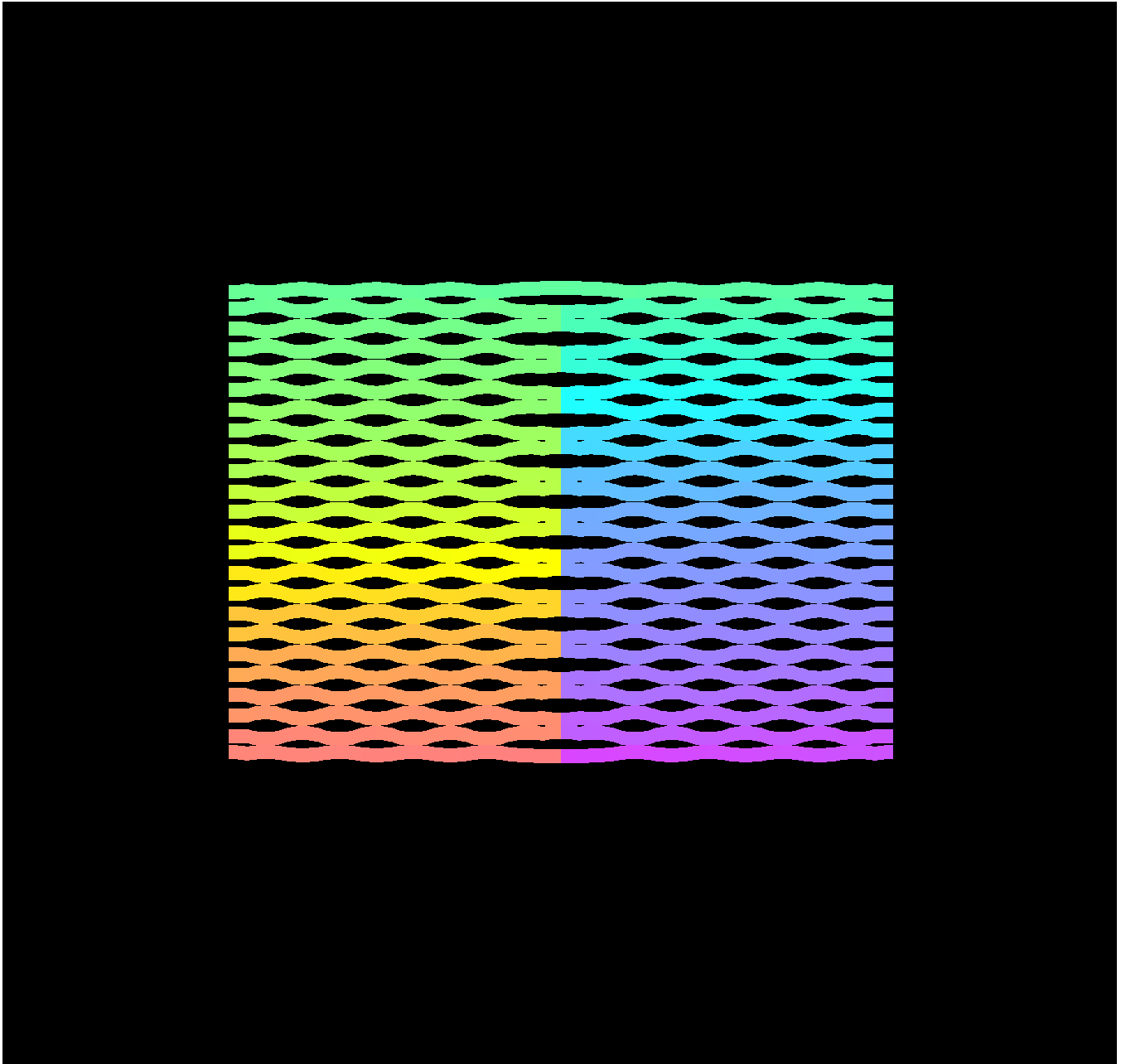
27 turns wide at 10.666 bases / turn -> 288 nt

24 helices tall

**b**



Supplementary Figure S19: Schematics for the rectangle Fig. 2b. **a** Block diagram. **b** Folding path.

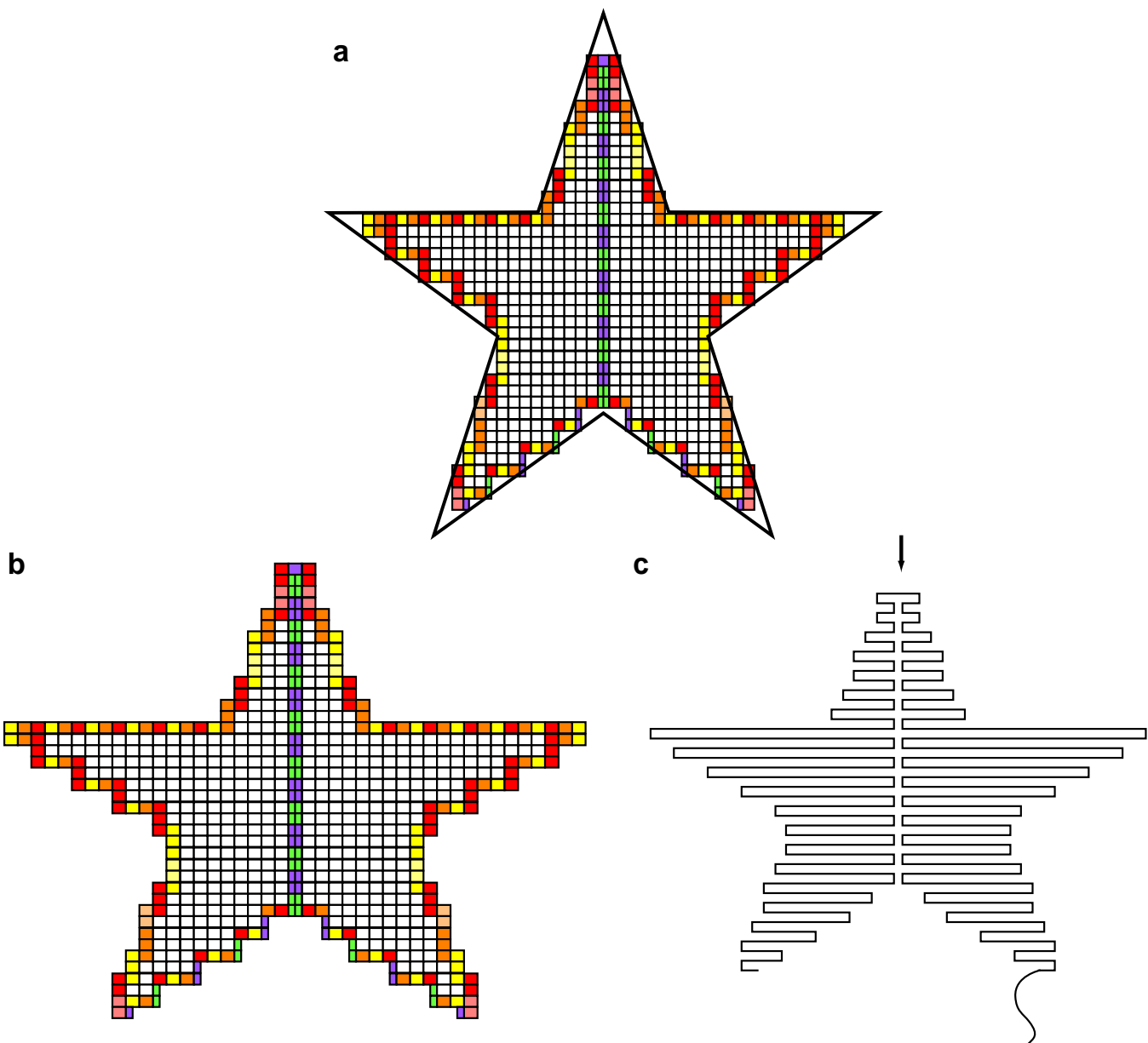


Supplementary Figure S20: Crossover diagram for the rectangle.

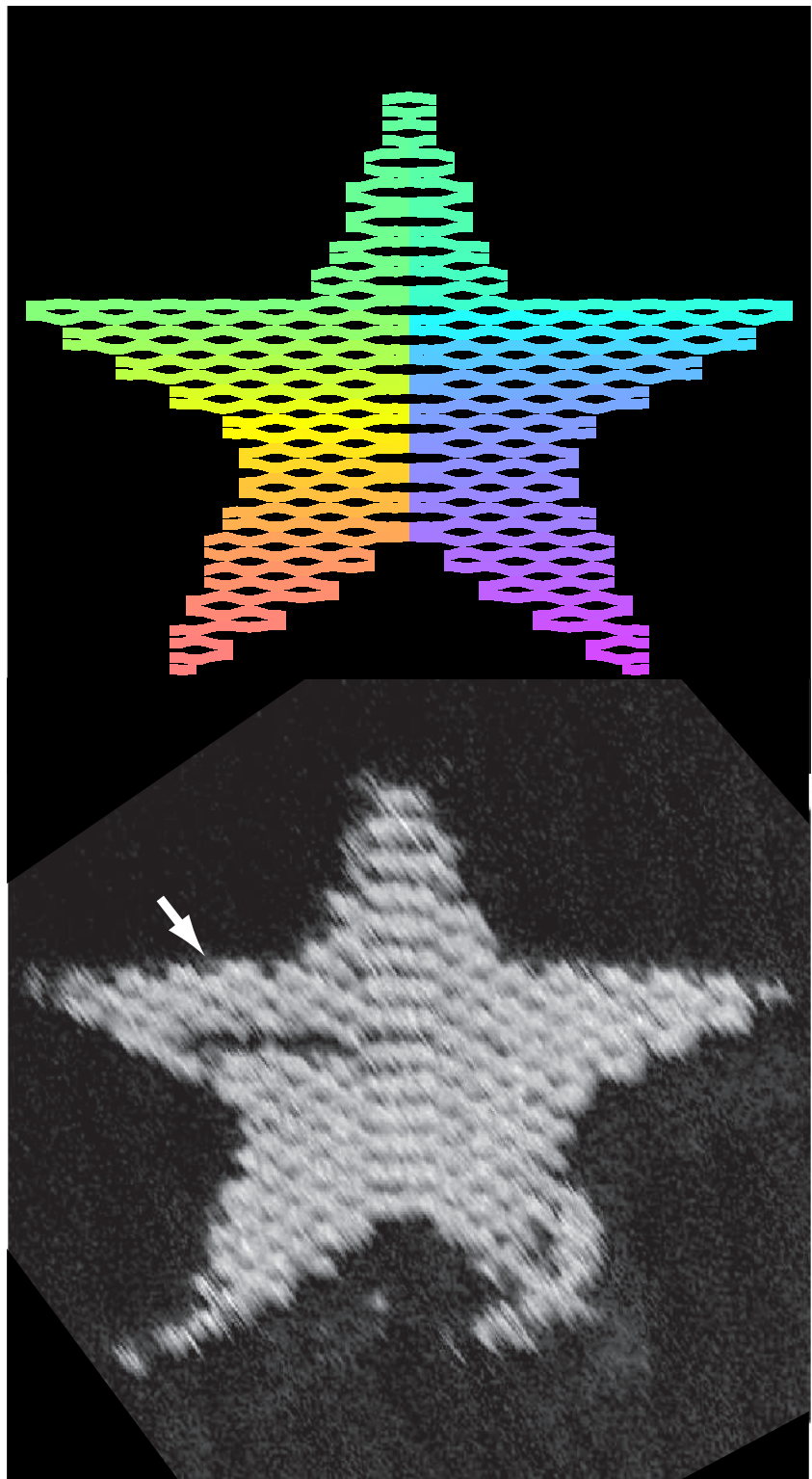
Plate number: 2  
r-9t0f, A1, TATACTGATAGCCGGCGCTGAG  
r-9t10f, B1, GCGGATTAGCTTACCGGTATTTAAATCAGA  
r-9t12f, C1, TATAGAACGCCAAAGGGTAAGTGAGAATA  
r-9t14f, D1, TAAAGTACCGGGAGAAAACCTTTATCGCA  
r-9t16f, E1, ACAAGAAAATTCATTAATTACCATCAC  
r-9t18f, F1, AAAAACAAATTCATCATATAATTCTACAG  
r-9t20f, G1, GTGGCAAATTAATCATTCGTCGACAAATTC  
r-9t22j, H1, AAACCCCTACCCATAAAGGGATTCACGCACAG  
r-9t2f, A2, AGGGTGAATAATTCATTAAGGATGATTC  
r-9t4f, B2, ACAACAAAATTCATTCAGGCGACGATGAG  
r-9t6f, C2, AGGCGCTTAAAGGTGGCAACATAGTAGAAAA  
r-9t8f, D2, TACATACAGGGAGGAATTAACCTACAGGAA  
r-1t0g, E2, TGAGTTCTGCTACAGGATCAACAACTTATGTA  
r-1t10e, F2, TTAAATTCGCGCAAGACTTCATTCAGGAG  
r-1t10f, G2, AAAGAGAACGACCTTAAAGCGGAATGATCATT  
r-1t12e, H2, TTTCATTTGGTCAATAACCTGTTAATCAATA  
r-1t12f, A3, TCGAAATGGGGCCGAGCTTAAATATGTGT  
r-1t14e, B3, AGACAGTCATCTAACAGGATGAGATTCATAT  
r-1t14f, C3, AGTAAAGAACATTCACATCAATAATTAATT  
r-1t16e, D3, GCTCATTTGCCATTAATTTAGCTTCTAGA  
r-1t16f, E3, GTTAAATTTAAACCAATTAGGAACCCGGAC  
r-1t18e, F3, TTGCGCATTCGGGAAACAGGGAAACAGTAC  
r-1t18f, G3, GCTCTGGTCAGCTGGCAACTGTGTATTC  
r-1t20e, H3, GCATAAGGTTCCACACACATCAAGAACAACT  
r-1t20f, A4, GCTCACATGTTAACGGCTTCTGGGGTTTGGC  
r-1t22e, B4, CGGAAATCCGAAAATCTCTGGTTAAATCCAG  
r-1t22f, C4, CCAGCAGGGGAAACATTCTTAAAGGCC  
r-1t24e, D4, GAACCTGGCGAGAAAGGAGGGGAAACAACTAT  
r-1t2e, E4, CTAAACATCAGCTTCTTCAGAACAGT  
r-1t2f, F4, TCCTGTTAGCTGATACAGTAGTCAC  
r-1t4e, G4, CTACATTTGGCACAAGAATCACCCTCTCA  
r-1t4f, H4, AAACGAATGACCCCGGGCAATTCTTATCATAC  
r-1t6e, A5, GAATAAGGCTAACAAAGCTGCTGGACGAGAA  
r-1t6f, B5, CCAAATCATCTGGCTTGGAGAACGCC  
r-1t8e, C5, CATAACCGGGAGCATAGTAAGAGCTTTTAAG  
r-1t8f, D5, GGAATTAAGCTTCTTACAGCAGCAAAAGATT  
r-3t0g, E5, TGAGACATTCACAGACGGCTTCTTC  
r-3t10e, F5, GAACCAAANAAAGCGGATTCAGATAGAAAA  
r-3t10f, G5, TCAAGACCTTCAACAGCTCAGATCTGGCA  
r-3t12e, H5, TCAATTCTTTAGTGTGACCATTAACCGAGC  
r-3t12f, A6, CGAGTAGACTAAATAGTAGCTAACACCTCTCA  
r-3t14e, B6, ACCGTTCAATAGCCTAGCTGGAGGTTGGCA  
r-3t14f, C6, TATATTTCAGCTGATAAATTATGTTGTTAA  
r-3t16e, D6, AAATAATTAAATTTAGTAAACCTGATATTC  
r-3t16f, E6, GCGAAATTCGCGCTTCGGCTTCCTGGCC  
r-3t18e, F6, GGCGATGCGCTTACCGACGAGCTTGGCCATCA  
r-3t18f, G6, GAAGATCGGGCCGGCTTCCTGGCAATCTGG  
r-3t20e, H6, CTGACTCTTCTCTCTGGTAAATTGGGAG  
r-3t20f, A7, TCTAGCTACTCATTAATGGCCCTTGAGA  
r-3t22e, B7, GATAAGCCGAGGCGCTTACGGCTCTTA  
r-3t22f, C7, GAGTGGAGGAGGAGGAGGAGGAGGAG  
r-3t24e, D7, CCCGATTATGAGCTTACGGGGAAATCAAAA  
r-3t2e, E7, CAATGACTCATCAAAAGGACCTTACACGCC  
r-3t2f, F7, AAAAAGAACCATCCCTCCACGGGGTAA  
r-3t4e, G7, GCGAACATGCGCATCTACGGAGATTCTGCGA  
r-3t4f, H7, ATACGTAAGAACATCACGGAGATTCTACAG  
r-3t6e, A8, AGCAGTAAGCAACAGGCGATTAACCAAGC  
r-3t6f, B8, ATGAACTTTAATGGCTTGGAGAACATACCA  
r-3t8e, C8, CAAAATATACTGACATACATAAACCCAGA  
r-3t8f, D8, CATTACAGCGGAGGCTTCTGCTATTATAG  
r-5t0g, E8, CCTAACGATCTAAAGTTTCTGCTGAATTCTGG  
r-5t10e, F8, TACCTTTAGGTCTTACCTCCAGAACAGA  
r-5t10f, G8, CAAAATCATCTGCTCTTGTATAAGTTCT  
r-5t12e, H8, CTAATAATCATACAGGCCAGGAC  
r-5t12f, A9, TCCCATATACAGGCCAGGAC  
r-5t14e, B9, GTGAGCTAGGATAAATTCTTGTGAGGATC  
r-5t14f, C9, CAAAGGAAATTCTTGGAGGATCTCTGATATC  
r-5t16e, D9, CTTTACATCCCCAAAACAGGAGACGGAG  
r-5t18e, E9, GAAAGAACCATTAATGCGATCTGGCA  
r-5t18f, F9, CAGCTGGCGGACGACGAGCATCTGAC  
r-5t18f, G9, GTTGAGGAAAGGGGGATCTGGTAGAGGATC  
r-5t20e, H9, ACTCGGCGGCCGAGCTTCAATTGCT  
r-5t20f, A10, CCTGGGTACTTCTCAGCTGGGAAACGGGAC  
r-5t22e, B10, AGTTTGGCCCTTCACGGCTTGTGGCTC  
r-5t22f, C10, AGCTGATTACAGAGCTTCTGATGTT  
r-5t24e, D10, GTAAAGCCTAACTTACGGAACCAACTTGT  
r-5t2e, E10, ATATAATTCTTTCTTCAGTGAATAGTTAG  
r-5t2f, F10, AATAATAAGCTGCTGGCTTACAGAACACT  
r-5t4e, G10, CGCGCTGTGGAGTTCTTCAATTAAACATAC  
r-5t4f, H10, TTTCATGAAATTGTGTCGAAATCTGTACAGA  
r-5t6e, A11, TTCAACTATAGCTGGCTGCGACCTTGT  
r-5t6f, B11, CCAGCGCTTACATCATTCGTAATAGCGGT  
r-5t8e, C11, TTGGCAGATCAGTGGAGATTGTTGGTTAA  
r-5t8f, D11, AAAGATTCTGGGGTAACTGAAACATTAAT  
r-7t0g, E11, AGCTTAACTGATGTTCTTACGGAG  
r-7t10e, F11, TTTTGGCGAACAAAAGGAGAATGT  
r-7t10f, G11, AAACAGTTGATGCTTGTGAGCTTAA  
r-7t12e, H11, CAAAATTTAGTCTGGTGTGGAGGAGCTA  
r-7t12f, A12, TGCACACTAACATTAACGGCTTGT  
r-7t14e, B12, CTGGCTGAGCTTCTGGGGAGAACAGGATT  
r-7t14f, C12, CTGTAATTCTGCTGAGCTGTC  
r-7t16e, D12, ACCGGTCTGCTTACGATCCGGGAAACAGGCTA  
r-7t16f, E12, CATGTCAGATCTGGCTGGGAAACGGTGT  
r-7t18e, F12, ATTAACTGGCTGATCATCAAGCTGGAGTAA  
r-7t18f, G12, TAGATGGGGGATCAGCCGGGGTTCTGG  
r-7t20e, H12, GCGACCTGGCTTCTGGAGCTTCTACAGGG

Plate number: 3  
 r-7<20f, A1, CTGGCATGATTAATGATCGGGCCCCAGGG  
 r-7<21e, B1, TTGGACTCTTCCTTTTCAACCTGAGAACCTGTCTG  
 r-7<22f, C1, TTGGTTTTTAACTGCAAGGGCGAACACCATC  
 r-7<24h, D1, ACCCAAATCAAGTTTTGGGTCAAGAACG  
 r-7<2e, E1, AAAGGCCAAGAACAACTAAGACCTTCCAG  
 r-7<2f, F1, GAGAGATGCTTTCGGCGATGTCGGTAGACA  
 r-7<4e, G1, GCTCATGAGAGGCTTGAAGGACTAGGGATT  
 r-7<4f, H1, ACGGCTACTTACTTACCGGCTTGCGTACCAA  
 r-7<6e, A2, CAATTTAGAGACGATAGAAGCCGGCAGCCT  
 r-7<6f, B2, CTGGAAAAGACTGCTTCATTAATAA  
 r-7<8e, C2, ACTGGATAACCGGAAACACATTACCTTATG  
 r-7<8f, D2, ACGACTAGCTCCATTACTCGGGAATGCTT  
 r-9<10e, E2, ATATAATGCTTGAATCCCCTCAATCGCTCA  
 r-9<11e, F2, CTGAAATCTCTGATGCTTCAACATGATTGCTGA  
 r-9<14e, G2, AGAGAATCTGGTTGATCAACAAACAGCATAA  
 r-9<16e, H2, GATTGACCGATGAGCCTTAATGCTGAGAACAA  
 r-9<18e, A3, CAGAGCTGTTAATGGTAGTGGCAACCGCG  
 r-9<20e, B3, GGGAGAGGTAAAAACGACCGCATTCCAGT  
 r-9<22e, C3, TATCAGGGGGTGTGCTTATGGGACCGCG  
 r-9<24e, D3, CGATGGCCCTACAGTCAACAGCT  
 r-9<21, E3, CGAGGAAACACTTCTCAAGCTTCTGGGATTTCGAAAC  
 r-9<4e, F3, ACGGCTAACAGCACCTGCGAACAGGCCCTCA  
 r-9<6e, G3, GAGCGTGTCTGATAGGGAACCCGGAG  
 r-9<8e, H3, TAAATATGGAGAAAATCTACGAGCAGCTCA  
 rt-rem1, A4, AACATCCTCTGGCTGAGTAAAGACT  
 rt-rem2, B4, TGATGCAACTACTTCTGGTATTGTAAT  
 rt-rem3, C4, AGCTGTCATCACCGGAAACCTGG  
 rt-rem4, D4, ATAACTAGTGAAGGCCAACCGGAAAG  
 rt-rem5, E4, ACCCGAAATCTCTGGAGGTTT  
 rt-rem6, F4, TTAAAGGGATTTCAGAACAGGCG  
 rt-rem7, G4, AGAGCGGAGCTAACAGGAGGCG  
 rt-rem8, H4, TATAACGTGCTTCTCTGGTAAATC  
 rt-rem9, A5, GACTATGGTTCTCTGGTACAGCAGC  
 rt-rem10, B5, CGCTTAACTGGCGCTACAGGGCGC

Supplementary Figure S21: Sequences for the rectangle.



Supplementary Figure S22: More design details for the star **a**, Original block diagram assuming that each block (1 turn of DNA) would have an aspect ratio of roughly 1:1 (3.5 nm per turn:3.5 nm per helix) based on the inter-helix gap for 2.5 turn spacing. In reality 1.5-turn spacing appears to have a ratio of roughly 1.2:1 (3.6 nm per turn:3 nm per helix) and so the stars were somewhat squat **b**. **c** reproduces the folding path for reference. In **a**, turns that occur between columns of red blocks and orange blocks have offset 0 with respect to the underlying crossover lattice. Other turns on the left and right outer edges have +1 or -1 offsets depending on which side of the star they occur. Purple and green half-blocks show that turns (in the scaffold) made on the seam or on the interior of the bottom left and right star arms are made an odd number of 1/2 turns (DNA half-turns) away from turns (in the scaffold) on the outer edges.



Supplementary Figure S23: Crossover diagram for the star (top) and high resolution AFM (bottom, taken by E. Winfree) which shows the crossover structure in great detail. Defects are probably tip damage. White arrow points to a section of helix that does not image well and appears to be a hole. On edges where helices can move unimpeded by neighbors helices often disappear at high tapping amplitude.

Plate number: 1

s10t15f,A1,AAAGACAAGCAAGGCCGGAAACGT  
s10t17f,B1,AGAGAGAACCAAGAAATTGAGTCCAGGGC  
s11t14e,C1,AGCACCAATTACCATTAAGGGCG  
s11t16e,D1,CATTCACATATCAGAGAGATAACTAATA  
s11t18g,E1,AAACAGGGAAACAGCAAGCCGTATTACCGCACTATCGAG  
s11t18h,F1,AAAGGCCATTAGACGGGGGTAAATGAGCGTAGATTGAG  
s12t17f,G1,AGAGGGAAACAGCAAATACCAAGT  
s13t14e,H1,ATTGGGAATTAGACCGTAAATA  
s13t16g,A2,TGACGGACCTGACAAAGTCAGAAAGATTAACTGACAC  
s13t16h,B2,AATTATTCAATTAAAGGTACCGACATTGAGCC  
s14t15b,C2,ATCACCTGAAT  
s10t18,D2,TATAGCCGGATAGCTGTATCCTACTA  
s10t19,E2,CCTTCAGGGAAAGCGCAGTCCTTCAACAG  
s12t21,F2,CAGGAGGTACCGGGCGCAAAGAG  
s14t14,G2,CCAGGCCTTTCATATAAATAATTATCGG  
s16t15,H2,ATTAAGGGGACCCGCGCTGC  
s18t18,I3,TTAAGACTGAACTAAAAGAACCGCG  
s18t20,J3,ATTTAGCTGTATTGGACCCGAACTACAT  
s17t21,K3,ACTTAAATTATTTAGTTAACTTACCAAAA  
s17t24,L3,AATTTCCTCTGTAAATCCTGCGAGATCT  
s17t26,M3,TTGAATACCAAAAGCAGTCCAAATCAG  
s17t28,N3,ATGATGGCTATCATATTCTGGGGAGCA  
s17t29,O3,ATTAAGGGGATATGCGCCCTCTCA  
s17t30,P3,ATCTTAAAGGTAAAGGAAATTAGTTGAA  
s17t32,Q3,GGCGGAACGTACAGTGGCAACTAACATTCTTAA  
s17t41,R4,BTACAGGTTAGATTAGCGGGGCTCTCAGA  
s17t61,C4,TTAAGGGCTATTATTCAGAAACAGTACCGTA  
s17t61,D4,TTGAATTAAGGTTAAAGGGCGCTAAAGCA  
s21t11f,E4,ATCGAGCTCATTAAAGCGAGATAAACGGC  
s21t13f,F4,ACCGGCCCTCCGGACAGACTGGCGAG  
s21t15f,G4,CCAGTATATTAGCTGTGGCCACACCAGGG  
s21t17f,H4,CAAGCTTAAACGAAATAACGCTTAA  
s21t19f,I5,AAAGCGCTTAAATCAAGGTTAACTTAC  
s21t21f,B5,TTGAATTAAGGTAAGTAACTTCTTAATGCA  
s21t23f,C5,CCTTGAATTAAGGTTAACTTAAATAATTAGT  
s21t25f,D5,AAATTCGGAGTGAATACTTCTCTTAA  
s21t27f,E5,AAATATACTTACATGGGAGAACAGTTAC  
s21t29f,F5,GGAGCACTCGAGGAGCGGAATAATTCATC  
s25t5g,G5,CAAGAGAAAGGA  
s27t5h,H5,TGCCCCAGTTAA  
s27t7g,A6,GTATAAACCTGCTATTGGAGACTCT  
s27t9h,B6,ATGATACCTTTTG  
s27t9f,C6,ATACATGGCAGGAGTGTACTGGTACAGTCCC  
s31t10e,D6,AAACAAACAAATAATTACCTTGGCT  
s31t12e,E6,TOATATTCCACCCACCTCAGAGGCCCTCAGA  
s31t14e,F6,GGCCGCCACCGGTCTAGGCCCTTGTAGCAA  
s31t16e,G6,AGTAGAACAGAGGAACAGCGAGGAGGT  
s31t18e,H6,CTTTCAGGGAGTTGAACTCTGTGTTAT  
s31t20e,H6,AAACAAATATAAAAGTACCGAACACCGCGT  
s31t22e,B7,GTGATAAAAGCAAGAACCGGAGACATACG  
s31t24e,C7,ATAGCTTAAATCAATTAATGTCAGAGGC  
s31t26e,D7,GAATTATTACAGTAACTAGCTCTCTGTG  
s31t28e,E7,TTTGGATTGGAGAACAGAAACCAAAACACTA  
s31t30e,F7,ATGATTTACATCAATCTGTTAGCGCTA  
s31t32h,G7,AAACATCGATTTGAGTGGCTATTAGTCCTTAA  
s31t34a,H7,ATGGAACAGCTC  
s41t13g,A8,TCACCCCTCAGA  
s41t15g,B8,CATAAAGGTTTCATGGCATTTCCTCAGAACCG  
s41t17f,C8,TTGCCAGTAGGCCAACAAAGTACATACATA  
s41t19f,D8,CTGAAACACCCCTGACAGGCGCTTAA  
s41t21f,E8,TAATAGGCGTAAATAGAGAGATAACTC  
s41t23f,F8,CCTGAGATGCAAATCCAATCGCATAAAGGCT  
s41t25f,G8,TTACCTTGAATTAAGGAAACAGTACGATTAAGA  
s41t27f,H8,GAATAATTAACCTGATGAACTATCATTAA  
s41t29f,A9,ATAGATATAACATTAATTCATTGATACCT  
s41t31f,B9,ATACCGACTCAATAATCAACCGAACGCTC  
s41t33f,C9,ATTTCAGACCTGGCACAGAACATCCATTAA  
s41t35f,D9,CATIGCAACAGAAAATACTCC  
s51t14e,E9,GTCAAGCTGTAGCGCTGGCAACA  
s51t16e,F9,TTAAAGAAAGGAGAAAGTACGAGTAA  
s51t18e,G9,AAACGCCCGAGGGCTTTAGCGGGAAAAATA  
s51t20e,H9,ATATCCCAGAGGCAATTGGCAAATAAAC  
s51t22e,A10,CGCGAACATTATGAAATGCGAGAGTC  
s51t24e,B10,TAATGAAATTGAACTTCTTGGAAAGA  
s51t26e,C10,AGATGTCCTGAGTTTCAAGGGTT  
s51t28e,D10,AGAACCTAATTAAAAGTTGAGATACATT  
s51t30e,E10,GAGGATTTCATCAGCTGGACAGAACCA  
s51t32e,F10,CGCACAGCTGAAGCTAAAGATGCTCA  
s51t34e,G10,GTCTGAAACAAATTACGCCAGC  
s51t36a,H10,GACTCTGTAAA  
s51t15f,A11,AGACACCAAGGAGTTGGCTTACAG  
s51t17f,B11,TATCCCCAACCGAGGCCCTTTAAACGCCA  
s51t19f,C11,TACGAGCACCGTATTCTAAGAACATATT  
s51t21f,D11,TAGAAAACCAACTGTAATTAGTCCTAATT  
s51t23f,E11,ATCATGGGGTTGGTTATAACATAATTAC  
s51t25b,F11,ATTAATTAACAA  
s51t25f,G11,ATCAAGAATCATTAACATTCTTATCAA  
s51t27b,H11,TTAAACACTGACAG  
s51t27f,A12,AAATTAGGAAATAAGGAAATTGAAACAAAC  
s51t29f,B12,TAGACTTTGCCGACGTTATTACCATATCA  
s51t31f,C12,CAGAGGTGAATGAAATACTTAAAGAGAAGTAT  
s51t33f,D12,TTACATTGATGACGGCTCTGACAGATAAAA  
s51t35f,E12,CGAACATTCTGGTAAATCCAGAACATGGATT  
s51t37f,F12,TCAGTAGGGCACCGACTCCATCA  
s51t34e,G12,TCAGTAGGGCACAGAACTGGAAATA  
s51t36e,H12,TTTATTAGGCAATAGCTATTCTTCCAAATA

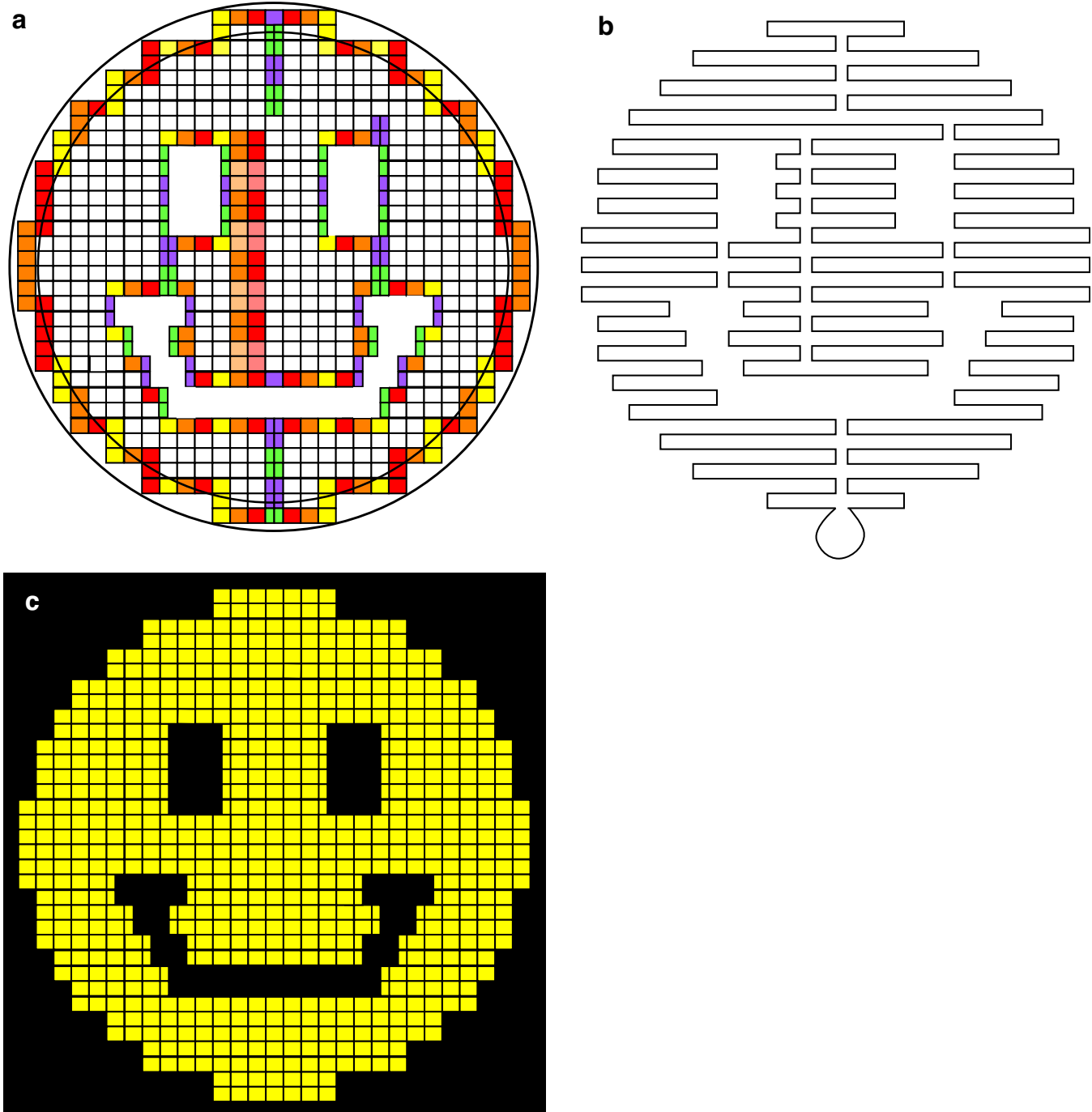
Plate number: 2

s7t18e,A1,AGAACAGAGATATAAGGCTTATTGAGAAA  
s7t20e,B1,CCAACTAACGGCCATTAACTAACAGCGCTT  
s7t22g,C1,AGTATCATTAACTCCCGCTTAACTCGAGACTACCTT  
s7t22h,D1,ATGCGTTATACAAATTGGCTTAATGAGAATCTAATCGC  
s7t28e,E1,CTCGTATTAACTCTTACAAACAA  
s7t30e,F1,TTGACAACTGAGAACGAGCAGCAAGCGGTC  
s7t31e,G1,AGTATTTAACTTCTGGCAACAGAGGCAATTG  
s7t34e,H1,ACAGTCACAAACTATCGGCTTGAACCGTTG  
s7t36e,A2,TGCAATAAGAAGTGTTTTATAA  
s7t38a,B2,AATCACTGGTAG  
s8t15f,C2,TCATAGAGATGAGCAGCGTAA  
s8t17f,D2,TTAACCTGCGAAAGAACATTCATGTC  
s8t19f,E2,TGCTTTCAATAGCAAGCAAATCATTGTTG  
s8t31g,F3,ACAGTGGCTCAG  
s8t33h,G2,ATTAAGGGGACCCGCGCTGC  
s8t35b,H2,CACTTGTAACT  
s8t35g,A3,ATTAGTAACCTGAGTAGAGAACCTACGACAGTA  
s8t37f,B3,CTAAACAGGTGGCCAGAACCTCTCTT  
s8t39f,C3,TATAACGTCCTTCTAGCGGGAG  
s9t14e,D3,CCAACTAACCATAACTTATCAT  
s9t16e,E3,ATGTTTTAAAGGCGAAATAAGAAGAATG  
s9t18e,F3,AAATAGCAAACTTACAGCGGCCCTTATCAT  
s9t20g,H3,CGGTATTAAACCAAGTTATTCTCATGCTAGGGCTTAC  
s9t20h,H3,CGGTATTAAACCAAGTTATTCTCATGCTAGGGCTTAC  
s9t36e,A4,ATTTAGACAGAACGGCC  
s9t38g,B4,TTAAGGGCTTGTGAGCAGCGCGCTACTATGGT  
s9t10f,C4,ATTAATTGACCTATGCACTAC  
s9t17f,D4,TCATAGCTGCTTAACTACAGTATCGCTG  
s9t11e,E4,AAAGCACCACAACTAACAGGAGA  
s9t11g,F4,TTTACAGGAGCTTGGAGAACACATTATTACAGG  
s9t12g,G4,TTAAGGAAACGGGAGATGCTCATAAAGAGAAG  
s9t15f,H4,AAAGTACACGAGGCAAAG  
s9t17d,I5,AATACATAAAACCTCCAGCTTATACCAA  
s9t18g,B5,AAAGCAACTACAGGGAAAATCTAGTTAATGCGGAA  
s9t14t5a,C5,TCGCCCCCT  
s9t11o,D5,TTGTAGGGAGTGGAGATAAGAAGTTCAGTT  
s9t11i,E5,TTTCAGGGCTTCTGAAACACTGAAATTAC  
s9t12e,F5,GAATAATTCTGTGTTCTAGCATGACAC  
s9t11e,G5,CCTTAAATGAGGCTTAAAGGCTTCAGGCT  
s9t14e,H5,AAACATCGCTTGTAGGGAGTTAATGCTG  
s9t14i,A6,TGCGTGGCCACRCGCATAACCGATCAGCG  
s9t16e,B6,CTTCATCAACCAAAATAACGTAATGCTT  
s9t16i,C6,TATTCTATTAGAATCTTCTGAGCATGATG  
s9t18e,D6,CAAAGAGTGGAGAACCCCCAGATGGTTAGTTGGA  
s9t18i,E6,AAATTTGGTTCTGGAGGGCTCAAAAT  
s9t20e,F6,TAATGCTTCTGAACTTACAGGCT  
s9t20i,G6,GTTTAAAGAAATAATGCTGTTAGAAACAC  
s9t22e,H6,AGAGCATACCTGTAATACTTTGAAATTAA  
s9t21f,H7,CATTATGCTGTTGAGTTCTGTTCTG  
s9t24e,B7,TGCGGAGTATCAGGGTATTCTTCTT  
s9t24f,C7,AAACAGGCTGAGTGTATTGTTAATT  
s9t26e,D7,TAATAATTCTAACCTAGAGCGGCCCATC  
s9t28e,F7,TCACCTTGTGGCATAGGAGATTGGTT  
s9t28i,G7,CGACAGTAGCATCTGCAGTTGATATTAC  
s9t21i,H7,GAACCCCGGAGGTTTACAGGCGAGGGT  
s9t13g,A8,CGCGAGGGCAGTGCAGCTGAGCTCAGTCCC  
s9t31j,B8,ACGAGCGCTTTCAGGCTACAGGAGGTT  
s9t32h,C8,CGTTCCAGTCGGGAAACCTCTGCTCCATT  
s9t14g,D8,CTCATTTTC  
s9t14i,E8,GCACACACCCATCAGAACCGCTTTC  
s9t16i,F8,ACACTGAGCCATTAGGAACCCATTGAAAGTA  
s9t18e,G8,TCACAGATTTGCTGTTCTGGAGATTTC  
s9t18i,H8,TCTAAAGTCAGCCCTTACAGTTGCTG  
s9t21f,A9,ATAAATTGGAAACAACTAAGGAAT  
s9t21f,B9,CGCCGACACTTCCTGGAGTGTGCAATA  
s9t21f,C9,GCATAGGCGAGGCCCTTGGGGAGTAGTTG  
s9t21f,D9,TAGCGAGAACAAAGCTGCTTACAGGAGC  
s9t21f,E9,C9GATGCAATACTGGGAATCTGTAACAAAA  
s9t21f,F9,TAAGCAATGGTTGCTGAGGTTCTCATT  
s9t23f,G9,CTAGCTGACGGAGAACGCTTATACAA  
s9t25f,H9,AACTTAAAGAGGCTTGGAGAACACCGTT  
s9t27f,I10,TGATGATGCTCATATAATTGCAAATTGTA  
s9t29f,J10,CGATTTAAAGGCGACTCCAGCGCAGT  
s9t23i,K10,CTGGTTGCTGGCATGGCTGACTCTGCAAGG  
s9t25g,D10,GGGATGCAACTTGTGACCAGTACATGAGCAT  
s9t27a,E10,AACGCCAACCTAC  
s9t29a,F10,GTAAATACGTTA  
s9t31g,G10,ATTCTCTTAAAC  
s9t31e,H10,GGTGTACAGTAATAAGGCTTGCCTCAGACG  
s9t31e,A11,ACGATAACACAAATAATTCTGACCTT  
s9t32e,B11,TAAGAGGTATTCTGATATAACAGT  
s9t32e,C11,AAAGATTTCAACGCAAGGATAACCATCAAT  
s9t32e,D11,ATGATATTCAGAGAATGCTGAGATATAAGC  
s9t32e,E11,AAATATTGCTGCTGCTTCTGCTG  
s9t32e,F11,GGATAGGTTCCGGCACCGCTTCTCGAAAG  
s9t32e,G11,GGGATGCTGAGGATTCCTGGAGTGTG  
s9t32e,H11,GCTAACTCCAGCTGCTTAAATGAAACAGCGG  
s9t34b,A12,CCCCAGGGTTG  
s9t34e,B12,TCCAGCTCAGGGAAAATCTCTG  
s9t41g,C12,ACGTGATACATCGTCACTCCAGCAGATGAC  
s9t41f,D12,AAAGGACCGCGAAAGACAGCATG  
s9t41f,E12,GGATAGGTTCTGAGGAGAACACCAACTTGA  
s9t41f,F12,TAATGCTTACCCCCCTAAATGCTTACATAC  
s9t42f,G12,ATCATACAGATCCAAATTCTGGAGTACCTT  
s9t42f,H12,TCAAATCAAATTGTTAGAAGCCCTTCAATAA

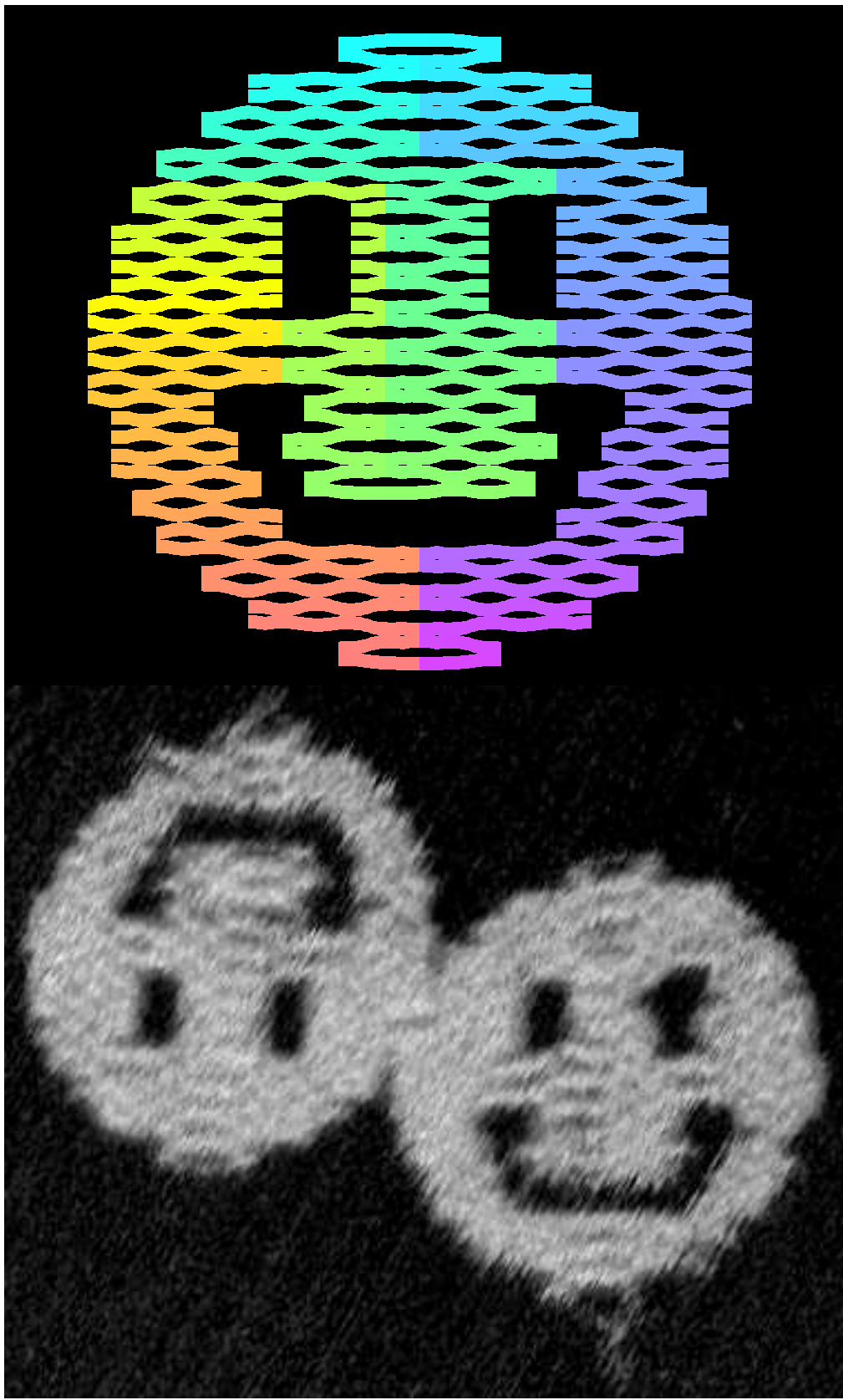
Plate number: 3

s-4t25f,A1,GGAAGATTGGTAATCGTAAACCTGGAGACAG  
s-4t27f,B1,CCGATTGAGCAGCGTTTCTACACAAAAAAC  
s-4t29f,C1,GCCAGCTGGTGGCGGAAACAGGACAACCG  
s-4t31f,D1,GGTGCTTACCGAGCTGAAATTGGCTTATTAC  
s-4t33f,E1,GAGTTGCTCATCGGCAACCGCGGAAAGCTGG  
s-4t35f,F1,TTGATGTTGTTGTCGACCTGAGA  
s-5t16e,G1,GAACGAGGGTAGCAACGGGAACCG  
s-5t16e,H1,AACTGACCGAACAGTAAATTAGTAGAAGA  
s-5t18e,A2,GCACACCTTAAACAGTTCAGAACAGCTGAG  
s-5t20e,B2,GAATTGAGAACGAGTAGATTAGTAGTAG  
s-5t22e,C2,CATTAACACATATTTAAATGCAAGGGT  
s-5t24e,D2,GAAGGGCAGGATGTCATCATATAATACAG  
s-5t26e,E2,AAAAGCCCCATAATAGTGGCGGAGGATT  
s-5t28e,F2,CCTGGGGACAAAGCCGCAATTCCCGGGT  
s-5t30e,G2,GCCTCTTGTAACTATGCTGATAGGGAAC  
s-5t32e,H2,AAAGTGTAGAGGGCTTGGGGTCCCT  
s-5t34e,A3,CGGCTTGGTAATCGGCAAATCCCTT  
s-5t36b,B3,AAACACGGGG  
s-5t36e,C3,AACTGCACTGCTATCGGGCAT  
s-6t15f,D3,AATCATAAAGCTACAGAGCTT  
s-6t17f,E3,ACAGGGCAGGGCTTGGAGTTAGACGTT  
s-6t19f,F3,AACTCCACAGAACATGACATAAAAGGAA  
s-6t21f,G3,CTACTAAATTGACCTTAAAGTACAGCG  
s-6t25a,H3,CCTGGTGTACCC  
s-6t26a,I4,AACTGAGCTGTT  
s-6t29f,B4,AGGGCGATATTAGCTGCTGCAAC  
s-6t31f,C4,TACGAGCCCTTGTCTGTGTAATGTTGG  
s-6t33f,D4,AGCTGATTATTGGGGCCAGGGTACAC  
s-6t35f,E4,AAAGAACGTTAAATCAAAAGATCGGAA  
s-6t37f,F4,CTACTAAATTGACCTTAAAGTACAGCG  
s-6t38e,G4,AGGACTAAAGACTTTAGCGGAA  
s-6t39e,H4,CGAGGGCAATTTCACAGTAACTGAG  
s-7t18e,C5,AACGCCAAATCAGGTTCAACAGG  
s-7t20g,B5,AAACAGACTTCCGAAATGGTCAACAGG  
s-7t22g,C5,CTAGGTTGAGTAACTGCAAGTGGT  
s-7t30g,D5,ATTGTTATCC  
s-7t36,E5,ACAAGGACTCATCCCCAAATCAAGATCGGA  
s-7t38b,F5,CCGATTGAGGCC  
s-7t38e,G5,CTTAAAGGTTAGAGCTTGGGG  
s-8t15f,H5,TGTTACTTTCTGAGGAATTTC  
s-8t17f,A6,ACTAATGCTGTTGTAATACCTTACTGCT  
s-8t19f,B6,TTTGAGCCTTACCCCTGACTTACATT  
s-8t31h,C6,CTCACATTGGTTTCTT  
s-8t33g,D6,CACCAAGTGAAGACCCCCAGATGGTTAGTTGGA  
s-8t35a,E6,TGTTCCAGAG  
s-8t37f,F6,AGGACTAAATTGTTGGGGT  
s-9t14e,G6,ATTAACCGGGTAAATGTCGAA  
s-9t16e,H6,TCGGCAGTCTGAGTTTAAAGACTGAGTT  
s-9t18e,A7,AGGAATACAGTCAAGGAAACAGGAAAGACTT  
s-9t22g,B7,ATTTCATTGGGGCTAACCTGTTAGCTT  
s-9t40g,C7,CGAGAAAGGAGGGAAAGCCGGGAACGTTG  
st-rem1,D7,CGCTTAATCGGCCGCTACA

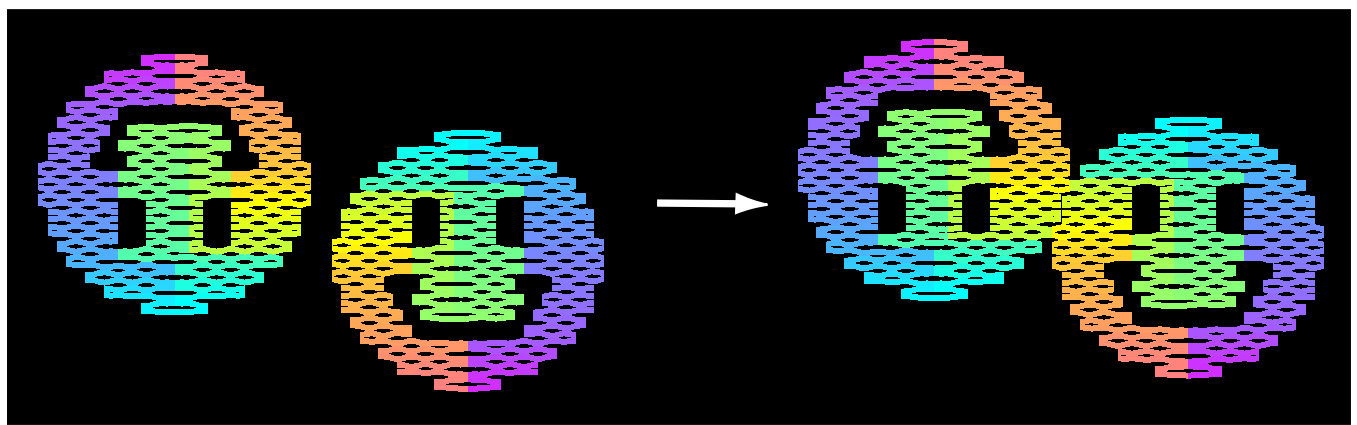
Supplementary Figure S24: Sequences for the star.



Supplementary Figure S25: More design details of the 3-hole disk (smiley). **a**, Block diagram. **b**, Reproduction of the folding path. **c**, Block diagram with all colors and notations removed. In **a**, turns that occur between columns of red blocks and orange blocks have offset 0 with respect to the underlying crossover lattice. Other turns on the left and right outer edges have +1 or -1 offsets depending on which side of the smiley they occur. Purple and green half-blocks show that scaffold turns made at most seams or on the interior of voids are an odd number of  $1/2$  DNA turns away from scaffold turns on the outer edges. A pair of columns with alternating light and dark orange and red blocks marks a seam of 0 offset, placed 1.5 turns to the left of the central seam.



Supplementary Figure S26: Crossover diagram for the disk with holes (smiley) with a high resolution zoom out of Fig. 2:d<sub>3</sub> for comparison of fine structure. Some tip damage has occurred to the right eye of the righthand smiley.



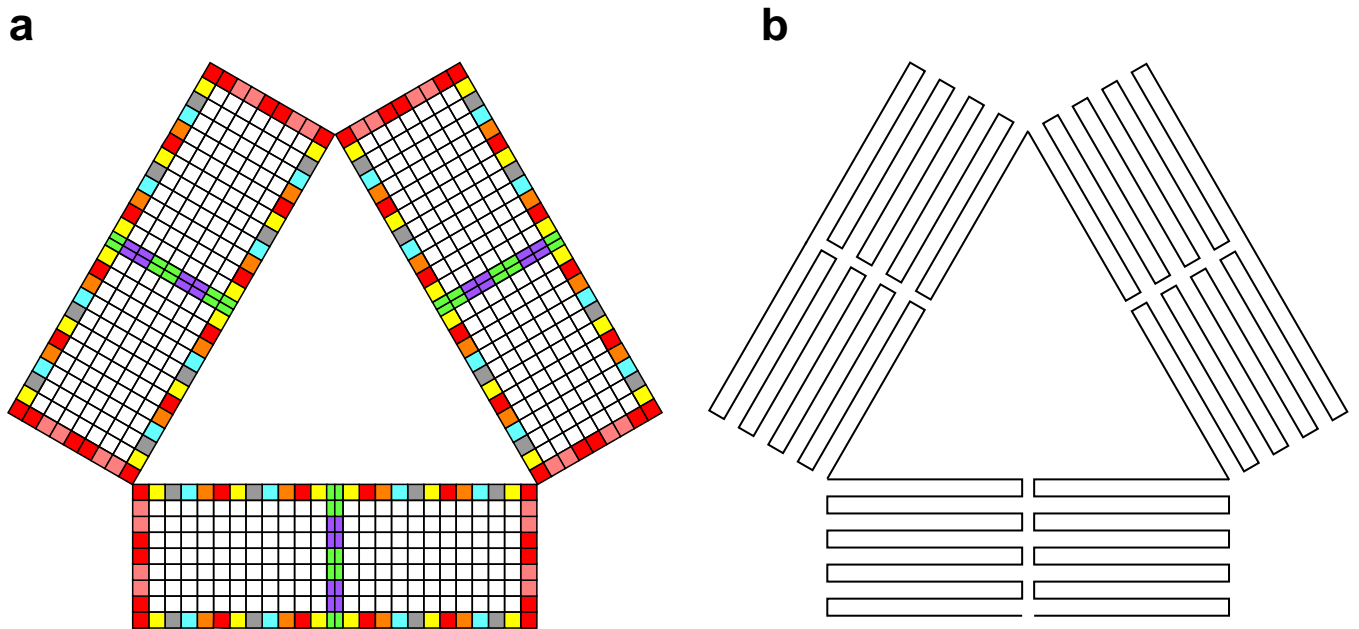
Supplementary Figure S27: Diagram showing how the smileys stick together to maximize the number of blunt end stacking interactions. Compare to previous Supplementary Fig. S26.

Plate number : 1  
s0m25k, A1, AAAACAGGACGAGCTTAAATTGGGCTTG  
s10m15g, B1, ATATATTTTAG  
s10m17g, C1, TCTCTGAAAACACTTTCAA  
s10m19g, D1, ATTCAATTCAATTCCTTGTAGAA  
s10m0j, E1, ACCGAAAGACCCAGGACAAAGTGTATTATTG  
s10m1e, F1, CGTACTCACCCCTCAGAACCCCACAGCG  
s10m12e, G1, CATAGGAAGGACCCAGGACAAAGTGTATTATTG  
s10m14e, H1, GATCTAAATTTCTGTGAGGATGAGAAT  
s10m16e, A2, AGAAAGGATGCTTCGAGGTTAGATGACATGA  
s10m18e, B2, CAACAACCCTCGGAAGGAGGTAGTTTCTCG  
s10m20e, C2, GAGGAAGTAAACACTTCTTGGAAACAG  
s10m22e, D2, GAGATTTGGGAACTTGTAAAGAAGGCTGG  
s10m24e, E2, TGACCTTCGGCTTGCGGAG  
s10m28i, F2, GCAACAGTGGCGCTGATTAAAGGGAGG  
s10m21, G2, ATGTAGGGATAAAGACTCTTACAGGATTG  
s10m30i, H2, GTAAATAAGCAGATTCAAGCTTAATAGGGTT  
s10m32i, A3, AGTAGAAAGATTGAGTAAACATCAATCGG  
s10m34g, B3, GTCTTCATCACCATGAACTCAACTTCTTGA  
s10m41, C3, GACCAAGAGATTGAGTAAAGCCCTAGCAGCA  
s10m61, D3, ATTATTAGCGGACTTACAAATAACCTCAGAG  
s10m8e, E3, CCTCGCTCGGATAAGTCGCGTGTATCAC  
s2m11f, F3, ACCGTAACCCCTTCAGAACCGCCGGAGGTT  
s2m13f, G3, GTCTTCACACTGAGTTCTGCACCAACCATG  
s2m15f, H3, AGQAATAGGAGCCTTGTAAATGAGTTTGT  
s2m15g, A4, CGAATAATTAATTGAGGACCTTAAATGGGCTATAT  
s2m17t, B4, CCCTTGTGACTGGTTATCTGACTCAACTAA  
s2m19f, C4, AACGGGTAAAGCGGAAAGACAGCTTGGCA  
s2m1b, D4, AACGGTGTACATA  
s2m1f, E4, AAAATACAGCAACATATAAAGAA  
s2m21f, F4, CCTGTAAGGCAAAAGAATACACTTCCATT  
s2m23f, G4, TAATCTTGTAGAAGGGACCGGATTTCTATCG  
s2m25f, H4, CTCACTGAGTAAATACTCAAGAG  
s2m27g, I5, AGCAGGAAATGAAAAATCAACCAAGCAGAGAGAT  
s2m29g, K5, TCTGCCAAGATTAACAGGAGTGGCCAGCTGAGAGCCA  
s2m31f, C5, CTATCGGCTGGATTATTCTACATGGAGGACAT  
s2m33b, D5, CGCTTGA  
s2m3f, E5, ATAAAGCAACCAAAAGAATCGCATAAACCTGAG  
s2m5f, F5, CAATAAAGGGAGAGATAACCCACCAAAACATGA  
s2m7f, G5, ACCTATATTACCGACGCTTAAATTTCCTAACAT  
s2m9f, H5, AGTACCGCTTGTGCTGACCTAACGAGATTTC  
s3m16i, A6, GGCTTCAACACGTGAAATTCTCTAACCTCC  
s3m18e, B6, TCGTGCCTGGGATGTCACCTCAAAATAGCT  
s3m18i, C6, CGCTTGTGAGGCTTGCAGGGAGTTTTAA  
s3m20b, D6, GGCAACCTACGAA  
s3m20e, E6, ATAGGCCACAACTTAAAGGAAATGTTGTC  
s3m22e, F6, GAATTCGGCGCACAGCGCTCAATCACAAAGAAC  
s3m24b, G6, CCAAACTATTAC  
s3m24e, H6, CGGATATTCAAGCTAACAAAGCTG  
s3m2e, A7, AAATAAACCGGAAATCTAGCTATC  
s3m30g, B7, AGAACCTCTCACTTCGCTAAACCTGTTAATATCC  
s3m32g, C7, AGACAAATATTACCGCTCATACCTATTTGACTCT  
s3m4e, D7, TTACCTGAACTTACGGCTTAACTATCAACAGATT  
s3m6e, E7, TTTTGTTACCGCTTACAGGCGCTTCTTGTAAA  
s3m8e, F7, CATGAAAGTTGAGATTCTGGGG  
s3m8i, G7, GAGAGGATNTAAAGGCTGAGATGAGG  
s4m23g, H7, ACTTACGGCGGAGCAGGCGACTCTCCATGTT  
s4m25g, A8, AGGAGCTTCATAGATAACAAACTAATAGTACTGAA  
s4m29g, B8, GAAAGCTTCATTAACAAACTGACCATAACGCTTC  
s4m3f, C8, TAAGGAAAAGAACCGGAAAGAAC  
s4m5f, D8, AAATGAAACAACTGAGGGTAAAGCCCTTT  
s4m9g, E8, CCAATTAATCGGCTACAGGCACTAGAAAATAGAGAA  
s5m12e, F8, TATAAGTATTCTGCGGACTAACGGAAATC  
s5m14g, G8, ATTAATCTAAATAAGAATAAA  
s5m16i, H8, GGCTTACTGAGGAGACTACCTTTAAAAAAA  
s5m18i, A9, TGGAAACATTCTATTGAAATTACCTTAAAGGC  
s5m22g, B9, TATCAAAATT  
s5m24a, C9, GAAACATTGGCG  
s5m28e, D9, CAAATATCTAGGCCCTAAACATCGAAGAATAC  
s5m26e, E9, ACAAAAGTACCGGAAAGGAG  
s5m30g, F9, GTGCGCACAAAAAGCGCTCATGGACAGCCATTGCAACAGG  
s5m30h, G9, GACAAATTTTTGTAAATTAGCGGCAACTGAAACCCCT  
s5m4e, H9, ATACCGGAAACTGACACCTTGAATAAGCAG  
s5m6j, A10, CTTACAGACCCAGCTTACATTATTCTGTAATCTACCA  
s5m8i, B10, TTACCGGCCAGGCAAACTCAGATACCTCTC  
s6m11f, C10, AAAGGAAATATTCTCATCTTAACTGTT  
s6m13f, D10, CTCTGGTTTAAATTGAGGAGCAGGCCAAC  
s6m15f, E10, TATAACTGAGTAAATAGCGCTTAAAGAAA  
s6m17t, F10, ATCAATATCTAAACATAGTCTTGGGTTA  
s6m19f, G10, TAATTCATTTAAACAAGTACATAA  
s6m23f, H10, CCAGAGGAGAACCTACCA  
s6m25f, A11, GAGGATTGTTGAGTAACTTATAGAAACCA  
s6m27f, B11, AATCAATATCTTACGGGACTTACATATT  
s6m29b, C11, TAGTCTGGCTTAT  
s6m5b, D11, AACGGCACAGGG  
s6m5f, E11, ACAAAAAATTAGACGGGAAATT  
s6m7f, F11, GAACGGCATTAGTGTCTATTGGAGAAGATA  
s6m9f, G11, CTTATCATATTACCGGCCCAATATTCTAA  
s7m10e, H11, CGGTTATTCTGCAACGAAAATGAGTAACT  
s7m12e, A12, GTTCCAGACTAACACCCCAACATGATCAT  
s7m14e, B12, ATGGCTTATGAAATACCGGCCATTGTA  
s7m16e, C12, TCTGCTGAGTCAATGTAATTGTGAGT  
s7m18e, D12, GAATAACCCATGAAAGAAAACAAATTACCGG  
s7m20e, E12, TTCCGCTGATACCGGGAAACATTGCA  
s7m22e, F12, TAAACAGGAAATAGGAGGCTGAGCGGAAAT  
s7m24e, G12, ATCATCAATTAAATTAAAGTGAAGAGTAT  
s7m26e, H12, TAGACTTGGAGGTTTCTAAATCTGGTCA

Plate number: 2  
s7m28g, A1, GTGGCCAAATCACACGTTG  
s7m8e, B1, AGCGAACCTTTCATCTAGGAATTCTCAAGAA  
s8m1f, C1, TAACACCAACCAAAATAGTCACCAACCAA  
s8m13f, D1, CTTACAGGAGAATGCCATATTGAGCAGCAA  
s8m15f, E1, ATCGGAAGACCTTAAATTATGTTGACCAATT  
s8m17f, F1, GTAATCTGTTAGACGCTGAGAACAAATCC  
s8m19f, G1, GATACCAAGATGTAGAACAAAATCTGCCT  
s8m21f, H1, AAATTGCCCCAGTAGAACACTTCTTATGCTT  
s8m23f, A2, ATTATCTGTTGGATTAATCTCTAAATAAG  
s8m25b, B2, TAAATCTCGTA  
s8m25f, C2, TTGACAACTTCTGGCCGAAGCTTATTCTCG  
s8m27g, D2, AAAGGAATTGACACAA  
s8m7g, E2, GGGGGTTTGAAGCTTAATCAAGAGGGCTTT  
s8m9b, F2, AGAACCATCTCG  
s8m9g, G2, TACCGCACAGACCGGTTTATTCCGACTTGC  
s9m10e, H2, GAACGCGCTGTATTATGTTCA  
s9m12e, A3, ATATGCAACAGCTGGCTTAATTATAAGC  
s9m14e, B3, CAACGCTTAAATTCTCTGCAAGAAA  
s9m16e, C3, CGCGGAATAAGCGCATGCTTGTGACCTT  
s9m18e, D3, AATTAATTCTGACGAAAGATTC  
s9m20e, E3, ATATGCCAGCTGAGTAATATAGATT  
s9m20f, F3, AGGGCGAAATT  
s9m29g, F3, CAGGTTAAATAATCTGATTGATGATGCCATTCA  
s-10m15g, H3, TAGATTTATCAAGGAAAGGGC  
s-10m17g, I4, AAAACAGGAGCGAACAA  
s-10m19g, B4, CCCCTGCGATT  
s-1m0e, C4, TCACAACTAATAGAACCTACAGCG  
s-1m10i, D4, AAATATCTGTTAGGCCGAATAGGAGGGTT  
s-1m10j, E4, GCCACCACTTAAAGGAGAACGGAGATTGCT  
s-1m12i, F4, CAAACAGGCTTCAATTCTGGAGGCTTCC  
s-1m12j, G4, ATCTTACAGCTGAGAACAGGCTTCC  
s-1m14i, H4, ACTATTATGACGCCCTCATAGTCTGTAGC  
s-1m14j, A5, AACACTTAACTAAAGCTTGTACAGGAAT  
s-1m16i, B5, GACCATAACACAGTTCTGGCGATTGCTAA  
s-1m16j, C5, CAGCTTGAAGACTGTAGGCTTAATAGTA  
s-1m18i, D5, AAATGTTTCTTACCGTAGTGTGCGCTTCTAAA  
s-1m18j, E5, ACAGGAGCATTAACACAGTTCTGGCGATT  
s-1m20i, F5, CGAACACTTTTGAGGACTAAAGAACACGGCT  
s-1m20j, G5, CGATTATAATTTAGGAATACACAAAGATT  
s-1m21i, H5, CGATTGAGGCCAAAGGGCAAAACACCC  
s-1m22j, I5, CGATTGAGGCCAAAGGGCAAAACACCC  
s-1m23j, A6, GACAGCTGTTATTACAGCTTGTAGGTTTAAG  
s-1m24i, B6, AACCTGGCTTACAGACCAAGCGCATGGACAGAT  
s-1m28i, C6, CGTTTGCATCGTACATACCGGAAAGGGCG  
s-1m2d, D6, CCAAGAACAGGAACTTGTACAGCA  
s-1m2e, E6, AGGGAGGGAAAGGGCAGATTCTACAGCG  
s-1m30e, F6, TATAATACTTCCTGGTAAACATTTTTG  
s-1m30i, G6, GAGTGTGAAAGAAATAGGCCGACGACCA  
s-1m32g, H6, GCTGAGGAGGCCCGGCTATTAGAACGGCGAACGCTG  
s-1m32i, A7, CCTAAAGGTGCGCTTAAGACTAACTGCTG  
s-1m34j, B7, CGAAAGAACAGGAGAACAGGAACTTAAAGA  
s-1m4e, C7, AACCTGCAACTGACGAACTACCC  
s-1m4i, D7, CCTCTAACTCCAAATGAACCTGAAATAA  
s-1m5e, E7, AACCCGAAAGAACACCACAGGAGGTT  
s-1m6i, F7, CGCGCACCCCTTCAGGACCAACAGGACCAT  
s-1m8e, G7, GACTAACACGTTTAAATGAGCTAACAGTTC  
s-1m8i, H7, GATAATAAGGTGCCCCTATAACAGTTAATGCC  
s-2m1l7, G8, AGGGGGGAAACTTGTGGAAGTTTAAACAGCTTCAA  
s-2m19f, B8, AGCGAACCAACAGCACGATAAACTTTTGG  
s-2m21f, C8, ATGTTTATCAT  
s-2m21f, D8, AGGTGAATTAACCTATGAGATAAGGAATT  
s-2m23f, E8, CTTATGGCAGTGTGGAGAAGAAAAATTATTAC  
s-2m25f, F8, GTGTTTAAATTCAGTAATTC  
s-2m27g, H8, ATTCGGCACTGGTTTCTTCTACTGGGAAACCTTC  
s-2m33a, I8, CGGGGAGCTGTG  
s-2m3f, B9, CCTTACAGGAAATTTCTTCA  
s-2m5f, C9, GAGCCGCCAGTTCTGGCTTCTAGCTC  
s-2m7f, D9, ACGGGGTCCGCCGCCAGCATTTGACTCTTC  
s-2m9f, E9, TCAAGCGAACAGCACAGTT  
s-3m16i, F9, CAAATGCTTAATATTCTATTGAGATGCTGG  
s-3m18i, G9, CAAAAGAAAACCAAAATAGCGGAGATT  
s-3m20a, H9, CCCAACATATA  
s-3m24a, A10, TCATTGCTTTAA  
s-3m2e, B10, GTGAAATTATCACCGTCAAA  
s-3m30g, C10, TTGATGTTAACGTGACTCCAACGGGCCACTACGTGA  
s-3m32g, D10, CATCCACCAAAATCACAGGCTTCAACTTAAAGGTT  
s-3m4e, E10, ACCATGACAGCTGTGCGGCTTCCCC  
s-3m6e, F10, GAAACCGGCAAGGAGTTGAGGCCAGGAGGTGA  
s-3m8e, G10, CTGGTAGTACGCCAACATCT  
s-4m11f, H10, GTAGCATTTTCTTACCTGAAATACAGTGTG  
s-4m13f, A11, TTCTTAAAGAACATCCAAATACTTAAATAGTA  
s-4m15g, B11, CCTCTCATATAATTAAATAA  
s-4m21g, C11, GAACTAAGGCAACACTTGTGTTAAAC  
s-4m27g, D11, TTGGCTCTTCTCTGTGAAATTCTGTGAGTCATAGCT  
s-4m27h, E11, TTGGCTCTTCTCTGTGAAATTCTGTGAGTCATAGCT  
s-4m29f, F11, CAGGGGAAGGCTGTGGCTTCAATAATTGCG  
s-4m3f, G11, TAGAGGCCACCCGACTTGTAGGCC  
s-4m5f, H11, AACCGAGGTCTACGGCTTCTGGGAAAT  
s-4m7f, I12, ATGATACAGTCAGCACGATGCCATT  
s-4m9f, B12, TCTGAAAGGAGCTGAGTGTAGAGGCCCTT  
s-5m10e, C12, CAACCTAAAGGTGATGCCCAATTCTGGC  
s-5m12e, D12, ATTTCTACTACAGGCAAGGAAATTT  
s-5m14e, E12, ACGGCAAGGATGTCAGCTGAGTAAGATCTAC  
s-5m16e, F12, AAAGGCTAACAGGAAATCTGAGTACAGATTC  
s-5m16i, G12, AGCAAAACATCAGGTCTTGTGCTTAATCC  
s-5m18e, H12, TAAATTTACCGCTTCA  
s-5m18i, I12, TAAATTTACCGCTTCA

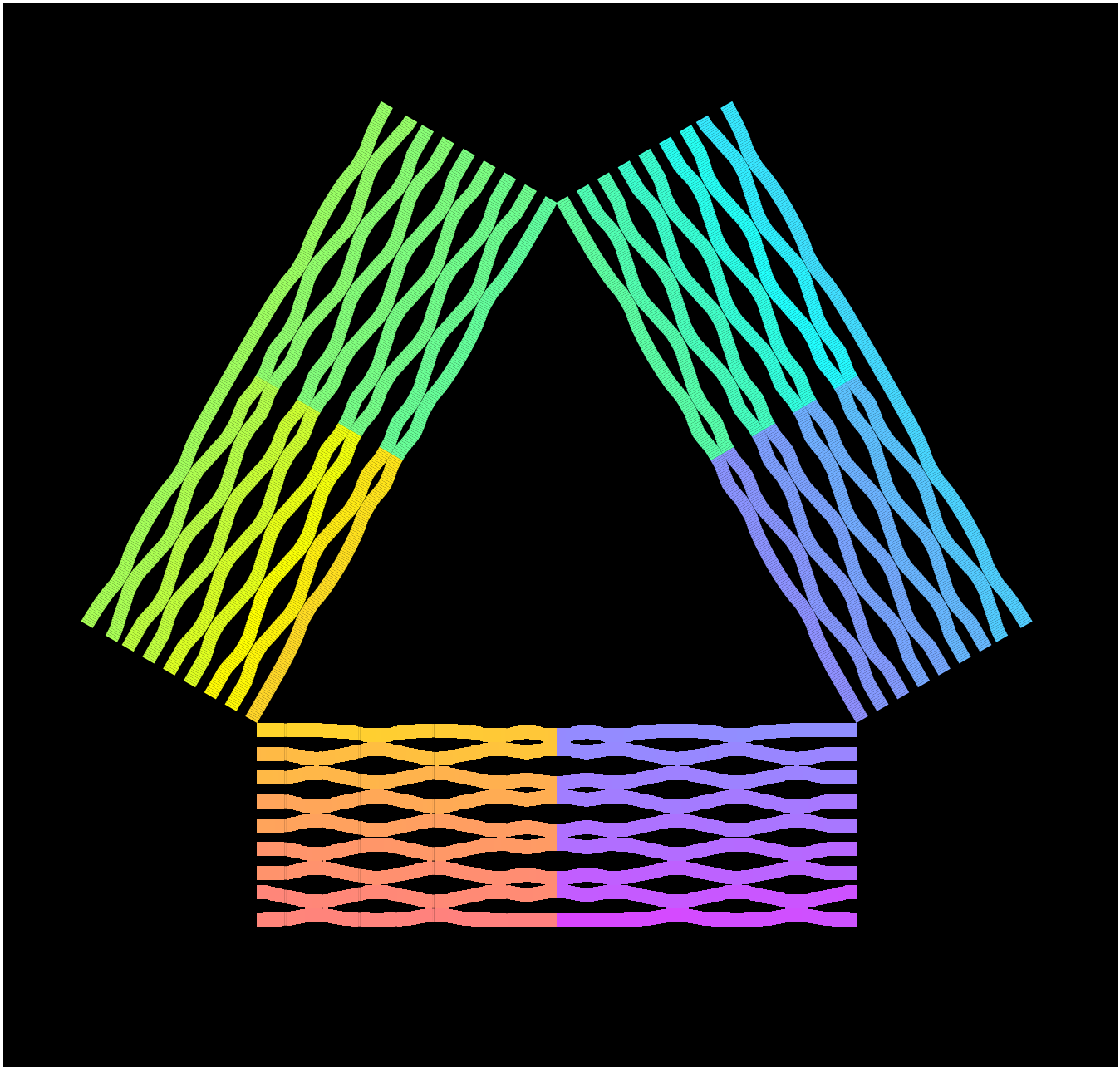
Plate number : 3  
s-5m18i, A1, CAATGAGATGTAAATCAGCTCATGGCTTTG  
s-5m22g, B1, GTGCCGGAAACTGTGCTGC  
s-5m24b, C1, GGTTAATAAGTT  
s-5m24e, D1, AAAGGCATGCGCAGGGTTTCCAGAGCTGA  
s-5m26e, E1, ATTCGTAATGGCCCTACAAATTGTCAGCTA  
s-5m28g, F1, ACTCACATCCGCTGGCCCTGAGAGCGCTGAGCGTGT  
s-5m22g, G1, TGTGATTCAGGGCACTAAAGGGCGAAAAGTCCCGCAG  
s-5m4e, H1, GTCATACAGGGCTTCTATTTCCTTA  
s-5m6e, A2, TAATCAAATGATTTACAACAAAGTAAGGG  
s-5m8e, B2, TCATACATAGTACCTTAACTGCTTAAATATG  
s-6m1f, C2, CTGAAAGTCGCCAGACGTAGATTTGACTCTA  
s-6m3f, D2, AAAGAGCTAAATTAGCAAAATTAGGGCCGAG  
s-6m5f, E2, TTTTTGAGATGTTAGTAAAGTTGGCG  
s-6m7f, F2, TTGTTAAAGTAGCTTAAACAGTGGGTGACTTA  
s-6m19e, G2, GTTACAGCTTTCGGCTGTCGCTTCAATTATT  
s-6m21f, H2, CTTTCCGGGTGAGATGGGCCATGGGATAG  
s-6m21g, A3, CACCGCTTCTG  
s-6m23f, B3, AAAGGGGACAGCGAACAGGCCATTCCAGCGAG  
s-6m25f, C3, CGGGTACCGCTACAGCGCTGTAAGCTGGCGA  
s-6m27f, D3, CCTTAATGACCACACACATCAGGAGGATCC  
s-6m29a, E3, CAGCGAAAGGTG  
s-6m5a, F3, TTGCCATAGCGT  
s-6m7g, G3, ACCGTTCCATAATCCTATTAAAGGCCAATGGA  
s-6m9f, H3, ACATGTTCTTCAATTAGGAGGCTTAAAGTT  
s-7m10e, A4, ATATAGCTTCTAGTTGACCATTAAGTATATT  
s-7m12e, B4, TCATTGCGCAATAGGCTTCAGATGACCT  
s-7m14e, C4, GTTAACTCTTAAAGGGCTGAGAAAATTANTG  
s-7m16e, D4, CGGGAGAGCTGTCACATCATATGTTTTAAAT  
s-7m18e, E4, TGAAACAGCTGTAGCCAGCTTCCAGGGATT  
s-7m20e, F4, GACCGTAACTTCAGCCGTCATCTCAGGAG  
s-7m22e, G4, ATCCGACTTCGCACTTCAGCGCTGCTTCTGTA  
s-7m24e, H4, TTACGCCAACAGGCCATGGCCATTGAGGTC  
s-7m26e, A5, GACTCTAGCGGCAAGATA  
s-8m1f, B5, CTGTTTGTACATTTCGAAATGG  
s-8m13f, C5, AAAACATTCAAAAGCTTAACTCGGTCAATAAC  
s-8m15f, D5, AGCTGATAGCGGCCAGACGACTCAATTGTCACCA  
s-8m17f, E5, AAACAAACATCCGGCTTAAATACCGCTT  
s-8m19f, F5, GACAAACACTAACATTAATAGTGGAGATTGTAT  
s-8m21f, G5, TATCGGCCGGCAATTGAGGGGACCTCGTGG  
s-8m25a, H5, TGTCCAGCTTGTG  
s-8m27g, A6, AAAGCTTCTGGGGTGG  
s-8m7g, B6, AAGCGCAGTCCTATTTCGCGATGGCTGCTGAAT  
s-8m9a, C6, CTAAATTAGAG  
s-9m14e, D6, ATCCACCATCA  
s-9m24g, E6, CTGCTGGCGGGCTCAAGTGGGAAGGGGACAG  
s-mrem1, F6, CCTGAGAAAGTTTTATAATCAGTGA  
s-mrem2, G6, ATTTAGACAGGACGAGCTGGACAGAAT  
s-mrem3, H6, CGACTAAACAGGAGGCCATTAAAGGG  
s-mrem4, A7, ACGTGCTTCTCTGTTAGAACATGAGCGC  
s-mrem5, B7, ATATAGCTGGCTTCAAGCAGACGCTATA  
s-mrem6, C7, CGCCTTAAATGCCGCCCTACAGGCCCGT

Supplementary Figure S28: Sequences for the disk with holes (smiley).



25 turns wide at 10.4 bases/turn -> 260 bases  
 9 helices / domain, 27 helices in all!

Supplementary Figure S29: Schematics for the triangle Fig. 2e. **a** Block diagram. Designed for 2.5-turn spacing blocks have 5 different offsets with respect to the underlying lattice of crossovers, hence the 5 different hues of blocks in different columns. As in other block diagrams, orange block/red block boundaries have an offset of 0 turns with respect to the underlying lattice of crossovers. **b** Folding path.



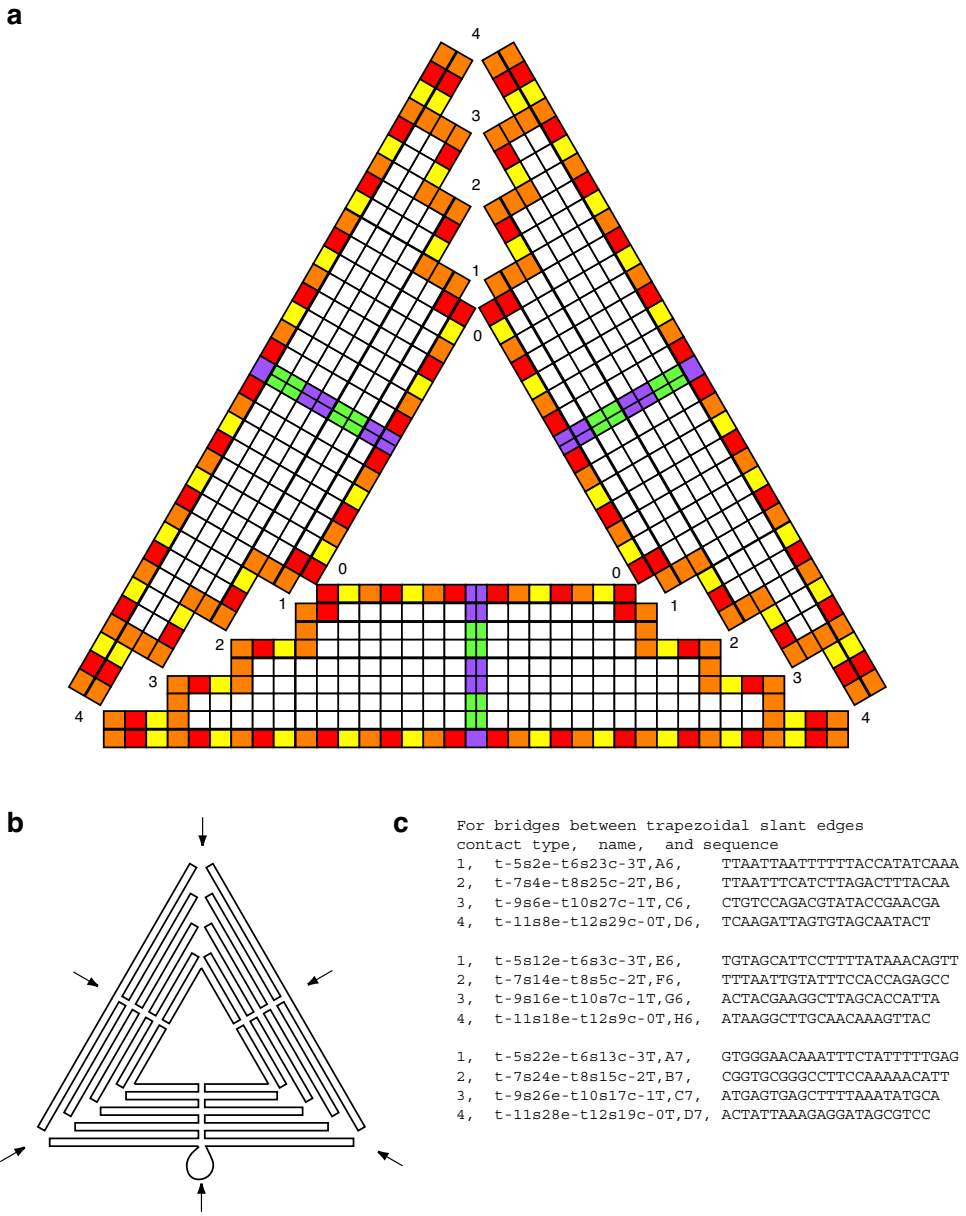
Supplementary Figure S30: Crossover diagram for the equilateral composed of rectangular domains.

Plate number: 1  
e0t1d, A1, CATAGTTAGCTTAAATCGTGAACGG  
e0t1c, B1, GCGGACAATGCACTGTAACTATT  
e0t1d, C1, GAGAACAAACAGGAGCATCTAAAGT  
e0t1c, D1, ACTCATCTTGTACTCATCCATATAA  
e0t1d, E1, AACCATTTAGCACCAACCATCGCC  
e0t1c, F1, AATCAACGTAACATATTATAGTCAGA  
e0t1d, G1, GTGTCTGGAAGTCCCGACGGGATAT  
e0t1c, H1, CTAATGCAAGATACAAAGGAAAG  
e0t1d, A2, TCTTACCCGCAAGCTGTCTTC  
e0t1d, B2, CAATAGTAATTGCTGCACTACAG  
e0t1d, C2, TAACAACCGCTGAGGAGG  
e0t2c, D2, CCAGCTGGAAAAGAGGAGCGAGA  
e0t2d, E2, TACCAAGTACCATGATCTGG  
e0t2c, F2, AGCTAACTCACATCAAATATCA  
e0t2d, G2, CAAAGAACCCGGGGGGATCTGG  
e0t2c, H2, CGGAAATCTTAAAGGAGCATT  
e0t2d, A3, ATCACCTGCTGATAATTGGCTGG  
e0t2c, B3, GAAAGGAAGGAAATATCAGTGAGG  
e0t2d, C3, ACAGCACGATTAATCAAAAG  
e0t3c, D3, GTATCATATGCTTACAAACAA  
e0t3d, E3, ATTAGCGGGTTATCAAAATCAG  
e0t5c, F3, CACATCTTAAATCAAGTGTCT  
e0t5d, G3, GATTGGCTTGTATTAACTTT  
e0t7c, H3, CTATTGCCCCAAAGTTATTG  
e0t7d, A4, CAGTAGCCAGACGAGCATGTAA  
e0t9c, B4, AGAGAGATAACCCACAAAGTGT  
e0t9d, C4, GACACCAGGAACTGACATTTA  
e0t10e, D4, TAAGCCCCATAAAGCAAGAAC  
e0t12a, E4, TAATCGTAAACCTGCTGAGTCT  
e0t12b, F4, CTATCAGTCAATTGATGCA  
e0t14a, G4, CGGGAGAACCTCGGTGACCA  
e0t14b, H4, GCATAAAAGCTTAAATTACCGCA  
e0t16a, A5, CAGTGTATCCCACAACTAAAGT  
e0t16b, B5, TGTGTTAAATGATCTGGCAAG  
e0t18a, C5, AGCAACCGGATTACAAATCAG  
e0t18b, D5, AGAAATGACCATAAAGGAAAG  
e0t20e, E5, GAATTAGGACATRACTAGAAC  
e0t22a, F5, CGAATTATTCATTGTTG  
e0t22b, G5, TAACGGGATTCACCTGGATG  
e0t24a, H5, TTATCATATTTCTGGCGA  
e0t24b, A6, TTAGAGTACATCTGATTATCAGA  
e0t26a, B6, AACCTCAATCAAAGATCTAAC  
e0t26b, C6, CCAGCAGAACATGTCTGGCT  
e0t28a, D6, CTGGCAACAGGAGTACCGTC  
e0t28b, E6, TATTACATGGCATAGAACCTCT  
e0t2a, F6, CGCGATAATGGAGGAGGATTAG  
e0t2b, H6, TGAGACTCTCACTGGAGGTTG  
e0t30e, H6, CCACCGGACCTTAAAGACTCT  
e0t4a, A7, TAAATCTCTTAAAGGAGCTCAG  
e0t4b, B7, TGAGGAGGTTGAGGAGCAAG  
e0t6a, C7, TTAGGGTCACTGGCAACCCATT  
e0t6b, D7, GAAAACATGATGACGGTTTC  
e0t8a, E7, CACAACTATAGAAAAGAACGAAA  
e0t8b, F7, GTGCCAACATTAATCATG  
e0t11e, G7, TATGTTACCCCGGTGATACTCAGAAA  
e0t13a, H7, AGGATAAAATTTAGTCTACAAAG  
e0t13b, A8, AGCTTATTTGAGGTAGAACCTCT  
e0t15a, B8, GTAGATTAGTTTAAAGCCTCAGA  
e0t15b, C8, GAAAATTAAAGCAGACATTAGATC  
e0t17a, D8, TAAGAGGAAAGCCCTGGTCAACA  
e0t17b, E8, CTGTAATATAAGGAAAGACTCTAA  
e0t19a, F8, ACTATCATACCCGTCAGAACAG  
e0t19b, G8, AAATGCTTAAACTCTTACAGAC  
e0t21e, H8, ATATAAGTATGGGGAAATAGTGT  
e0t21e, A9, CAAAGAGGTGATGAAACATC  
e0t23a, B9, TGATGCCATTACCGGAAACAA  
e0t25b, C9, AGTACCTTACATCAATATACT  
e0t25a, D9, GGCAATCACAGTAACTTTAAAGT  
e0t25b, E9, GCGGGAACCTTAAAGGAAATG  
e0t27a, F9, GACCTGAAAGCTGGCAGCTGAG  
e0t27b, G9, CGCTGCAAGTAAAGTACCTGG  
e0t29a, H9, AGCGAAATTAACTCTGAATG  
e0t29b, A10, TTGACGCTCAATGTTGAGCA  
e0t2a, B10, AAAGGCAGCTCTGATTAGGAC  
e0t3b, C10, TCTGAAATCATGAAGATTACCG  
e0t25c, D10, ATCGGCACTTACCGGAAAC  
e0t5b, E10, ACCACACCAAGGGCTATGCC  
e0t27a, F10, TTACCGGCCCCAACCTTACCA  
e0t27b, G10, TTAGCAAGGGGGAGAACAGG  
e0t29a, H10, ATGAAATAGCAATACATCA  
e0t29b, A11, CAAAGCTTAAAGTCTTAC  
e0t10e, B11, GAGGCCCTTAAAGGAAAG  
e0t12a, C11, AGGCCCCAACATCCGGAGGG  
e0t12b, D11, OCTGATAATTAAGGAAATG  
e0t14a, E11, ATTTTTAAATCAGGAAAG  
e0t14b, F11, ATCATACGCAATGCTGTAG  
e0t16a, G11, ATTCTGAAATGGTAAAGCTTAA  
e0t16b, H11, TTTCGGGAGGCTTAAACATCT  
e0t18a, A12, TATCGCTTAAATGATCT  
e0t18b, B12, TCATAATATTCATCGGCTTCA  
e0t20e, C12, GACGATAAAACCAAAATAGC  
e0t22a, D12, AGAAAACAAATATACAGTAA  
e0t22b, E12, TTACCTCAGATGTAATAC  
e0t24a, F12, GATTGTTGGATTATAATCCTT  
e0t24b, G12, ATTCGACAACTCGTACTCT  
e0t26a, H12, AGGAGGTATCTCGATTAAAC

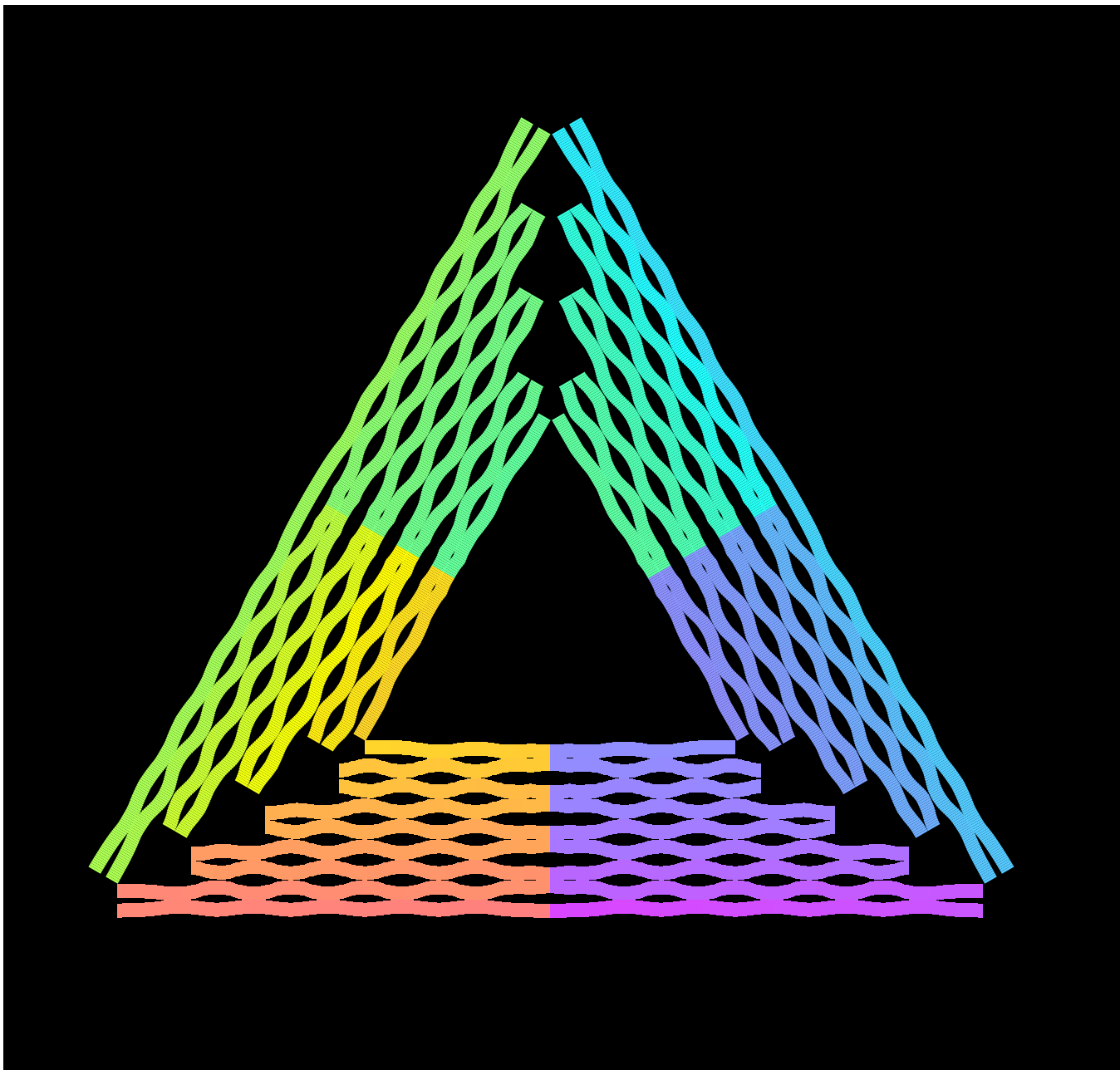
Plate number: 2  
e0t26b, A1, AGAGGTGAGGGGGAAATATCTT  
e0t28a, B1, AGAGACATATTAACTAC  
e0t28b, C1, AAAAGCCTCATGTTGAATGGCT  
e0t28d, D1, ATACCGTACTACGGAAACCTT  
e0t28b, E1, CCCCTGCCTATTGGAGGT  
e0t30e, F1, TTCTTGTAGTAAATACAT  
e0t3a, G1, CAGTAACGCTATAGGCCAC  
e0t3b, H1, CACCAACCTTACAGCATGGTT  
e0t6a, A2, TATAGGGTTGAGCACCATT  
e0t6b, B2, CAAAATACCACTGATCTT  
e0t8a, C2, ACATCACCGCAGTGGCT  
e0t8b, D2, AGACTCTTATTAGGAGGAG  
e0t11e, E2, AGCAAAATTATGTAATG  
e0t13a, F2, TGTGAGGTAAAGCTTCA  
e0t13b, G2, CATCAATATGATAATCAA  
e0t15a, H2, TAGCTATTTCTTCA  
e0t15b, A3, AAATGAGTACGCA  
e0t17a, B3, CGGAAACAGGAGTAT  
e0t17b, C3, AATGGCTCTTGA  
e0t19a, D3, GCTTGGAAAAGCTG  
e0t19e, E3, GGATAGCGTAAAGATT  
e0t1f, F3, CGCCGCTTCA  
e0t21e, G3, CAATTCTTGTAACT  
e0t23a, H3, ATGGAGGGTTAGT  
e0t23b, A4, TAAAGAAATTGCGAAC  
e0t25a, B4, GAGCTACTAACAGCT  
e0t25b, C4, TTAGAGTATTAGT  
e0t27a, D4, AGCTTAACTGGC  
e0t27b, E4, AACGAAACCCAGG  
e0t29a, F4, GCTGTAGGATG  
e0t29e, G4, TATTACCGCAGCA  
e0t29a, H4, GATACGAGGAACT  
e0t23b, A5, ACAGTGTGCTT  
e0t25b, B5, TCAAATACCGGG  
e0t25c, C5, CACCCCTGAGAAC  
e0t27a, D5, GTAAATTGAGGAA  
e0t27b, E5, TTAGGCAATT  
e0t29a, F5, GATAGCGAAC  
e0t29e, G5, ATAGGAGGTTAG  
e0t23b, A6, TAAAGAAATTGCGAAC  
e0t25a, B6, GAGCTACTAACAGCT  
e0t25b, C6, GCTTGGAGGAGT  
e0t27a, D6, TTGAGCAATT  
e0t29a, E6, AAAATTATGCA  
e0t23b, F6, CGCTCAAGT  
e0t28a, G6, CTAAACATCC  
e0t28b, H6, GAAACGGC  
e0t28c, A7, TTACGGGG  
e0t28d, B7, ACCGGG  
e0t28e, C7, AAAGGT  
e0t10e, D7, TCAGGGGTA  
e0t12a, E7, GCTGTAGC  
e0t12b, F7, TTGCGTCT  
e0t14a, G7, TTAAACAGG  
e0t14b, H7, ACCCATAC  
e0t16a, A8, AAAGGG  
e0t16b, B8, ACCAGG  
e0t18a, C8, GACAG  
e0t18b, D8, AGTGA  
e0t20e, E8, TTGAG  
e0t22a, F8, TTTCAT  
e0t22b, G8, AACAA  
e0t24a, H8, TCGTGG  
e0t24b, A9, CAGGG  
e0t26a, B9, GAAAG  
e0t26b, C9, CTAC  
e0t28a, D9, ATCT  
e0t28b, E9, AAATAG  
e0t28c, F9, GCTT  
e0t28d, G9, GTCT  
e0t30e, H9, AGCG  
e0t4a, A10, CATA  
e0t4b, B10, ACCAG  
e0t6a, C10, AAGT  
e0t6b, D10, ACCA  
e0t8a, E10, TTGAA  
e0t8b, F10, TTCTG  
e0t11e, G10, TTCTG  
e0t13a, H10, ATCG  
e0t13b, A11, TGA  
e0t14a, B11, ATTT  
e0t14b, F11, TTAT  
e0t16a, G11, ATT  
e0t16b, H11, TTTC  
e0t18a, A12, TATCG  
e0t18b, B12, TCATA  
e0t20e, C12, GACG  
e0t22a, D12, AGAAA  
e0t22b, E12, TTACCT  
e0t24a, F12, GATT  
e0t24b, G12, ATTC  
e0t26a, H12, AGGAGG

Plate number: 3  
e0t29b, A1, GTTCCAGTTGGAGATTAG  
e0t23a, B1, CGCTTAAATA  
e0t23b, C1, CGCTTAAAG  
e0t25a, D1, AACCGCCT  
e0t25b, E1, TAGGGCTTAA  
e0t27a, F1, CGAACCT  
e0t27b, G1, TATAC  
e0t29a, H1, GAATTA  
e0t29b, A2, CGCTT  
e0t310e, B2, AAAACAGGG  
e0t312b, D2, AACAA  
e0t314b, F2, TTTC  
e0t316b, H2, GTG  
e0t318a, A3, CGGT  
e0t318b, B3, CTTG  
e0t320e, C3, TAATA  
e0t322a, D3, CCA  
e0t322b, E3, GCAT  
e0t324a, F3, CCAG  
e0t324b, G3, AAC  
e0t326a, H3, AAT  
e0t326b, A4, ATCG  
e0t328a, B4, CCT  
e0t328b, C4, ATTA  
e0t32a, D4, AAT  
e0t32b, E4, ATG  
e0t330e, F4, GCG  
e0t34a, G4, AAATAC  
e0t34b, H4, TTAA  
e0t36a, A5, ATAA  
e0t36b, B5, CCA  
e0t38a, C5, GTAT  
e0t38b, D5, TTAC  
e0t411e, B5, CTCA  
e0t413a, F5, TGA  
e0t413b, G5, TGAG  
e0t415a, H5, TAA  
e0t415b, A6, CGAA  
e0t417a, B6, ACC  
e0t417b, C6, GTT  
e0t419b, D6, ATC  
e0t41e, E6, TTG  
e0t41b, F6, TTG  
e0t423a, G6, TCCC  
e0t423b, H6, TGAG  
e0t425a, A7, CAT  
e0t425b, B7, GCT  
e0t427a, C7, CAG  
e0t427b, D7, TT  
e0t429b, E7, AAGGG  
e0t43a, F7, TCT  
e0t43b, G7, CCA  
e0t45a, H7, AA  
e0t45b, A8, CAG  
e0t47a, B8, CAA  
e0t47b, C8, GCA  
e0t49b, D8, AT  
e0t510e, E8, AAA  
e0t512b, F8, AT  
e0t514b, G8, GCA  
e0t516b, H8, CGG  
e0t518b, A9, TT  
e0t520e, B9, CATT  
e0t522b, C9, CAG  
e0t524b, D9, CCG  
e0t526b, E9, TT  
e0t528b, F9, GAT  
e0t529b, G9, TT  
e0t530e, H9, GTG  
e0t54b, A10, GAG  
e0t56b, B10, GAAT  
e0t58b, C10, TT  
e0t59b, D10, AT  
e0t61b, E10, TT  
e0t63b, F10, AG  
e0t64b, G10, TT  
e0t65b, H10, AT  
e0t67b, A11, TGA  
e0t69b, B11, TT  
e0t71b, C11, GAG  
e0t73b, D11, GCG  
e0t75b, E11, AGA  
e0t77b, F11, TT  
e0t79b, G11, AAC  
e0t81b, H11, TT  
e0t83b, A12, TAT  
e0t85b, B12, TCG  
e0t87b, C12, GAT  
e0t89b, D12, CAA  
e0t91b, E12, AGC  
e0t93b, F12, GGT  
e0t95b, G12, ACC  
e0t97b, H12, AAAGGG

Supplementary Figure S31: Sequences for the equilateral composed of rectangular domains.



Supplementary Figure S32: More details of sharp triangle design. **a** Block design for the sharp triangle composed of trapezoidal domains. Contacts between trapezoids on their slant faces are of type 0, 1, 2, 3, and 4. Contacts of type 0 are bridged by the scaffold strand as shown in the folding path (**b**). Other contacts are bridged by special staples (**c**) that each replace two of the staple strands in the staple sequences (Supplementary Fig. S34), identified by the composite names of the bridging staples. Assuming a 1 nm inter-helix gap and 32 bases/3 turns, I calculated that the contacts would have gaps of width of 1.5696 nm, 1.0822 nm, 0.5944 nm, 0.1070 nm for contact types 1,2,3, and 4. (The gap widths drawn in the block diagram above are not accurate; contact type 4 has essentially no gap given an inter-helix gap of 1 nm.) Assuming that an unpaired thymine can bridge .43 nm (the length per base-pair of single stranded DNA<sup>34</sup>), this would require adding 3.7, 2.5, 1.4, or 0.25 T's in the bridging staple for each contact point. In fact, 4T loops are often used to bridge 2 nm wide double helices to make them into hairpins assuming .5 nm per T. I used 3, 2, 1, and 0 T's for contacts of type 1, 2, 3, and 4 as can be seen inserted into the middle of the sequence in **c**. As in other block diagrams, in **a**, turns that occur between columns of red blocks and orange blocks have offset 0 with respect to the underlying crossover lattice. Other turns on the left and right outer edges have +1 or -1 offsets depending on which side of the trapezoid they occur. Purple and green half-blocks show that scaffold turns made at the central seams are an odd number of DNA 1/2 turns away from scaffold turns on the outer edges.



Supplementary Figure S33: Crossover diagram for the sharp triangle composed of trapezoidal domains.

Plate number: 1

t10s17c,A1,TTAAATATGCA  
t10s27c,B1,ATACCGAACGA  
t10s7c,C1,TAGCACCAATT  
t11s18h,D1,AATACTCGGAAATCGTAGGGGTAATAGTAAATGTTTACGCT  
t11s28h,E1,TCTTTGATGTAATAGTCTGCCATCGCAAATTAAACGGT  
t11s8h,F1,CAGAAGGAAACCGAGGTTTTAAGAAGAATAGCAGATAGCCG  
t12s19c,G1,GGATAGCGCTC  
t12s29c,H1,GTGCAACTACT  
t12s9c,A2,AACAAAGTTAC  
t13s10g,B2,GACGGGAAATTAACTCGGATAAGTTTATTCAGCGC  
t13s11c,C2,TCATATGTAATCGAAACTAGTCATTTC  
t13s14i,D2,TTGAGAAAATGTTGAGTAAAGTACAACCTT  
t13s16i,E2,GGCATCAATTGGGGCGAGCTAGTTAAAG  
t13s18i,F2,TTCGAGCTAAGAGCTAAATCGGAAACGAG  
t13s20g,G2,GAATACCAACTTCACTAAAGGAGAACGCGATCAAGCG  
t13s21c,H2,TCGGGGATTCCTGAGCTAAAGGAAATTAAAT  
t13s24i,A3,CCTGATTAAGGGCGGAATTATCTCGGCTC  
t13s26i,B3,CGAACATCCTCACTAAATCTGCACTG  
t13s28i,C3,CGACAGCTATGGCGAATTCACTGATG  
t13s21,D3,CGGGGTTTCTCGAGAAGGAGATTGTTAG  
t13s30g,E3,TTGACGAGCGATGATGAAATGTTAAATAAAG  
t13s4i,F3,AGCGTCATGTCCTGAAATTACCGACTACCTT  
t13s11i,G3,TTCAATACCTCCATTAGTCAGTAAAG  
t13s11i,H3,ATGTTTATGTCACATCAATAGTAAAT  
t13s11g,A4,AGAAAAGCCCCAAAAGGTCTGAGCAAAACATCACC  
t13s23g,B4,CACTGAAAGATGATGAAAGCAGCCGGTGTATACT  
t13s15f,D2,ATAGTGTATGCTGCTGAGTAAAGGGGG  
t13s27f,D4,AAACAGACCTTACGCTATATTCTCTACTA  
t13s19g,E4,GATAAGTCGGTCCAGCTGAAATAGAATACAGGAG  
t13s21g,F4,CTGATTTGCTTGTAGATTCAGGCACTAATA  
t13s23g,G4,TGCAATTTCAGCTGAGTAAACATAACCGATTG  
t13s25f,H4,AAAGAACATACAGGCAACCTGAGTGA  
t13s27f,A5,GGACATTCACTTAACTACAAACAGTGT  
t13s29g,B5,TTTGATGTAAGGCGTAGCTGCTAGCAGCGGC  
t13s25f,C5,CCGAAACCCAGATGGAAAGCCAGCTG  
t13s17f,D5,AAAGACACATTTTCTGCTAGCCAAATCA  
t13s10g,E5,GTCAAGGTTTGTAGTGGCAATATAAGCGATTG  
t13s14e,F5,CAATATGACCTTATATTATTTAAAGCATTA  
t13s16e,G5,CTTGTGAACTTACAGCTAAAGGAGCA  
t13s18g,H5,AACTCCAAGATTCATCAAAAGATAATCGAGATACATA  
t13s20g,I5,TTTGTGAACTTACAGCTGAGAAGACCGCAGTC  
t13s24e,B6,TAATCTCTGATTCAGGAGAAGGG  
t13s26e,C6,TTATCAAAAGCATCCTGCTGATGCCAAC  
t13s28g,D6,AGAGTATGTTGAGTACATCTGAGTCTCTCGTT  
t13s30g,E6,AGAATCAGCGGGAGATGGAAATACCTCAAACTTCC  
t13s4e,F6,TGTACTGGAATTCCTTACCTAAAGCAGCAC  
t13s6e,G6,CACCGGAAAGCGCTTCTCATGGAGGGCGA  
t13s8g,H6,CATTCAACAAACGAGCAACAGGACACCTGGACAAAA  
t13s11g,A7,GAAATATTAAATTATGAGATCTAACAGGCTACTGTATAA  
t13s13g,B7,CTTCTCTGAGTGTAGCTATGGCTGACAGGAATGTATAA  
t13s15f,C7,CAGCGAACATTTAAAGTACATTCAGGAAATT  
t13s17f,D7,GATTAGAGATTAGATACTTCTGCAATCAT  
t13s19g,E7,TAGCCCGGAATAGGTGAATGGCCCTCTGGTAG  
t13s21g,F7,GGCAGAGCGCAATTATTTGGAGCTAACTTC  
t13s23g,G7,GATTATAACAGCAATAAGAAATACCAAGTTAAC  
t13s25f,H7,TAGGAGCATAAAGGTGAGTATGTT  
t13s27f,A8,TGACCTGACAATAGAAAATCTAAATATCTT  
t13s19g,B8,TTAACCGTTGGCACCTTATTAGGGCTGATATAAGT  
t13s5f,C8,CTCAGACCATTCACAAACAAATTAAAGT  
t13s17g,D8,GGAGGAATTAGGCGTAGCGACAGCGCTTC  
t13s10g,E8,GATAACCCACAAGATTTAGCAACCTGGGTTAG  
t13s14e,F8,TTAACCGCTTACCCCTGACTACAGGCTGGGACAGA  
t13s16e,G8,TTAACGATAGATTGTTGAGCTGACAG  
t13s18g,H8,TAATGCTTACCCCTGACTATGGAGCTAGTAAGAGC  
t13s20g,A9,AAACATCTCATACCCCAATTAGGTCTCTTGT  
t13s24e,B9,AATOGAGGCGAACGTTTAATTTCTAACAC  
t13s26g,C9,TTAAGATGCTGAGGCCAGAACAGCTGAA  
t13s28g,D9,GAATACCTGAAAGGAAACCGCTTAAACAGGAGGCC  
t13s30g,E9,TTAACGGGTTTACCTGACTACAGGCTGGGACAGA  
t13s4e,F9,CCTGAGTCAGCAGATTGGCTTGGCCACCC  
t13s6e,G9,TCAGAACCCAGAATGAGTGGCTGAGGAAATA  
t13s8g,H9,TTGAGGAAATCATACATAAGGGCTAATATCAGAGA  
t13s13c,A10,CTATTTTGAG  
t13s15g,B10,ATAAGGCTTGGGGAGAACGCTGGAGGGTAG  
t13s17f,C10,TAAGAGGTCAATTCTGCCAACAGGATTAAGCA  
t13s23c,E10,ACCATATC  
t13s25g,E10,TCATAGTATTAATACCTTGGCTTAGAACCT  
t13s27f,F10,CAATTTGGCTGCAACAGTGGCATAGAGCG  
t13s30c,G10,TATAAACAGT  
t13s16g,H10,CAGGCCAGGGAGTTGAGCAGGTAACAGTGGCG  
t13s7f,A11,ATTAAGGCGAACATGCGATGAGGACCCCT  
t13s10g,B11,ATAGAGCAAGAACATGCGATGAGTAAAGCTCGACTG  
t13s14e,C11,ATGACCTGCTGAACTTACAGCA  
t13s16e,C11,TAACAGCTTAACTAACAGTTTCCATT  
t13s18g,E11,CGGAGCCGACGAGGAAATGACCGGTTACAGAGC  
t13s20g,F11,GATAAAAACCAAAATTAAACAGGCTAACAGGAAATTAGAGCT  
t13s24e,G11,ACAACTGACAACCTGTAATCAT  
t13s26e,H11,TTGAGGTGTCAGTATTAACCTTGTAG  
t13s28g,A12,CTTATAGTATCATCGAACATAATCGAACGGTAGC  
t13s30g,B12,GAATCTGAGAAGGAGTATCGGCTCTGCTGTACTTAA  
t13s4e,C12,CGCCGAGGAGTACAGAACCCCT  
t13s6e,D12,AGAGCCGACCCATGATAGCCAGCTGAGATT  
t13s8g,E12,CACCGTCACCTTATTACCGAGTATTGAGTTAACCCA  
t13s15c,F12,CCAAAACATT  
t13s17g,G12,TAATGCTGGAAGTTTCACTCCAAATCGGTTGA  
t13s25c,H12,AGACCTTACAA

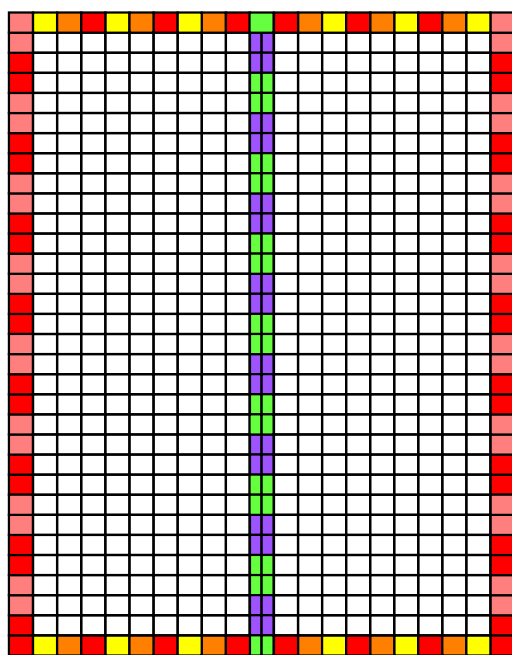
Plate number: 2

t8s27g,A1,CGCGAACTAAACAGAGGTTGAGCTTAAAGTATT  
t8s5c,B1,CCACAGAGGCC  
t8s7g,C1,AGCCATTAAACAGTCACCAATGAAACAGGAAACCA  
t9s10h,D1,TATCTTACCGGAAGCCAAACGCAATAATACGAAATTACCGAG  
t9s16e,E1,ACTAAAGTACGGTGTGAAATA  
t9s18g,F1,TCGTTGAGATCCCCTCAATAGTGGAGGGCTTTGCA  
t9s20h,G1,AAAGAAGTTTGCAGCATAAATTCATGACTAACATGTT  
t9s26e,H1,ACCCACAGAGAACATGATAGCCC  
t9s28g,A2,TAACACATTAGAGAACCTCAACATTTTATAATCAGTGA  
t9s30h,B2,GGCCAGGAGTAAAGACATACCTGGCTGAGGCCATTAAA  
t9s6e,C2,CCATTAGGGGAATT  
t9s8g,D2,GAGCAGGGAAATACCCCAAAGAGATTAAGGAAATAG  
t10s17h,D2,TTCGAGCTTAAATCAAAAGAGACCTACCC  
t10s27h,F2,AACTCATTATGAGTTGTTGAGCAAGCTCTTAC  
t10s7h,G2,ACGAAATAAATCCGAGTTCGGGGAGATCTGAATCTTACCA  
t11s18e,H2,ATAAGGCTTGA  
t11s28e,A3,ACTTAAAGAAG  
t11s18e,B3,TCAGAATTAGT  
t12s19h,C3,CCTGACGAAACACAGAGAAGCTGCTATTAGTGA  
t12s28h,D2,ACCTGAGCTACCAAGCTAACAGGAAATTGGGACAGAGTCC  
t12s9h,E3,TGCTATTGTCAGCAGCTACATAATTGTTGAGCCTTAA  
t13s10e,F3,AGAGAAATAACATAAAACAGGGAGGAGCATT  
t13s12i,G3,AGGGATAGCTGAGCACCCAGGAGCATT  
t13s14e,H3,ATTTCCTGAGCAGGAGTGAAGATACGGATAT  
t13s14i,H2,CAGAGTGTGGATTGAGTTGCTAATCAAAAGG  
t13s16e,B4,ATTCCGTTGCGGGAGCTGTCACCCGAAATCC  
t13s16i,C4,GGCCGTTTGGCTGAGTACGGAGGGAAAGGT  
t13s18g,D4,CGACCTGGGCTCAATCATAGGGAGGACAAACATT  
t13s18i,D4,GGCAGACTTCTGTTTACAGTGAAGGTTTAA  
t13s20e,F4,CGAGTAGAAAGATTCAGTTGAGGTTTAA  
t13s21i,G4,CGGCTGTGATAGGAAACGCATCAACATT  
t13s24e,H4,CAGTTTGGACGCCCTCAGGAGCTAACAGCAG  
t13s24i,A5,AGGAAGATGGGAGCAGCAGACATTA  
t13s26e,B5,GGCATGGGATCCGGGAGTACCGAGTTTCT  
t13s26i,C5,CTCTAGACGAACTGGCATCTGCTGTT  
t13s28g,D5,TTTACCGAGCGGCCAGGAGAAGCCGGAGCTGG  
t13s28i,E5,CCTTACCGAGCTGGAGGCAACGAGCTC  
t13s21i,F5,CCTTTTCTCATTAACATTTCATGAGTTAG  
t13s18e,B5,CGAGAAAGGGAGGAGCTACTGGTT  
t13s4e,H5,TTTACCAACGGCTTACGGTTGAGCTGT  
t13s14i,A6,TTTACCTATCATGGCTGAGTGGCTTCA  
t13s16e,B6,TATGTTCTCAGCAGGAAACAGCATTCT  
t13s16i,C6,AGTAAATAATGTTGAGTTAAACAGGCTAC  
t13s18g,D6,TTTCTCTGAGCTTACGAGAACATGAGCCTTAC  
t13s81i,E6,CAAGTACCTTACCAAGAACGGAAATT  
t13s25i,E7,CCTCAGAACGCCAACCCAGGAACTTAC  
t13s13g,G6,AGACGTTACCATGCTGAGGTT  
t13s25g,F8,AGAGTAAACATGAGGTTTACAGGAACT  
t13s17f,A7,ATTGTGTTCTCAGCAGGAAACAGCATT  
t13s21g,B7,AGAGTAAACATGAGGTTTACAGGAACT  
t13s21g,C7,GTCTTACCTTACGAGCCTTCTGAGGAGCAGCT  
t13s23g,D7,GTAAACCGTTTCATCAACATTAAATTTGTT  
t13s25f,E7,ACGTTGATTCGGCAGGCCGAG  
t13s27f,F7,CGAGGTGGCTCGAGTAACTGAGT  
t13s29g,G7,AGAGTAAACATGAGGTTTACAGGAACT  
t13s25f,H7,ACTAGAAATAATACATATGAGCTGAG  
t13s27f,A8,TCATAACTAGGGCTTAAAGGAGAT  
t13s21g,C7,GTCTTACCTTACGAGCCTTCTGAGGAGCAGCT  
t13s23g,D7,GTAAACCGTTTCATCAACATTAAATTTGTT  
t13s25f,E7,ACGTTGATTCGGCAGGCCGAG  
t13s27f,F7,CGAGGTGGCTCGAGTAACTGAGT  
t13s29g,G7,AGAGTAAACATGAGGTTTACAGGAACT  
t13s30g,B8,AGAGTAAACATGAGGTTTACAGGAACT  
t13s31e,D8,GACAACAGCATCGAACGGAGGTGAGATT  
t13s18g,E8,TATCATCTGAGAAGGGACAGTGGAGAAATT  
t13s20g,F8,TTAGTGTGGTGGCGGAGAACGGCG  
t13s24e,H8,GGTTCTTACCTGATAGCTGTTGAGGAGCG  
t13s28g,A9,TTTGGGCTCAGCTGGTCTGGGAACTGGGAG  
t13s30g,B9,TTAGGCTGAGGGAGTTGAGCAGGCTAC  
t13s31e,C9,TTTGGGCTCAGCTGGTCTGGGAACTGGGAG  
t13s31e,D9,CACCGGAACTGGCTCATTTAAACAAATT  
t13s31g,E8,TATCATCTGAGAAGGGACAGTGGAGAAATT  
t13s32g,F8,TTAGTGTGGTGGCGGAGAACGGCG  
t13s32g,H8,GGTTCTTACCTGATAGCTGTTGAGGAGCG  
t13s32g,B9,TTAGGCTGAGGGAGTTGAGCAGGCTAC  
t13s34e,C9,TTTGGGCTCAGCTGGTCTGGGAACTGGGAG  
t13s34e,D9,GATAAAAGATCTGAGTAACTGAG  
t13s35g,E9,AGGTTAGTACCCGAGTGGAGAAATT  
t13s31g,F9,AGGTTAGTACCCGAGTGGAGAAATT  
t13s31g,G9,AGGTTAGTACCCGAGTGGAGAAATT  
t13s45f,H9,TAGTTGGCAATTTCAGCTGT  
t13s17f,A10,GTACAAACGAGAACGGCTACAGGAGTACCGA  
t13s18g,B10,AGGAAAGAGTTGAGTGAATTAACCT  
t13s21g,C10,GTAAAATTCTGCAATTAGTGAGCAGGAGTA  
t13s23g,D10,GAGATGGTACCCGTCGGATTCTCT  
t13s25f,E10,AGTTGGCTAACGGCCATT  
t13s27f,F10,CGCCGGCTCTGGTGAAT  
t13s32g,G10,ACATAGGGCTTAATCTGCTGTT  
t13s45f,H10,GTAAAATTCTGCAATTAGTGAGCAGGAGTA  
t13s47f,A11,CCCATCTCTGCCAACATGTAATTAAAGG  
t13s50g,B11,TCCCAATTCAAAATAGATTACCGGCC  
t13s51e,C11,TGTGAGTAC  
t13s51e,D11,ACAGACTTGTGAGGACTAAAGCGATT  
t13s51g,B11,CCAAAGCCAGGGCTAGGGCTGGCAAG  
t13s52g,F11,ACAGACTTGTGAGGACTAAAGCGATT  
t13s52g,H11,GTGGAACAACT  
t13s52g,A12,TTAATGAGTT  
t13s53g,C12,CTAACATGGAACTGCAATT  
t13s56e,D12,AGAGTGAATGGAGGAGGCTTAC  
t13s58g,E12,ACAGAAAGCAAGAACATGAGTA  
t13s61g,F12,ACAGACAGGCCAAATCTCC  
t13s61g,G12,CGAGGTGAGGCTCCAAAAGGAGC  
t13s61g,H12,ACCCCGAGACTTTCTCATGAGGA  
t13s61g,I12,AGACCTTACCCGAGGCTTAC

Plate number: 3

t-6s23f,A1,CGGGGATTGAAATTCAAGGCTGCCAACGGGGATG  
t-6s25c,B1,TGGCGAAATGTTGGGAAAGGGCGAT  
t-6s27f,C1,TGTCGTCGACAAACATAGGAGGCCAC  
t-6s3f,D1,CCCTCTGAAATAACGGGAAACATT  
t-6s5c,E1,GTGGAATTCAAAATT  
t-6s7f,F1,AATAGATGAGCCAGTA  
t-7s10g,G1,GGCAGTTACAAATAATAGAGGTTTAT  
t-7s14e,H1,TTTAAATTGTT  
t-7s18g,A2,AAACACTTAATCTGACAGAACTTA  
t-7s20g,B2,ACCTTATGCGATTTTATGACCTTC  
t-7s24e,C2,CGGCTGGGG  
t-7s24h,D2,TTCAAGCTTAACTGGGCT  
t-7s30g,E2,CAAGTTTTGGGTCGAATCGGCAAAACGG  
t-7s4e,F2,TTAGTGTGAGCT  
t-7s8g,G2,GGCGCTGTTTACAGCGGCT  
t-7s8g,H2,CGGGCTGTTTACAGCGGCT  
t-7s8g,I2,GGGGCTGTTTACAGCGGCT  
t-7s8g,J2,GGGGCTGTTTACAGCGGCT  
t-7s8g,K2,GGGGCTGTTTACAGCGGCT  
t-7s8g,L2,GGGGCTGTTTACAGCGGCT  
t-7s8g,M2,GGGGCTGTTTACAGCGGCT  
t-7s8g,N2,GGGGCTGTTTACAGCGGCT  
t-7s8g,O2,GGGGCTGTTTACAGCGGCT  
t-7s8g,P2,GGGGCTGTTTACAGCGGCT  
t-7s8g,Q2,GGGGCTGTTTACAGCGGCT  
t-7s8g,R2,GGGGCTGTTTACAGCGGCT  
t-7s8g,S2,GGGGCTGTTTACAGCGGCT  
t-7s8g,T2,GGGGCTGTTTACAGCGGCT  
t-7s8g,U2,GGGGCTGTTTACAGCGGCT  
t-7s8g,V2,GGGGCTGTTTACAGCGGCT  
t-7s8g,W2,GGGGCTGTTTACAGCGGCT  
t-7s8g,X2,GGGGCTGTTTACAGCGGCT  
t-7s8g,Y2,GGGGCTGTTTACAGCGGCT  
t-7s8g,Z2,GGGGCTGTTTACAGCGGCT  
t-7s8g,A3,GGGCTGTTTACAGCGGCT  
t-7s8g,B4,GGGGCTGTTTACAGCGGCT  
t-7s8g,C5,GGGCTGTTTACAGCGGCT  
t-7s8g,D6,GGGGCTGTTTACAGCGGCT  
t-7s8g,E7,GGGGCTGTTTACAGCGGCT  
t-7s8g,F8,GGGGCTGTTTACAGCGGCT  
t-7s8g,G9,GGGGCTGTTTACAGCGGCT  
t-7s8g,H10,GGGGCTGTTTACAGCGGCT  
t-7s8g,I11,GGGGCTGTTTACAGCGGCT  
t-7s8g,J12,GGGGCTGTTTACAGCGGCT  
t-7s8g,K13,GGGGCTGTTTACAGCGGCT  
t-7s8g,L14,GGGGCTGTTTACAGCGGCT  
t-7s8g,M15,GGGGCTGTTTACAGCGGCT  
t-7s8g,N16,GGGGCTGTTTACAGCGGCT  
t-7s8g,O17,GGGGCTGTTTACAGCGGCT  
t-7s8g,P18,GGGGCTGTTTACAGCGGCT  
t-7s8g,Q19,GGGGCTGTTTACAGCGGCT  
t-7s8g,R20,GGGGCTGTTTACAGCGGCT  
t-7s8g,S21,GGGGCTGTTTACAGCGGCT  
t-7s8g,T22,GGGGCTGTTTACAGCGGCT  
t-7s8g,U23,GGGGCTGTTTACAGCGGCT  
t-7s8g,V24,GGGGCTGTTTACAGCGGCT  
t-7s8g,W25,GGGGCTGTTTACAGCGGCT  
t-7s8g,X26,GGGGCTGTTTACAGCGGCT  
t-7s8g,Y27,GGGGCTGTTTACAGCGGCT  
t-7s8g,Z28,GGGGCTGTTTACAGCGGCT  
t-7s8g,A3,GGGGCTGTTTACAGCGGCT  
t-7s8g,B4,GGGGCTGTTTACAGCGGCT  
t-7s8g,C5,GGGGCTGTTTACAGCGGCT  
t-7s8g,D6,GGGGCTGTTTACAGCGGCT  
t-7s8g,E7,GGGGCTGTTTACAGCGGCT  
t-7s8g,F8,GGGGCTGTTTACAGCGGCT  
t-7s8g,G9,GGGGCTGTTTACAGCGGCT  
t-7s8g,H10,GGGGCTGTTTACAGCGGCT  
t-7s8g,I11,GGGGCTGTTTACAGCGGCT  
t-7s8g,J12,GGGGCTGTTTACAGCGGCT  
t-7s8g,K13,GGGGCTGTTTACAGCGGCT  
t-7s8g,L14,GGGGCTGTTTACAGCGGCT  
t-7s8g,M15,GGGGCTGTTTACAGCGGCT  
t-7s8g,N16,GGGGCTGTTTACAGCGGCT  
t-7s8g,O17,GGGGCTGTTTACAGCGGCT  
t-7s8g,P18,GGGGCTGTTTACAGCGGCT  
t-7s8g,Q19,GGGGCTGTTTACAGCGGCT  
t-7s8g,R20,GGGGCTGTTTACAGCGGCT  
t-7s8g,S21,GGGGCTGTTTACAGCGGCT  
t-7s8g,T22,GGGGCTGTTTACAGCGGCT  
t-7s8g,U23,GGGGCTGTTTACAGCGGCT  
t-7s8g,V24,GGGGCTGTTTACAGCGGCT  
t-7s8g,W25,GGGGCTGTTTACAGCGGCT  
t-7s8g,X26,GGGGCTGTTTACAGCGGCT  
t-7s8g,Y27,GGGGCTGTTTACAGCGGCT  
t-7s8g,Z28,GGGGCTGTTTACAGCGGCT  
t-7s8g,A3,GGGGCTGTTTACAGCGGCT  
t-7s8g,B4,GGGGCTGTTTACAGCGGCT  
t-7s8g,C5,GGGGCTGTTTACAGCGGCT  
t-7s8g,D6,GGGGCTGTTTACAGCGGCT  
t-7s8g,E7,GGGGCTGTTTACAGCGGCT  
t-7s8g,F8,GGGGCTGTTTACAGCGGCT  
t-7s8g,G9,GGGGCTGTTTACAGCGGCT  
t-7s8g,H10,GGGGCTGTTTACAGCGGCT  
t-7s8g,I11,GGGGCTGTTTACAGCGGCT  
t-7s8g,J12,GGGGCTGTTTACAGCGGCT  
t-7s8g,K13,GGGGCTGTTTACAGCGGCT  
t-7s8g,L14,GGGGCTGTTTACAGCGGCT  
t-7s8g,M15,GGGGCTGTTTACAGCGGCT  
t-7s8g,N16,GGGGCTGTTTACAGCGGCT  
t-7s8g,O17,GGGGCTGTTTACAGCGGCT  
t-7s8g,P18,GGGGCTGTTTACAGCGGCT  
t-7s8g,Q19,GGGGCTGTTTACAGCGGCT  
t-7s8g,R20,GGGGCTGTTTACAGCGGCT  
t-7s8g,S21,GGGGCTGTTTACAGCGGCT  
t-7s8g,T22,GGGGCTGTTTACAGCGGCT  
t-7s8g,U23,GGGGCTGTTTACAGCGGCT  
t-7s8g,V24,GGGGCTGTTTACAGCGGCT  
t-7s8g,W25,GGGGCTGTTTACAGCGGCT  
t-7s8g,X26,GGGGCTGTTTACAGCGGCT  
t-7s8g,Y27,GGGGCTGTTTACAGCGGCT  
t-7s8g,Z28,GGGGCTGTTTACAGCGGCT  
t-7s8g,A3,GGGGCTGTTTACAGCGGCT  
t-7s8g,B4,GGGGCTGTTTACAGCGGCT  
t-7s8g,C5,GGGGCTGTTTACAGCGGCT  
t-7s8g,D6,GGGGCTGTTTACAGCGGCT  
t-7s8g,E7,GGGGCTGTTTACAGCGGCT  
t-7s8g,F8,GGGGCTGTTTACAGCGGCT  
t-7s8g,G9,GGGGCTGTTTACAGCGGCT  
t-7s8g,H10,GGGGCTGTTTACAGCGGCT  
t-7s8g,I11,GGGGCTGTTTACAGCGGCT  
t-7s8g,J12,GGGGCTGTTTACAGCGGCT  
t-7s8g,K13,GGGGCTGTTTACAGCGGCT  
t-7s8g,L14,GGGGCTGTTTACAGCGGCT  
t-7s8g,M15,GGGGCTGTTTACAGCGGCT  
t-7s8g,N16,GGGGCTGTTTACAGCGGCT  
t-7s8g,O17,GGGGCTGTTTACAGCGGCT  
t-7s8g,P18,GGGGCTGTTTACAGCGGCT  
t-7s8g,Q19,GGGGCTGTTTACAGCGGCT  
t-7s8g,R20,GGGGCTGTTTACAGCGGCT  
t-7s8g,S21,GGGGCTGTTTACAGCGGCT  
t-7s8g,T22,GGGGCTGTTTACAGCGGCT  
t-7s8g,U23,GGGGCTGTTTACAGCGGCT  
t-7s8g,V24,GGGGCTGTTTACAGCGGCT  
t-7s8g,W25,GGGGCTGTTTACAGCGGCT  
t-7s8g,X26,GGGGCTGTTTACAGCGGCT  
t-7s8g,Y27,GGGGCTGTTTACAGCGGCT  
t-7s8g,Z28,GGGGCTGTTTACAGCGGCT  
t-7s8g,A3,GGGGCTGTTTACAGCGGCT  
t-7s8g,B4,GGGGCTGTTTACAGCGGCT  
t-7s8g,C5,GGGGCTGTTTACAGCGGCT  
t-7s8g,D6,GGGGCTGTTTACAGCGGCT  
t-7s8g,E7,GGGGCTGTTTACAGCGGCT  
t-7s8g,F8,GGGGCTGTTTACAGCGGCT  
t-7s8g,G9,GGGGCTGTTTACAGCGGCT  
t-7s8g,H10,GGGGCTGTTTACAGCGGCT  
t-7s8g,I11,GGGGCTGTTTACAGCGGCT  
t-7s8g,J12,GGGGCTGTTTACAGCGGCT  
t-7s8g,K13,GGGGCTGTTTACAGCGGCT  
t-7s8g,L14,GGGGCTGTTTACAGCGGCT  
t-7s8g,M15,GGGGCTGTTTACAGCGGCT  
t-7s8g,N16,GGGGCTGTTTACAGCGGCT  
t-7s8g,O17,GGGGCTGTTTACAGCGGCT  
t-7s8g,P18,GGGGCTGTTTACAGCGGCT  
t-7s8g,Q19,GGGGCTGTTTACAGCGGCT  
t-7s8g,R20,GGGGCTGTTTACAGCGGCT  
t-7s8g,S21,GGGGCTGTTTACAGCGGCT  
t-7s8g,T22,GGGGCTGTTTACAGCGGCT  
t-7s8g,U23,GGGGCTGTTTACAGCGGCT  
t-7s8g,V24,GGGGCTGTTTACAGCGGCT  
t-7s8g,W25,GGGGCTGTTTACAGCGGCT  
t-7s8g,X26,GGGGCTGTTTACAGCGGCT  
t-7s8g,Y27,GGGGCTGTTTACAGCGGCT  
t-7s8g,Z28,GGGGCTGTTTACAGCGGCT  
t-7s8g,A3,GGGGCTGTTTACAGCGGCT  
t-7s8g,B4,GGGGCTGTTTACAGCGGCT  
t-7s8g,C5,GGGGCTGTTTACAGCGGCT  
t-7s8g,D6,GGGGCTGTTTACAGCGGCT  
t-7s8g,E7,GGGGCTGTTTACAGCGGCT  
t-7s8g,F8,GGGGCTGTTTACAGCGGCT  
t-7s8g,G9,GGGGCTGTTTACAGCGGCT  
t-7s8g,H10,GGGGCTGTTTACAGCGGCT  
t-7s8g,I11,GGGGCTGTTTACAGCGGCT  
t-7s8g,J12,GGGGCTGTTTACAGCGGCT  
t-7s8g,K13,GGGGCTGTTTACAGCGGCT  
t-7s8g,L14,GGGGCTGTTTACAGCGGCT  
t-7s8g,M15,GGGGCTGTTTACAGCGGCT  
t-7s8g,N16,GGGGCTGTTTACAGCGGCT  
t-7s8g,O17,GGGGCTGTTTACAGCGGCT  
t-7s8g,P18,GGGGCTGTTTACAGCGGCT  
t-7s8g,Q19,GGGGCTGTTTACAGCGGCT  
t-7s8g,R20,GGGGCTGTTTACAGCGGCT  
t-7s8g,S21,GGGGCTGTTTACAGCGGCT  
t-7s8g,T22,GGGGCTGTTTACAGCGGCT  
t-7s8g,U23,GGGGCTGTTTACAGCGGCT  
t-7s8g,V24,GGGGCTGTTTACAGCGGCT  
t-7s8g,W25,GGGGCTGTTTACAGCGGCT  
t-7s8g,X26,GGGGCTGTTTACAGCGGCT  
t-7s8g,Y27,GGGGCTGTTTACAGCGGCT  
t-7s8g,Z28,GGGGCTGTTTACAGCGGCT  
t-7s8g,A3,GGGGCTGTTTACAGCGGCT  
t-7s8g,B4,GGGGCTGTTTACAGCGGCT  
t-7s8g,C5,GGGGCTGTTTACAGCGGCT  
t-7s8g,D6,GGGGCTGTTTACAGCGGCT  
t-7s8g,E7,GGGGCTGTTTACAGCGGCT  
t-7s8g,F8,GGGGCTGTTTACAGCGGCT  
t-7s8g,G9,GGGGCTGTTTACAGCGGCT  
t-7s8g,H10,GGGGCTGTTTACAGCGGCT  
t-7s8g,I11,GGGGCTGTTTACAGCGGCT  
t-7s8g,J12,GGGGCTGTTTACAGCGGCT  
t-7s8g,K13,GGGGCTGTTTACAGCGGCT  
t-7s8g,L14,GGGGCTGTTTACAGCGGCT  
t-7s8g,M15,GGGGCTGTTTACAGCGGCT  
t-7s8g,N16,GGGGCTGTTTACAGCGGCT  
t-7s8g,O17,GGGGCTGTTTACAGCGGCT  
t-7s8g,P18,GGGGCTGTTTACAGCGGCT  
t-7s8g,Q19,GGGGCTGTTTACAGCGGCT  
t-7s8g,R20,GGGGCTGTTTACAGCGGCT  
t-7s8g,S21,GGGGCTGTTTACAGCGGCT  
t-7s8g,T22,GGGGCTGTTTACAGCGGCT  
t-7s8g,U23,GGGGCTGTTTACAGCGGCT  
t-7s8g,V24,GGGGCTGTTTACAGCGGCT  
t-7s8g,W25,GGGGCTGTTTACAGCGGCT  
t-7s8g,X26,GGGGCTGTTTACAGCGGCT  
t-7s8g,Y27,GGGGCTGTTTACAGCGGCT  
t-7s8g,Z28,GGGGCTGTTTACAGCGGCT  
t-7s8g,A3,GGGGCTGTTTACAGCGGCT  
t-7s8g,B4,GGGGCTGTTTACAGCGGCT  
t-7s8g,C5,GGGGCTGTTTACAGCGGCT  
t-7s8g,D6,GGGGCTGTTTACAGCGGCT  
t-7s8g,E7,GGGGCTGTTTACAGCGGCT  
t-7s8g,F8,GGGGCTGTTTACAGCGGCT  
t-7s8g,G9,GGGGCTGTTTACAGCGGCT  
t-7s8g,H10,GGGGCTGTTTACAGCGGCT  
t-7s8g,I11,GGGGCTGTTTACAGCGGCT  
t-7s8g,J12,GGGGCTGTTTACAGCGGCT  
t-7s8g,K13,GGGGCTGTTTACAGCGGCT  
t-7s8g,L14,GGGGCTGTTTACAGCGGCT  
t-7s8g,M15,GGGGCTGTTTACAGCGGCT  
t-7s8g,N16,GGGGCTGTTTACAGCGGCT  
t-7s8g,O17,GGGGCTGTTTACAGCGGCT  
t-7s8g,P18,GGGGCTGTTTACAGCGGCT  
t-7s8g,Q19,GGGGCTGTTTACAGCGGCT  
t-7s8g,R20,GGGGCTGTTTACAGCGGCT  
t-7s8g,S21,GGGGCTGTTTACAGCGGCT  
t-7s8g,T22,GGGGCTGTTTACAGCGGCT  
t-7s8g,U23,GGGGCTGTTTACAGCGGCT  
t-7s8g,V24,GGGGCTGTTTACAGCGGCT  
t-7s8g,W25,GGGGCTGTTTACAGCGGCT  
t-7s8g,X26,GGGGCTGTTTACAGCGGCT  
t-7s8g,Y27,GGGGCTGTTTACAGCGGCT  
t-7s8g,Z28,GGGGCTGTTTACAGCGGCT  
t-7s8g,A3,GGGGCTGTTTACAGCGGCT  
t-7s8g,B4,GGGGCTGTTTACAGCGGCT  
t-7s8g,C5,GGGGCTGTTTACAGCGGCT  
t-7s8g,D6,GGGGCTGTTTACAGCGGCT  
t-7s8g,E7,GGGGCTGTTTACAGCGGCT  
t-7s8g,F8,GGGGCTGTTTACAGCGGCT  
t-7s8g,G9,GGGGCTGTTTACAGCGGCT  
t-7s8g,H10,GGGGCTGTTTACAGCGGCT  
t-7s8g,I11,GGGGCTGTTTACAGCGGCT  
t-7s8g,J12,GGGGCTGTTTACAGCGGCT  
t-7s8g,K13,GGGGCTGTTTACAGCGGCT  
t-7s8g,L14,GGGGCTGTTTACAGCGGCT  
t-7s8g,M15,GGGGCTGTTTACAGCGGCT  
t-7s8g,N16,GGGGCTGTTTACAGCGGCT  
t-7s8g,O17,GGGGCTGTTTACAGCGGCT  
t-7s8g,P18,GGGGCTGTTTACAGCGGCT  
t-7s8g,Q19,GGGGCTGTTTACAGCGGCT  
t-7s8g,R20,GGGGCTGTTTACAGCGGCT  
t-7s8g,S21,GGGGCTGTTTACAGCGGCT  
t-7s8g,T22,GGGGCTGTTTACAGCGGCT  
t-7s8g,U23,GGGGCTGTTTACAGCGGCT

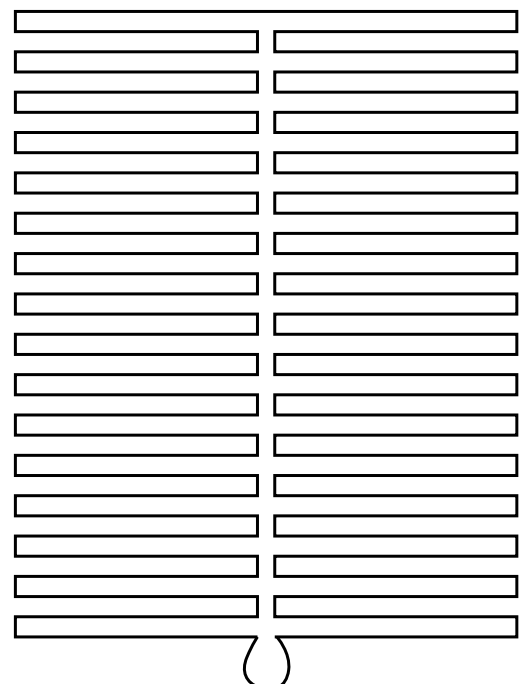
**a**



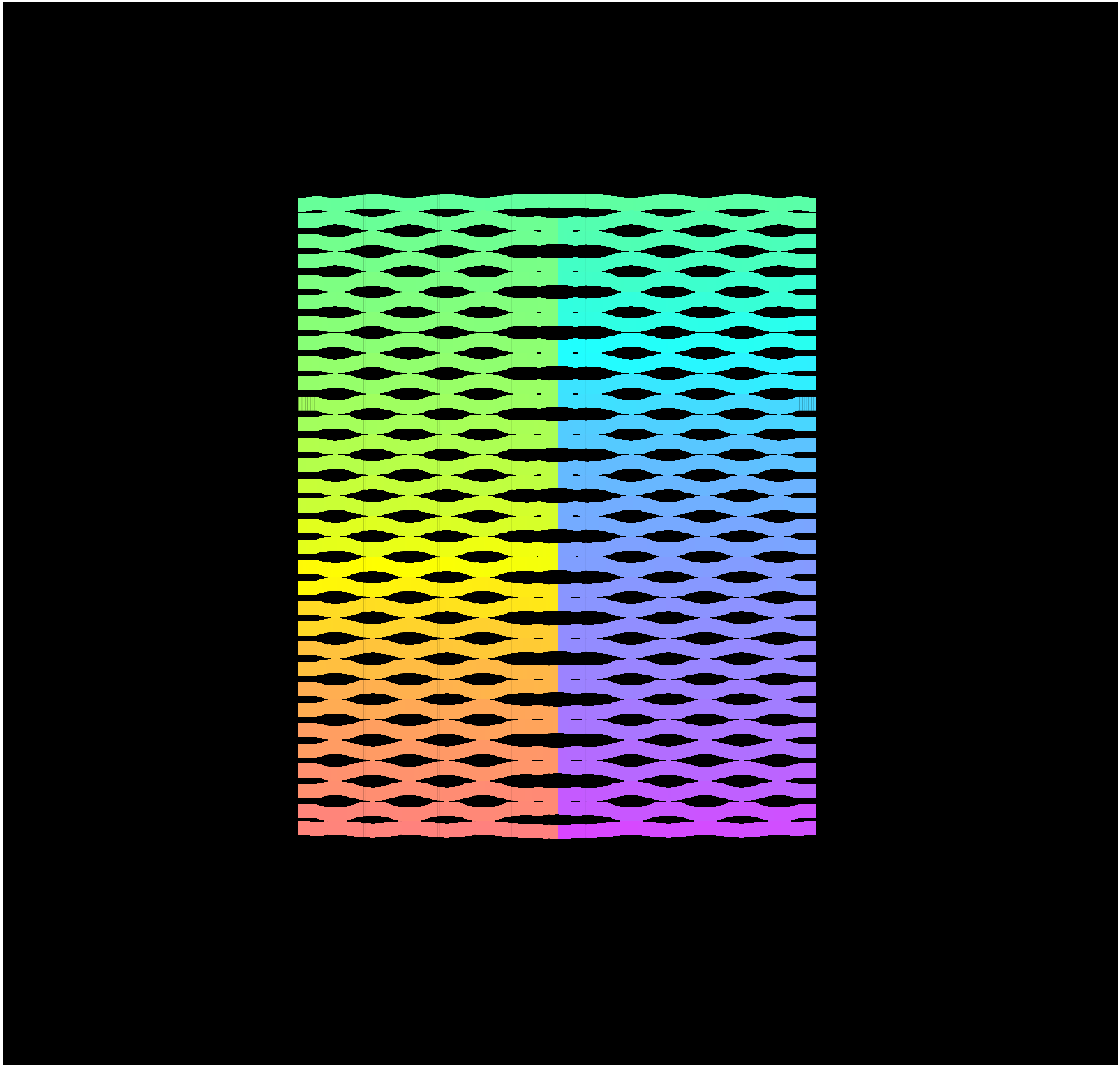
21 turns wide at 10.666 bases / turn -> 224 nt

32 helices tall

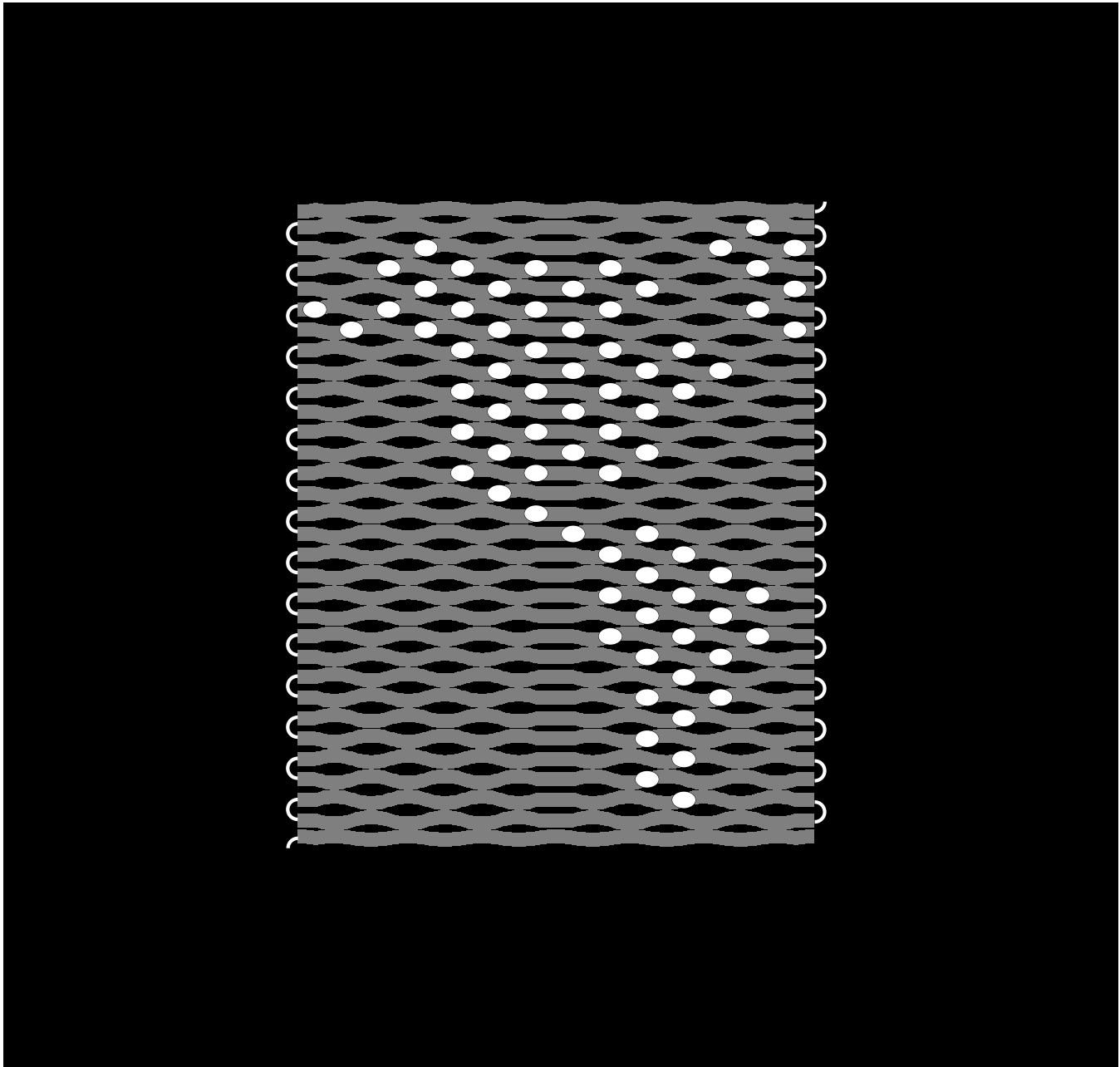
**b**



Supplementary Figure S35: Schematics for the “tall” rectangle used for the map pattern shown in Fig. 4e-i. **a** Block diagram. **b** Folding path.



Supplementary Figure S36: Basic crossover diagram for the “tall” rectangle used for the map pattern shown in Fig. 3e-i. Note, here I show the crossovers at the seam as bridged by staple strands. In the experiments shown in Fig. 3f and g, the seam was unbridged and only stacking interactions held it together, as diagrammed in Fig. 3e. For comparison, Fig. 3e is reproduced in the next figure, Supplementary Fig. S36



Supplementary Figure S37: Actual crossover diagram for the “tall” rectangle used for the map pattern shown in Fig. 3e–i. The seam is unbridged and staple strands with ‘TTTT’ loops have been added to the edges to discourage blunt-end stacking. At two corners 4-T tails have been added.

Plate number: 1

tir0g,A1, AGGGTTGATATAAGTATAGCCCGGAATAGGTG  
tir10e,B1, TGAAACAAAGATAACCCACAAGAATAAGACTCC  
tir12e,D1, TATTITTCAGCCTAACAGGCCTCTGAAACCC  
tir12f,E1, TCTTACCAACCCAGACTAACATTTTAAAGAAGT  
tir14e,F1, ATCCGGCTGACCAGATACCGCACTCTAGTGG  
tir14f,G1, GGTATTAACTTTCCTTATCATTCATATCCCG  
tir16e,H1, CATATTATTTCGGCAGTAATAAACATA  
tir16f,A2, AGAGGCCATACACCCACCATGATCTGGCAA  
tir18e,B2, ATAGGAGACTTCTTCGACAGATCG  
tir18f,C2, TTTTAGTCGGAGAAAACCTTTTATGACC  
tir20e,D2, AAATCAATCTGTCGCTTAAATTCAGGCAAG  
tir20f,E2, CTGAAATATATGTGTAAGTAAAGGCTA  
tir22e,F2, TTAACGTCGGAGAACATAACAGTACAT  
tir22f,G2, CTTTTACACAGATAATCACGTCATCA  
tir24e,H2, TTATTAAAGAACAAAACCCCTTTCAGG  
tir24f,H3, ATTTTCGGTTAAAGAATTGACCGGACC  
tir26e,B3, CTAAAGCAACATCATATCTGGTACCCGAACG  
tir26f,C3, AAACCCCTTACCTCTCTGCAACGGAGATC  
tir28e,D3, GCCACAGATACGGTCAGACATGAAAAT  
tir28f,E3, GGTAGAAGATAGAACCCCTTGAACGCCG  
tir2e,F3, TAAGCGTCGGTAGAAGTAACTTTCAG  
tir2f,G3, AGTGFACTATACATGCGTTTGTATCTTCAG  
tir3e,H3, GTTGTTAGCCGAGTGAAGAATGATCTG  
tir30f,A4, ATCACTGAATACTTCTTGTAGTTGTTCTC  
tir32h,A4, TAACGGGGCCCTGATCTGGTTAAATTAAC  
tir4e,C4, ACACAGAGACCCCTAACGGCACCTCCAG  
tir4f,D4, GAGCCGCCAACCGGCTGGCCG  
tir6e,E4, ACTTGGGTAGCACCATACCATAACCGG  
tir6f,F4, ATACACCCATTGGGAAATTAGCAACACTA  
tir8e,G4, TTATTACGTTAACGCAATACCGTCACC  
tir8f,H4, TACATACACAGTATGTTAGCAACTTACAGA  
tir9e,O5, ATGCTCAGTACCGGGGATAAGTGGGGTCA  
tir10e,B5, GCGCATTAAGAACGCAAGAACATAACCGA  
tir10f,C5, GCCCAATAGACGGGAAATTACTTCCAGAG  
tir12e,D5, AGGTTTGGGCAAGTAAACAAATACGGGAA  
tir12f,E5, CTAAATTAAAGCCTTAATCAAGAATCGAAA  
tir14e,E6, CTAAATTACCGCTTAACTTCTTCAGCGG  
tir14f,G5, CAACGACAGGAGCATGTAAGAACAGAGATA  
tir16e,H5, ACGCTCACGACAAAGGTTACCTTCATC  
tir16f,A6, TAAGACTTACCGTAGGCTTAAATGCTAAATT  
tir18e,B6, TATCTGAAAGAATTACGCCGCTTAAAGGCA  
tir18f,C6, AATGGTTTGGCTGTGAACTAACCTTCCCT  
tir20e,D6, TGIAATTATGAAAATACAGGATAATTAAC  
tir20f,E6, TAGAACCCCTTAACTTACGGGACATTG  
tir22e,F6, ACAGAAATCTTGTAACTAACAGGAAACAT  
tir22f,G6, CCTGATTTGAAAGGATGAGTAAAGGAGG  
tir24e,H6, CGAACACTTACATCATTCCTGATCAGTAA  
tir24f,A7, CGGAAATTACGTATTAATCCCTTGGTGGCAA  
tir26e,B7, GCCACGCTTGGCATGATTGGAGAACATT  
tir26f,C7, ATCACAGGAGACGCCAGCAAAATTTT  
tir28e,D7, GTACACAGTACTTTACGGGCAACAGT  
tir28f,E7, GAATGGCTTACCAAGTAAAGGAAACAT  
tir2e,F7, CCTGATTTGAAAGGATGAAAGGAGG  
tir2f,G7, TGCGCTGACAGTCTGTAATTACCCCTCAGA  
tir30e,H7, GTAAAAGACTGTGTAATTCAGAAATTACCA  
tir30f,A8, CGGCCCTGGTCTGTCATCACGCAITGAGG  
tir32h,B8, CACTATAAACGTCCTTCTGTTGCCACCG  
tir3e,C8, GTTGCCCACCTTACGGGCAACAG  
tir4f,D8, GCCCCACACTTTCAATAATCAAGCAAG  
tir6e,E8, TTATTCATGTCACCAAGAACATTATGAC  
tir6f,F8, CCGAAACTAACAGGTGAATTATCAAAAAGA  
tir8e,B8, ATACCCAACACCCAGGAATAAGTGCAGGAAA  
tir8f,H8, ACGCHAAGAAGACTGGCATGATTGAGTTAA  
tir9g,A9, CCTCAAGAGAGATTGAGATTGAGAACAGTT  
tir10e,B9, CTTACACGATTTACTTACCGGACCGTACCA  
tir10f,C9, GCAATAGCAGGAAATACATAAACACGGAT  
tir12e,D9, GAGGCCCTTCCCAATTAAGATGACAGC  
tir12f,E9, ATTATTTATAGCGAACCTCCCGAGCTGAA  
tir14e,F9, TAAGTCTTGCAGGAACTAGCAGAACAGC  
tir14f,G9, TCATACCGAACAGAAATTATAATTCTG  
tir16e,H9, GGCTTACGACAATAAACACATACAATAGA  
tir16f,A10, CGAGACGACAACTTACCGAGATAAATA  
tir18e,B10, TAACCTTCAATAAGAATAAACACATATAT  
tir18f,C10, AGGGTTAGGCTTACGGTTGGGAACTTGA  
tir20e,D10, AAACAAACTGAGAACGACTTAATACCTTT  
tir20f,E10, TTAAGACGATAATTACATTAACAAACATC  
tir22e,F10, AACTTACCGGAAATCATTCATCATCACAG  
tir22f,G10, GCCCAAGAGATACAAAATTATTGTTACAG  
tir24e,H10, GGATTAGTTCTCATTAATACCAAGGTTAG  
tir24f,A11, GATGCCAAAGATTAGACTTTACCAAGGTT  
tir26e,B11, AGGGCTCTTCTTAAATACGTGAGAGATCAG  
tir26f,C11, CTAAATAAGATTACACCCGCTCGAAGTGA  
tir28e,D11, GAATAGCAGAACATGCCATTAAAGCAGGTG  
tir28f,E11, TAGCCCTTATTATTAATTCAGAACGAACTTAA  
tir2e,F11, ACAAACACTGCTTACCGGAACTCGAGACT  
tir2f,G11, AATGGGAAATCATGAGGAAACCGGAAAC  
tir3o,H11, AGAGTCATGTCACACGAAAATCTGCTT  
tir30f,A12, CGCCGACGCTTAAATACGTGAGAGATCAG  
tir32h,B12, AGGGGAGCTAACAGGAGGAGAACATCTG  
tir34e,C12, TGCGCATTCGGCCGGAGCATGATGATATT  
tir4f,D12, CACCAAGGTCTGGTCTAGACCCCTCGATAG  
tir6e,E12, ATTGAGGAATCATGAGCAGACAGCTTCA  
tir6f,F12, AGCCCGTAGGGAAGGAAATTTATTT  
tir8e,G12, GAAGAAAAATGAAAGATCATTCACCG  
tir8f,H12, TCACATCCGAGGAAACGCCATAATGAAATA

Plate number: 2

t7r0f,A1, TGAAAGTATAGAGGCTATTATT  
t7r10f,B1, AAAAGTAAACGTCAAAATGAAAAAACGATT  
t7r12f,C1, TTTGTGTTCTCGTATCTGCTTAAATCAGA  
t7r14f,D1, TATAGAACGGCGCTTGTATTCAGTCAGT  
t7r16f,E1, AAATGCAAGAAAAGCCTTGGAGGAATCAT  
t7r18f,F1, AAATTACTACATGCTGAGAGACTGTGAATT  
t7r20f,G1, ATCAAATGAAGATGATGAAACAAAATTACCT  
t7r22f,H1, GAGCAA AAAACTGTAATAAGATGATGTT  
t7r24f,A2, TGGATTATGCCCTAGATAATACTAAT  
t7r26f,B2, AGATTAGACAGGAGAAAGATAAAAATACCGA  
t7r28f,C2, ACGAACCACTACATTGACGCCACGCTCAT  
t7r28f,D2, CTGAAACAGCTGAGGATTGGAGGAGT  
t7r30j,E2, GGAATACGAGAACGAGTACGCCATTAAAGGTTT  
t7r4f,F2, TGAGGAGGGCTCAGACTGTAGGATCAAGT  
t7r6f,G2, TGAGGAGGGCTCAGACTGTAGGATCAAGT  
t7r8f,H2, AGCGCAACAGCATGAGGCCAACATTTTAG  
t7r9g,A3, TATCCGGTACTCGAGGAGTTAGATGTTAG  
t7r10e,B3, CGAGCTGAGACTCTGCTTACATGCTTAAT  
t7r12e,C3, CGATTTTAGAGAAAATCTGAGGAAATTT  
t7r12e,D3, TGCGCTTACGCTTAAAGGGTCA  
t7r12f,E3, CCAAAATAGGGGTTAAGTAAAGGAAAT  
t7r14e,F3, TTTAAATTGAGAACAGTACACAGAACAGC  
t7r14f,G3, AGAGGAAACGAGCTTACAGGAAAGTTCAT  
t7r16e,H3, CGAGTAGAGGCTTAACTTAAATTAGGC  
tir16f,A4, TCTCATATATTAGTGTACCATTAAGCAATAA  
tir18e,B4, CTGTAATAGGTGTTACGGCATTAAGCAATAA  
t7r18f,C4, GCTTAATCTTTCGGAGGAGCTTCCAGAG  
t7r20e,D4, TCAGGTCTATTGAGATCTACCTCTGTT  
t7r20e,E4, GGTAGCTATTGAGATCTGGTGTGAAAT  
t7r22e,F4, AAATAATTAACTTAACTAAGGAAACAGTAC  
t7r22f,G4, GCTCATTTTCGGCTTCTCCGCTCAG  
t7r24e,H4, CTCTTCGACTTCCAGGCTTACATTCAT  
t7r26f,D5, GAAGATGCGGAAACCCAGGCTGCGAG  
t7r26e,B5, CCCGGTACCTGGAGGCTGATCTAAATTC  
t7r26f,C5, CTTGCATGCCAGGCTGAACTGCTCTGCT  
t7r28e,D5, GGGAGAGGGCTTACGGTGTGAACTGCG  
t7r28e,E5, CGCAGCTGGTTTGGCTATTGGGAATCAAAA  
t7r2e,F5, ACGTTAGCTTAAAGTGGTGTGAACTGAG  
t7r2f,G5, CGAGGAGGCTTACGGTGTGAACTGAG  
t7r2f,G5, CGTAACAAAGATAATTCTCTGTTGAAATT  
t7r30e,H5, AGTTGGGAGGAGTGGTGTGAACTTAAAC  
t7r30f,A6, GAATAGCACAAGGCTTACCTAAAGGGC  
t7r32h,B6, GAAGCTGCGGAGAAGGAGGAATGGCCGC  
t7r4e,C6, CAATGACAGCTTGTGACCTAGTCTCC  
t7r4f,D6, CTTAAACACACACATGCCAACCGCGTAA  
t7r12e,D6, AAACAAAGATGCAACTTACGGGACAGCAA  
t7r12f,G5, CGTAACAAAGATAATTCTCTGTTGAAATT  
t7r30f,A6, GAATAGCACAAGGCTTACCTAAAGGGC  
t7r32h,B6, GAAGCTGCGGAGAAGGAGGAATGGCCGC  
t7r4e,C6, CAATGACAGCTTGTGACCTAGTCTCC  
t7r4f,D6, CTTAAACACACACATGCCAACCGCGTAA  
t7r12e,D7, ACTGGATATTGCTTACAGACGACTTAATAA  
t7r12f,E7, CTATAACCCCTCCATACCTCGCGTATTAG  
t7r14e,F7, GAAGCAAAAGGGGATTGGCATTAATTGTTAG  
t7r14f,G7, CTAGAGCCTCCACAGGTAGGATTAAATA  
t7r16e,H7, TCAGAAATTAAAGTACCGGTGTGAGACAGC  
t7r16f,A8, TGCAACTTAGGTCTACACCTTGTGAAATTAG  
t7r18e,B8, CAAGCAGAACATAAAAGCCCTGGATACAT  
t7r18f,C8, CAAAATTAGGATAAAAATTGGATATTICA  
t7r20e,D8, AGAGAATCAGCTGATAATTATGTTT  
t7r22e,F8, ACCGTTCTGATGAGCGTTCTGTAATT  
t7r22f,G8, GTAAAAAAACATTAATGTCAGCATCTGCGA  
t7r24e,H8, TTGCCTATGGACGACAGCTGAGTCTGAGG  
t7r24f,A9, TTTGCAGTGGAGCTGGCAACACTGTTCCAGT  
t7r26e,B9, TCATAGCTTGAACAGCAGGCTTACGGGCA  
t7r26f,C9, CACGAGCTGTTCTGTTGAAATTTCGCTC  
t7r28e,D9, TGGTTTTCTTCCAGTGGGAAAATCATGG  
t7r28f,E9, ACTGCCGCTTACAGCTGAGATGGTGGTT  
t7r2e,F9, TGCTAAACTCAGACAGCAGCCCTACCGCCA  
t7r3r2f,G9, TGTCAGATAACTTCAACAGTTCTTAATGTA  
t7r30e,H9, TGGACTCCGAAACCTTACACCGCAGGG  
t7r32e,A10, CCGAAACATCAACCTAAAGGGGAAAAGGGC  
t7r32h,B10, CCCCGATTAGAGCTTACGGGAAAGAACG  
t7r34e,C10, ATATATTCTGAGCTTACGGCTTACGGT  
t7r34f,D10, TCGTTTTAGTCGCTGAGGCTTACAGAAC  
t7r36e,E10, CTCATCTGAGCTTACGGCTTACGGT  
t7r36f,F10, TTTCATGATGACCCCCAGGATTAAGGGCAG  
t7r38e,G10, AGTAATCTTACAGGAAACCGAACTAAAC  
t7r38f,H10, ACGGCTTACGACAAGAACCGGATATGGTTAA  
t7r50g,A11, CTCAGAGCCACACCCCTTACCTGGTACAC  
t7r510e,B11, AAAGATCTTAAATTGGGCTTGGAGTTAC  
t7r510f,C11, ACAGCTAGATCAGTTGGATTTACGGC  
t7r512e,D11, AAATATTTGAGGCTTACAGGCAAGGTAG  
t7r512f,E11, GGAAATTACATTGTAATCCCTCACCAATAA  
t7r514e,F11, TACCTTAAAGGTTCTACCCCTGACATCG  
t7r514f,G11, CAAAACATTCGCTTACGGGAAAGGGG  
t7r516e,H11, TTTCATTCGAGCTTACATGTTAGAGAG  
tir516f,A12, ATATAATGGGGGGGGAGCTGAAATTACATC  
tir518e,B12, TATATTTCATACAGGAAACGCTTATAT  
tir518f,C12, CAATAATAAGTCAATGGCTTACGGAGAGCC  
t7r520e,D12, CATGTCACAAATACCATTAACACCTCA  
t7r520f,E12, AGACAGCTCTGATGACCCCCAGGTTGTTA  
t7r522e,F12, ACCCGTCGTTAAATTGAAACGTTAAACTAG  
t7r522f,G12, GCAAAATGATTCTCTGTTGGAAACCGT  
t7r524e,H12, GGCGATCGCCATGTCGAGGAGTAAACA

Plate number: 3

t-5r24f,A1, TAGATGGGGGGGGCTTCTCGCGAAGCG  
t-5r26e,B1, GCTCACAGGGTAAACGCCAGGGTTGGGAAG  
t-5r28e,D1, ATTAAGTCTTACACACATACGGCTTAAATG  
t-5r28f,E1, AGCTGATTACTACATTAATGCGTGTATTTC  
t-5r28f,F1, GTGAGCTGGCCCTTACCCGCTGGGTTGGC  
t-5r28e,P1, GAGAAATAGGGTACAGTACAACCTCGC  
t-5r28f,G1, TGAGTGTGAGGAACTTACGGTAAACG  
t-5r28f,H1, GAGCAA AAAACTGAAACTAGTCTCCAA  
t-5r28f,I1, GGTAAATGAGGCTTACGGGAAAGGGG  
t-5r28f,J1, GGTAAATGAGGCTTACGGGAAAGGGG  
t-5r28f,K1, GGTAAATGAGGCTTACGGGAAAGGGG  
t-5r28f,L1, GGTAAATGAGGCTTACGGGAAAGGGG  
t-5r28f,M1, GGTAAATGAGGCTTACGGGAAAGGGG  
t-5r28f,N1, GGTAAATGAGGCTTACGGGAAAGGGG  
t-5r28f,O1, GGTAAATGAGGCTTACGGGAAAGGGG  
t-5r28f,P1, GGTAAATGAGGCTTACGGGAAAGGGG  
t-5r28f,Q1, GGTAAATGAGGCTTACGGGAAAGGGG  
t-5r28f,R1, GGTAAATGAGGCTTACGGGAAAGGGG  
t-5r28f,S1, GGTAAATGAGGCTTACGGGAAAGGGG  
t-5r28f,T1, GGTAAATGAGGCTTACGGGAAAGGGG  
t-5r28f,U1, GGTAAATGAGGCTTACGGGAAAGGGG  
t-5r28f,V1, GGTAAATGAGGCTTACGGGAAAGGGG  
t-5r28f,W1, GGTAAATGAGGCTTACGGGAAAGGGG  
t-5r28f,X1, GGTAAATGAGGCTTACGGGAAAGGGG  
t-5r28f,Y1, GGTAAATGAGGCTTACGGGAAAGGGG  
t-5r28f,Z1, GGTAAATGAGGCTTACGGGAAAGGGG  
t-5r28f,A2, GGTAAATGAGGCTTACGGGAAAGGGG  
t-5r28f,B2, GGTAAATGAGGCTTACGGGAAAGGGG  
t-5r28f,C2, GGTAAATGAGGCTTACGGGAAAGGGG  
t-5r28f,D2, GGTAAATGAGGCTTACGGGAAAGGGG  
t-5r28f,E2, GGTAAATGAGGCTTACGGGAAAGGGG  
t-5r28f,F2, GGTAAATGAGGCTTACGGGAAAGGGG  
t-5r28f,G2, GGTAAATGAGGCTTACGGGAAAGGGG  
t-5r28f,H2, GGTAAATGAGGCTTACGGGAAAGGGG  
t-5r28f,I2, GGTAAATGAGGCTTACGGGAAAGGGG  
t-5r28f,J2, GGTAAATGAGGCTTACGGGAAAGGGG  
t-5r28f,K2, GGTAAATGAGGCTTACGGGAAAGGGG  
t-5r28f,L2, GGTAAATGAGGCTTACGGGAAAGGGG  
t-5r28f,M2, GGTAAATGAGGCTTACGGGAAAGGGG  
t-5r28f,N2, GGTAAATGAGGCTTACGGGAAAGGGG  
t-5r28f,O2, GGTAAATGAGGCTTACGGGAAAGGGG  
t-5r28f,P2, GGTAAATGAGGCTTACGGGAAAGGGG  
t-5r28f,Q2, GGTAAATGAGGCTTACGGGAAAGGGG  
t-5r28f,R2, GGTAAATGAGGCTTACGGGAAAGGGG  
t-5r28f,S2, GGTAAATGAGGCTTACGGGAAAGGGG  
t-5r28f,T2, GGTAAATGAGGCTTACGGGAAAGGGG  
t-5r28f,U2, GGTAAATGAGGCTTACGGGAAAGGGG  
t-5r28f,V2, GGTAAATGAGGCTTACGGGAAAGGGG  
t-5r28f,W2, GGTAAATGAGGCTTACGGGAAAGGGG  
t-5r28f,X2, GGTAAATGAGGCTTACGGGAAAGGGG  
t-5r28f,Y2, GGTAAATGAGGCTTACGGGAAAGGGG  
t-5r28f,Z2, GGTAAATGAGGCTTACGGGAAAGGGG  
t-5r28f,A3, GGTAAATGAGGCTTACGGGAAAGGGG  
t-5r28f,B3, GGTAAATGAGGCTTACGGGAAAGGGG  
t-5r28f,C3, GGTAAATGAGGCTTACGGGAAAGGGG  
t-5r28f,D3, GGTAAATGAGGCTTACGGGAAAGGGG  
t-5r28f,E3, GGTAAATGAGGCTTACGGGAAAGGGG  
t-5r28f,F3, GGTAAATGAGGCTTACGGGAAAGGGG  
t-5r28f,G3, GGTAAATGAGGCTTACGGGAAAGGGG  
t-5r28f,H3, GGTAAATGAGGCTTACGGGAAAGGGG  
t-5r28f,I3, GGTAAATGAGGCTTACGGGAAAGGGG  
t-5r28f,J3, GGTAAATGAGGCTTACGGGAAAGGGG  
t-5r28f,K3, GGTAAATGAGGCTTACGGGAAAGGGG  
t-5r28f,L3, GGTAAATGAGGCTTACGGGAAAGGGG  
t-5r28f,M3, GGTAAATGAGGCTTACGGGAAAGGGG  
t-5r28f,N3, GGTAAATGAGGCTTACGGGAAAGGGG  
t-5r28f,O3, GGTAAATGAGGCTTACGGGAAAGGGG  
t-5r28f,P3, GGTAAATGAGGCTTACGGGAAAGGGG  
t-5r28f,Q3, GGTAAATGAGGCTTACGGGAAAGGGG  
t-5r28f,R3, GGTAAATGAGGCTTACGGGAAAGGGG  
t-5r28f,S3, GGTAAATGAGGCTTACGGGAAAGGGG  
t-5r28f,T3, GGTAAATGAGGCTTACGGGAAAGGGG  
t-5r28f,U3, GGTAAATGAGGCTTACGGGAAAGGGG  
t-5r28f,V3, GGTAAATGAGGCTTACGGGAAAGGGG  
t-5r28f,W3, GGTAAATGAGGCTTACGGGAAAGGGG  
t-5r28f,X3, GGTAAATGAGGCTTACGGGAAAGGGG  
t-5r28f,Y3, GGTAAATGAGGCTTACGGGAAAGGGG  
t-5r28f,Z3, GGTAAATGAGGCTTACGGGAAAGGGG  
t-5r28f,A4, GGTAAATGAGGCTTACGGGAAAGGGG  
t-5r28f,B4, GGTAAATGAGGCTTACGGGAAAGGGG  
t-5r28f,C4, GGTAAATGAGGCTTACGGGAAAGGGG  
t-5r28f,D4, GGTAAATGAGGCTTACGGGAAAGGGG  
t-5r28f,E4, GGTAAATGAGGCTTACGGGAAAGGGG  
t-5r28f,F4, GGTAAATGAGGCTTACGGGAAAGGGG  
t-5r28f,G4, GGTAAATGAGGCTTACGGGAAAGGGG  
t-5r28f,H4, GGTAAATGAGGCTTACGGGAAAGGGG  
t-5r28f,I4, GGTAAATGAGGCTTACGGGAAAGGGG  
t-5r28f,J4, GGTAAATGAGGCTTACGGGAAAGGGG  
t-5r28f,K4, GGTAAATGAGGCTTACGGGAAAGGGG  
t-5r28f,L4, GGTAAATGAGGCTTACGGGAAAGGGG  
t-5r28f,M4, GGTAAATGAGGCTTACGGGAAAGGGG  
t-5r28f,N4, GGTAAATGAGGCTTACGGGAAAGGGG  
t-5r28f,O4, GGTAAATGAGGCTTACGGGAAAGGGG  
t-5r28f,P4, GGTAAATGAGGCTTACGGGAAAGGGG  
t-5r28f,Q4, GGTAAATGAGGCTTACGGGAAAGGGG  
t-5r28f,R4, GGTAAATGAGGCTTACGGGAAAGGGG  
t-5r28f,S4, GGTAAATGAGGCTTACGGGAAAGGGG  
t-5r28f,T4, GGTAAATGAGGCTTACGGGAAAGGGG  
t-5r28f,U4, GGTAAATGAGGCTTACGGGAAAGGGG  
t-5r28f,V4, GGTAAATGAGGCTTACGGGAAAGGGG  
t-5r28f,W4, GGTAAATGAGGCTTACGGGAAAGGGG  
t-5r28f,X4, GGTAAATGAGGCTTACGGGAAAGGGG  
t-5r28f,Y4, GGTAAATGAGGCTTACGGGAAAGGGG  
t-5r28f,Z4, GGTAAATGAGGCTTACGGGAAAGGGG  
t-5r28f,A5, GGCCTAA

Supplementary Figure S38: Sequences for the “tall” rectangle used for the map pattern shown in Fig. 3e-i. These sequences are for a bridged seam.

Supplementary Figure S39: New England Biolabs sequence for M13mp18 used to design the staples for all origami. It is based on an unpublished resequencing of M13mp18, F.J. Stewart 5/28/02.

## Supplementary Note S4: Experimental Methods

### Supplementary Note S4.1: Design, synthesis, and sample preparation.

Single-stranded M13mp18 DNA (New England Biolabs), resequenced in 2002, was quantitated by UV absorbance at 260 nm. (Different clones of M13mp18 have small sequence differences, with the potential to affect folding; by AFM no qualitative difference was observed for a Bayou Biolabs clone—see Supplementary Note .) Staple and remainder strands were purchased unpurified (Integrated DNA Technologies; the manufacturer's mass spectrophotometry indicated that strands had a few percent  $n - 1$  truncation products.) in water at 100  $\mu\text{M}$  or 150  $\mu\text{M}$  and stored at -20°C. The desired set of up to 273 short strands was mixed with M13mp18 (typically 160 nM of each short strand, 1.6 nM M13mp18 circular or linear, a 100-fold excess of short strands) in a 100  $\mu\text{l}$  volume of 1X Tris-Acetate-EDTA (TAE) buffer with 12.5 mM magnesium acetate (pH=8.3) and annealed from 95°C to 20°C in a PCR machine (Eppendorf) at a rate of 1°C/minute in .1°C steps. When composing sharp triangles into hexagons or lattices the best results were obtained when staples that mediated the interaction, i.e. extended staples, were used in only 4-fold excess. To create linear DNA for the square and star, circular single-stranded M13mp18 DNA was incubated in restriction buffer with a short complementary strand at 37°C for 15 minutes, then linearized by digestion with BsrB I (New England Biolabs), phenol-chloroform extracted, and ethanol precipitated.

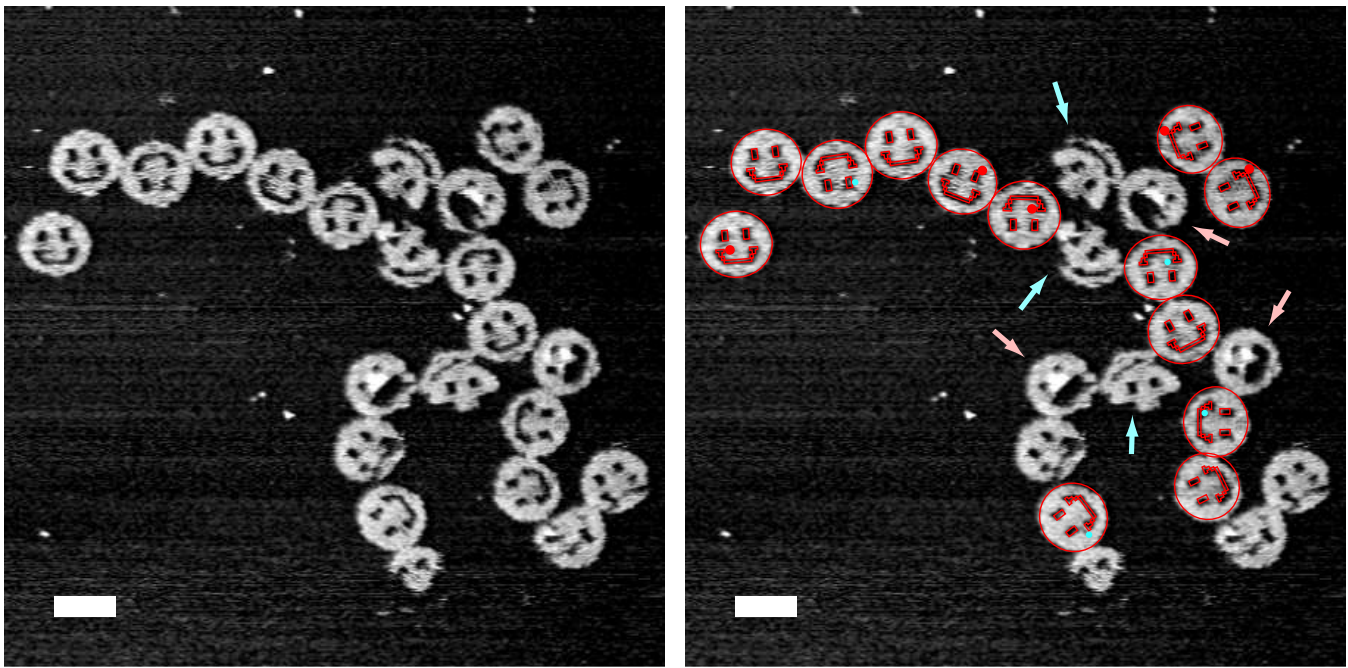
### Supplementary Note S4.2 Atomic force microscopy.

Imaging was performed in Tapping Mode under TAE/Mg<sup>2+</sup> buffer on a Digital Instruments Nanoscope III Multimode AFM (Veeco) with a nanoAnalytics Q-control III (Asylum Research) and a vertical engage J-scanner, using the ≈9.4 kHz resonance of the narrow 100  $\mu\text{m}$ , 0.38 N/m force constant cantilever of an NP-S oxide-sharpened silicon nitride tip (Veeco). Samples were prepared by deposition of ≈5  $\mu\text{l}$  onto freshly-cleaved mica (Ted Pella).

After self-assembly was complete, samples were prepared for AFM imaging by deposition of ≈ 5  $\mu\text{L}$  onto a freshly-cleaved mica surface (Ted Pella) attached by hot melt glue to a 15 mm metal puck; an additional 30  $\mu\text{L}$  of buffer was added to both sample and cantilever (mounted in the standard Tapping Mode fluid cell) before the sample and fluid cell were positioned in the AFM head. The tapping amplitude setpoint, after engage, was typically 0.2 - 0.4 volts, the drive amplitude was typically 100-150 millivolts, scan rates ranged from 2-5 Hz. Fine structure associated with crossovers was most clearly resolved for low amplitude setpoint and high drive amplitude values. However, under such conditions, the greatest damage is done to the sample and the hairpin labels are less distinct, sometimes disappearing entirely. Thus, to prevent damage to samples, drive amplitude was minimized subject to the constraint that fine structure was still visible; this often involved lowering the amplitude setpoint. After this procedure, the drive amplitude was typically 70-90 millivolts and the amplitude setpoint .15-.25 volts. Drive amplitude was often further reduced through use of the Q-control.

The single most important factor in acquiring high resolution images appears to be the quality of the AFM tip. In a single AFM session only 1 in 10 NP-S AFM tips might prove capable of revealing fine structure in origami or distinguishing individual hairpin labels. Practically the best approach seems to be to change tips as quickly as possible until the desired resolution is achieved.

Images were flattened by subtracting a low-order polynomial from each scan line, or by adjusting each scan line to match intensity histograms. In Fig. 2:a<sub>3</sub>-f<sub>3</sub> the scale of AFM images was adjusted (by < 5%) so that the width of experimental structures matched the theoretical widths of origami. Theoretical widths were calculated assuming .34 nm/base. The width change due to bending of helices by small angles between crossovers (~10 degrees) was ignored; simple geometry suggests it would change theoretical widths by <2% (Supplementary Note 2).



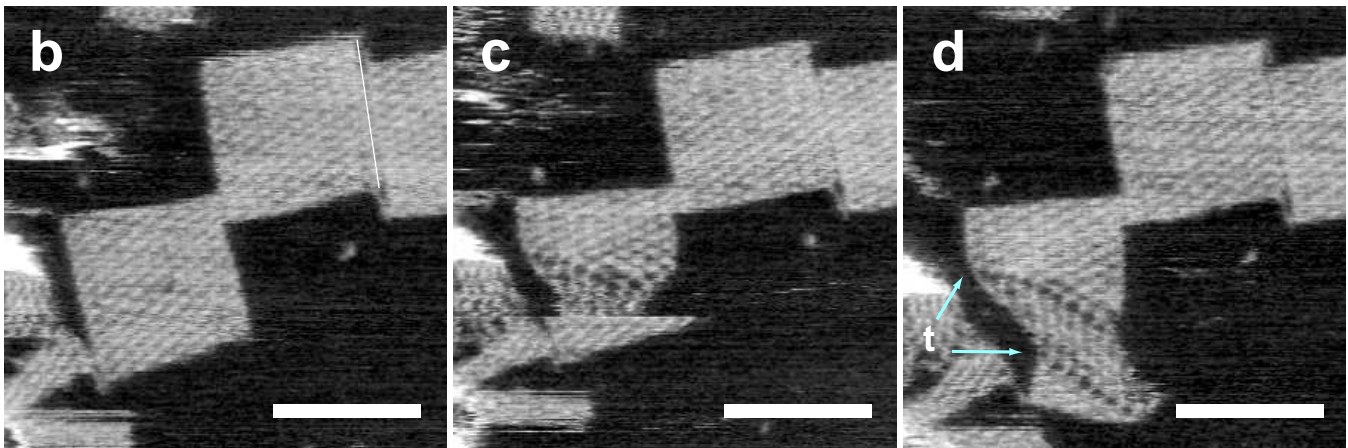
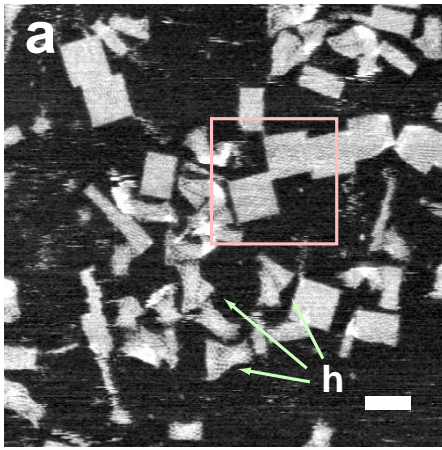
Supplementary Figure S40: Scale bar, 100 nm.

### Supplementary Note S5: Experimental variations and controls

In this note I give a text or data for any experimental variation, control, or phenomena that was mentioned in the text but not shown.

#### Supplementary Note S5.1: Counting well-formed structures

Supplementary Fig. S40 shows one of the fields (reproduced from Fig. 2:d<sub>4</sub>) used to obtain the frequency of well-formed structures smileys (here a smiley variant that has the seam above its right eye unbridged). Red dots are 15 nm in diameter, blue dots are 10 nm in diameter. These dots help determine the size of holes. Deciding which apparent holes are defects and which are correct high-resolution crossover structure (see Supplementary Fig. /refsmileyrainbow) is a matter of judgment. At right, templates of smileys are superimposed over experimental structures. To better fit the smileys some templates have been stretched up to 10%. In this field 13 structures have been judged well-formed, and 10 structures have been judged malformed. Two characteristic deformations of smileys are indicated: pink arrows indicate structures in which the ‘upper lip’ of the smiley has been flipped up onto the nose; light blue arrows indicate structures in which the ‘jaw’ has become dislocated, landing over the ‘forehead’ of the smiley.



Supplementary Figure S41: Scale bars, 100 nm.

### Supplementary Note S5.2: Stretching of squares into hourglasses

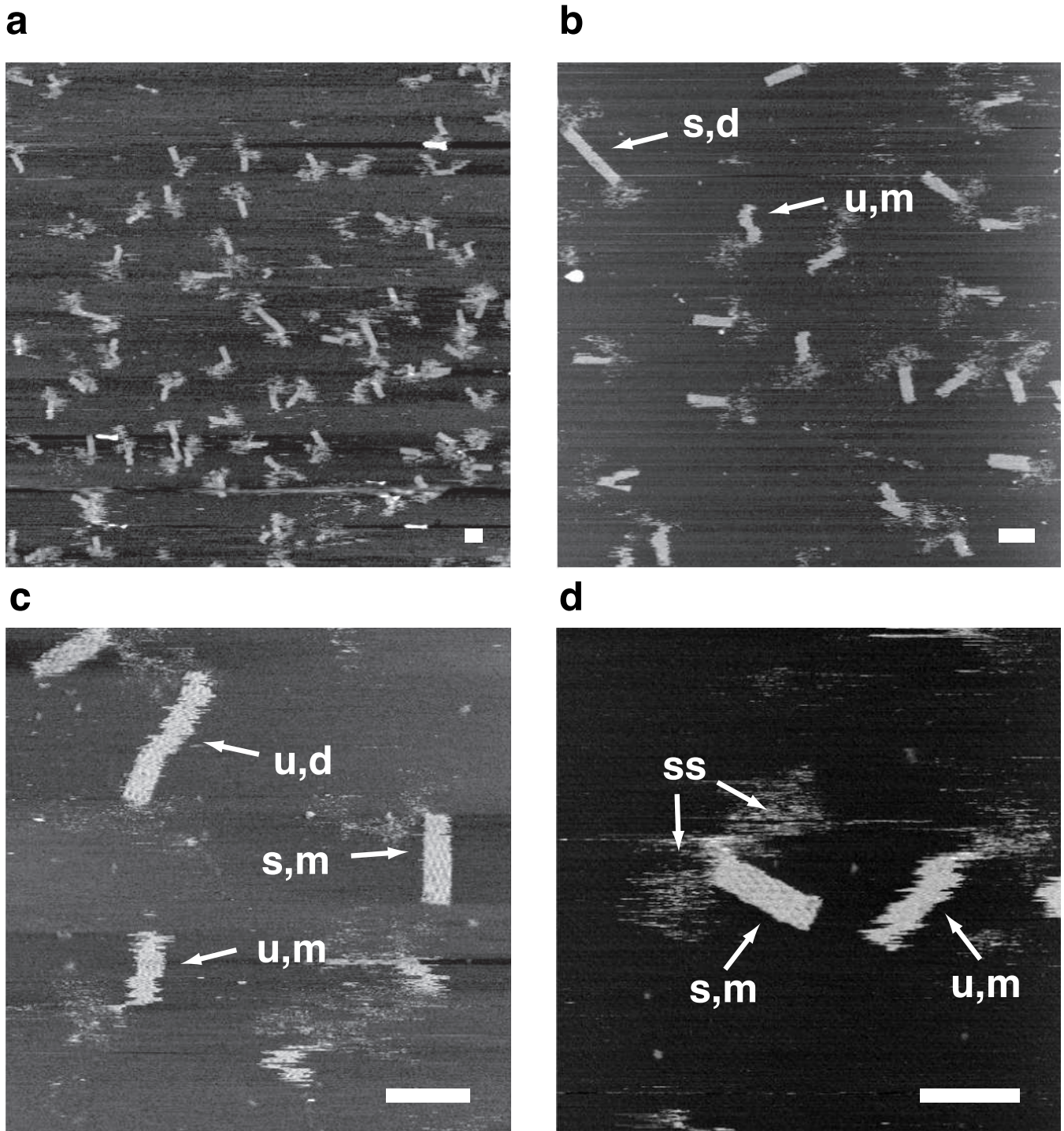
Supplementary Fig. S41a shows a typical field of 26-helix squares. A few structures are square, but many others are rectangular fragments or hourglass shapes (green arrows, marked 'h'). Supplementary Fig. S41b–d document the stretching of a square, over the course of three AFM scans, into an hourglass shape. The hourglass shape that results has what appear to be transitions between the normal folded lattice, and stretched lattice, along diagonals in the structure (blue arrows marked 't'). This is in contrast with the hourglass shown in the main text (Fig. 2:a<sub>4</sub>) which appears to have a continuous deformation of the lattice.

### **Supplementary Note S5.3: One third of the square**

The first test of the scaffolded DNA origami method, before the creation of the full square, was the creation of the bottom  $\sim 1/3$  of the square (Supplementary Fig. S42). Also, a circular M13mp18 scaffold DNA was used rather than a linearized one, because the corners of the rectangle were close enough that the unfolded portion of the M13mp18 scaffold DNA could easily bridge the corners without deforming the rectangle. No remainder strands were used on the  $\sim 2/3$  of M13mp18 DNA left unfolded. Apparently long, unfolded single-stranded sections of the scaffold do not adversely affect folding and remainder strands (where they are used for other designs) are probably unnecessary.

The  $1/3$  squares were observed singly (Supplementary Fig. S42, structures marked ‘m’ for monomer) or as dimers (Supplementary Fig. S42, structures marked ‘d’ for dimer). Dimers always appeared to be the result of stacking of  $1/3$  squares by vertical edges *opposite* from the unfolded single scaffold. Thus the unfolded scaffold appeared to prevent stacking at adjacent vertical edges. Single-stranded scaffold takes on a ‘cloud-like’ appearance that varies from AFM image to AFM image (Supplementary Fig. S42, marked ‘ss’).

Coplanar helices in DNA nanostructures appear to bind mica cooperatively; the larger a DNA nanostructure, the more tightly it appears to bind mica. This trend is apparent in the mobility of DNA nanostructures deposited on mica and imaged by tapping mode AFM under buffer. Most of the structures described in the main paper move infrequently during imaging, occasionally rotating by a few degrees or slipping by a few tens of nanometers (as judged by stationary structures around the mobile structure). The  $1/3$  squares, however, were more difficult to image because they often slipped, as shown by structures marked ‘u’ (for “unstable”) in Supplementary Fig. S42. In the same field, other structures may stick well (and are thus labelled ‘s’ for “stable”); when structures are stable, their fine structure (the lattice of crossovers) can often be observed. Sometimes, a structure that appears stable in one image moves in the next (data not shown). Thus, as for DNA nanotubes<sup>15</sup> and other DNA nanostructures, the interaction of scaffolded DNA origami with the mica surface (under buffer) is complex and dynamic and must be taken into account when interpreting AFM images.



Supplementary Figure S42: The first experiment performed for this paper was to create  $\sim 1/3$  of the 2.5-turn spacing square by adding  $\sim 1/3$  of the staples for the square to circular M13mp18 DNA. Structures that appear to be moving under imaging are marked with a 'u' for "unstable"; structures that appear to be stable are marked with an 's'. Monomers of the  $1/3$  square are marked with an 'm'; dimers are marked with a 'd'. Single-stranded scaffold, unfolded by staples is marked with an 'ss'. Scale bars, 100 nm.

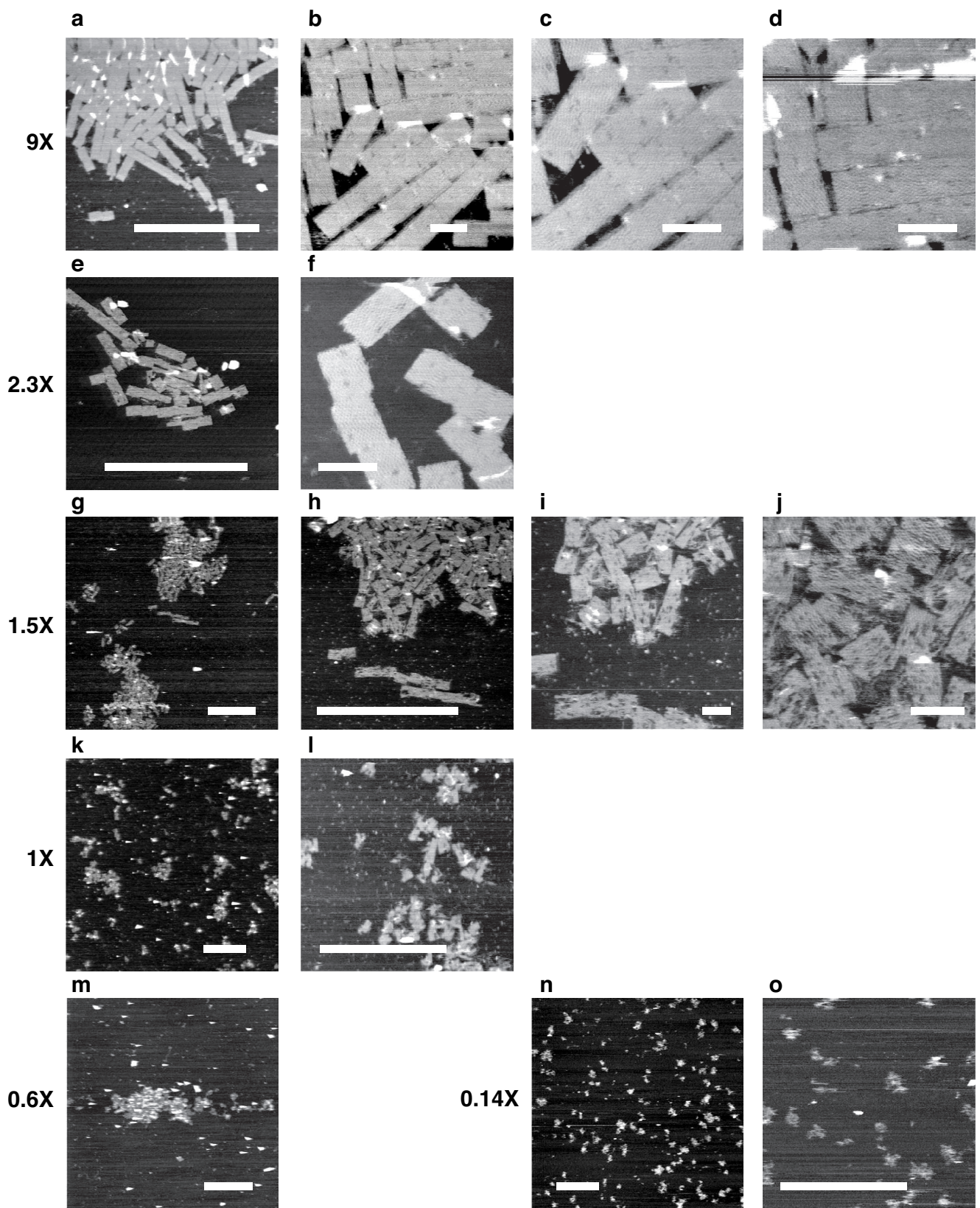
## Supplementary Note S5.4: Stoichiometry

Oligos were received from the manufacturer (Integrated DNA technologies) at a nominal concentration of 100 or 150  $\mu\text{M}$  as determined by UV absorbance at 260 nm. To estimate the error in stoichiometry, the concentration of 10 staple strands were remeasured by UV absorbance upon receipt by diluting 4  $\mu\text{l}$  of stock solution with 196  $\mu\text{l}$  of distilled water. This modelled the type of pipetting errors that occurred in the experiments since typically 3-7  $\mu\text{l}$  of each staple stock solution was used when staples were mixed. (In a given experiment a fixed volume of each staple strand was used so no renormalization was performed.) Concentrations were calculated based on extinction coefficients calculated according to a nearest neighbor model<sup>35</sup>. Assuming that the nearest neighbor model is correct, errors in absolute concentrations ranged from -5% to +13% and averaged +6% with a standard deviation of 6%. This may have reflected a systematic difference between the manufacturer's and the laboratory's spectrophotometers or measurement of volume. Nevertheless, this means that errors in relative concentration had a range of roughly 20%, and thus I estimate the error in concentration to be  $\sim 10\%$ . The M13mp18 scaffold strand was similarly quantitated but variable volumes of it were used to achieve a desired concentration in the final experiment. Pipetted in small 1-2  $\mu\text{l}$  volumes, its stoichiometry relative to the staple strands is assumed to have, similarly, at least  $\sim 10\%$  error.

In most experiments, a vast excess of staple strands (100 to 300-fold) over the scaffold were used. A question becomes, how small an excess can be effectively used to create DNA origami. Supplementary Fig. S43 shows AFM images of samples in which a smaller staple:scaffold ratio (from 9-fold down to .14-fold) was used. At a 9-fold excess (Supplementary Fig. S43a-d), rectangles are indistinguishable from those at higher molar excess of staple strands. Small 'hole' defects were sometimes observed but these defects are often observed upon repeated high resolution scanning even at high (100 to 300-fold) molar excess of staple strands. Rectangles created with just a 2.3-fold excess (Supplementary Fig. S43e-f) were difficult to distinguish from rectangles created with higher staple strand excess – that is, I am not sure they are distinguishable. It appeared that fewer long stacked chains formed, and that there were more malformed rectangles, but I made no attempt to quantify this.

In contrast, at a 1.5-fold excess of staple strands (Supplementary Fig. S43g-j), clear differences from normal rectangles were observed. Rectangles take on a "moth-eaten" appearance and have holes that often cover over 10% of their area. Linear stacks of rectangles may still be observed, however (bottom of Supplementary Fig. S43h). At a 1:1 staple:scaffold ratio (Supplementary Fig. S43k,l) no clear stacking is observed and it requires imagination to make out rectangular structures. At a 0.5 staple:scaffold ratio (Supplementary Fig. S43m) aggregates of partially folded scaffold strands still form but at a 0.14 ratio (Supplementary Fig. S43n,o) no large aggregates are formed; Instead, structures that appear to contain 1-3 scaffold strands are observed and they have a "streaky" appearance characteristic of structures that are mobile on the mica surface.

Because of the sloppiness with which strands were quantitated, no precise conclusions should be drawn from these experiments. However, I conclude that a 10-fold excess of staple strands is a "safe" concentration to work with for DNA origami containing 32-mer staple strands and that, because of the structures observed at a 2.3-fold excess, the use of a *vast* excess of staple strands should not be seen as a fundamental requirement of scaffolded DNA origami. Better control of concentrations may allow a 2-fold excess to be used for the construction of well-formed origami.



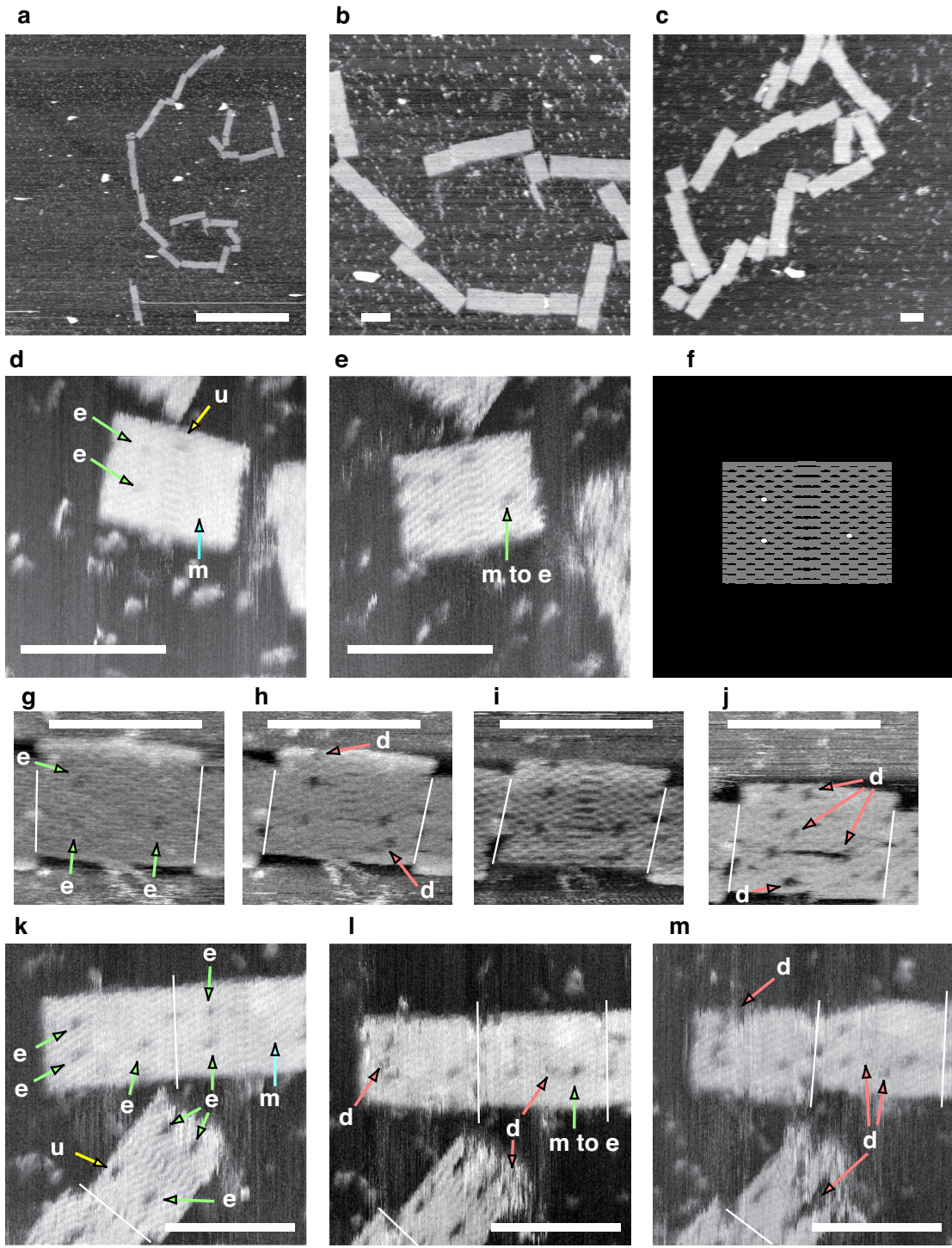
Supplementary Figure S43: Changing the concentration of staple strands relative to the scaffold. Scale bars in a,e,g,h,k–o are 1 micron. Scale bars in b–d, f, i, j are 100 nm

### **Supplementary Note S5.5: Removal of a strand**

To test the ability of atomic force microscopy to detect defects in origami, rectangles were prepared with three staple strands intentionally omitted (**r-5t8e**, **r-5t16e** and **r5t14f**). The positions of the omitted strands in the rectangle are diagrammed in Supplementary Fig. S44f as white dots. At low magnification, no defects could be observed (Supplementary Fig. S44a–c). Even at high magnification, in images of typical resolution, no defects were observed; the majority of AFM tips did not provide resolution that allowed imaging of the defects. Roughly 1 in 5 tips were sufficiently sharp to allow ‘holes’ at the position of the omitted strands to be observed (features marked ‘e’ for ‘expected’ in Supplementary Fig. S44d–e, and g–m), although not all rectangles showed all three holes immediately upon imaging (features marked ‘m’ for ‘missing’). It sometimes took repeated imaging for holes to appear (features marked ‘m to e’), as if repeated scanning of the AFM tip was enlarging the defect.

A difficulty is that unexpected defects (features marked ‘u’) were sometimes observed during initial scans and further, repeated scanning often created holes and tears in structures (features marked ‘d’). Two examples, in which (upon an initial scan) holes appear in the expected positions without other holes elsewhere, convinced me that the observed defects were associated with the omission of strands. These examples were not culled from hundreds of images, only about a half-dozen high-resolution examples of the sample were obtained. Thus these examples appear to be statistically significant (although I have made no attempt to calculate their significance based on the rate of appearance of holes in high-resolution images of pristine rectangles).

I conclude that, while omitted strands are difficult to observe, any strands systematically missing from structures (say because of bad secondary structure in a staple strand or the scaffold) should be detectable in multiple high-resolution images.



Supplementary Figure S44: Visualization of the positions of omitted strands in rectangles. **a–c** show that at low magnification and resolution, defects due to omitted strands cannot be observed. **f** diagrams the position of the three omitted strands. **d–e** and **bf** **g–m** show high resolution images of rectangles with omitted strands. ‘e’ marks expected defects, ‘u’ marks unexpected defects, ‘m’ marks a missing defect, and ‘d’ marks AFM damage. Defects on the vertical edges of rectangles (ragged edges) are so common that I do not mark them. Such defects seem to be created or enhanced easily by AFM imaging. White lines mark boundaries between rectangles. Rectangles do not always land in the ‘canonical’ orientation and under imaging roughly 50% appear flipped. Thus **d–e** and **k–m** have been flipped left to right so that the rectangles they contain may be more easily compared with **f**. In **k–m** the diagonally oriented rectangle at bottom is flipped with respect to **f**. Inspect **f** and note that the singleton omission on the right hand side is slightly raised with respect to the pair of omissions on the left; AFM defects show a similar pattern. Scale bar in **a**, 1 micron. Scale bars in **b–e** and **g–m** are 100 nm.

## **Supplementary Note S5.6: Unbridged seams**

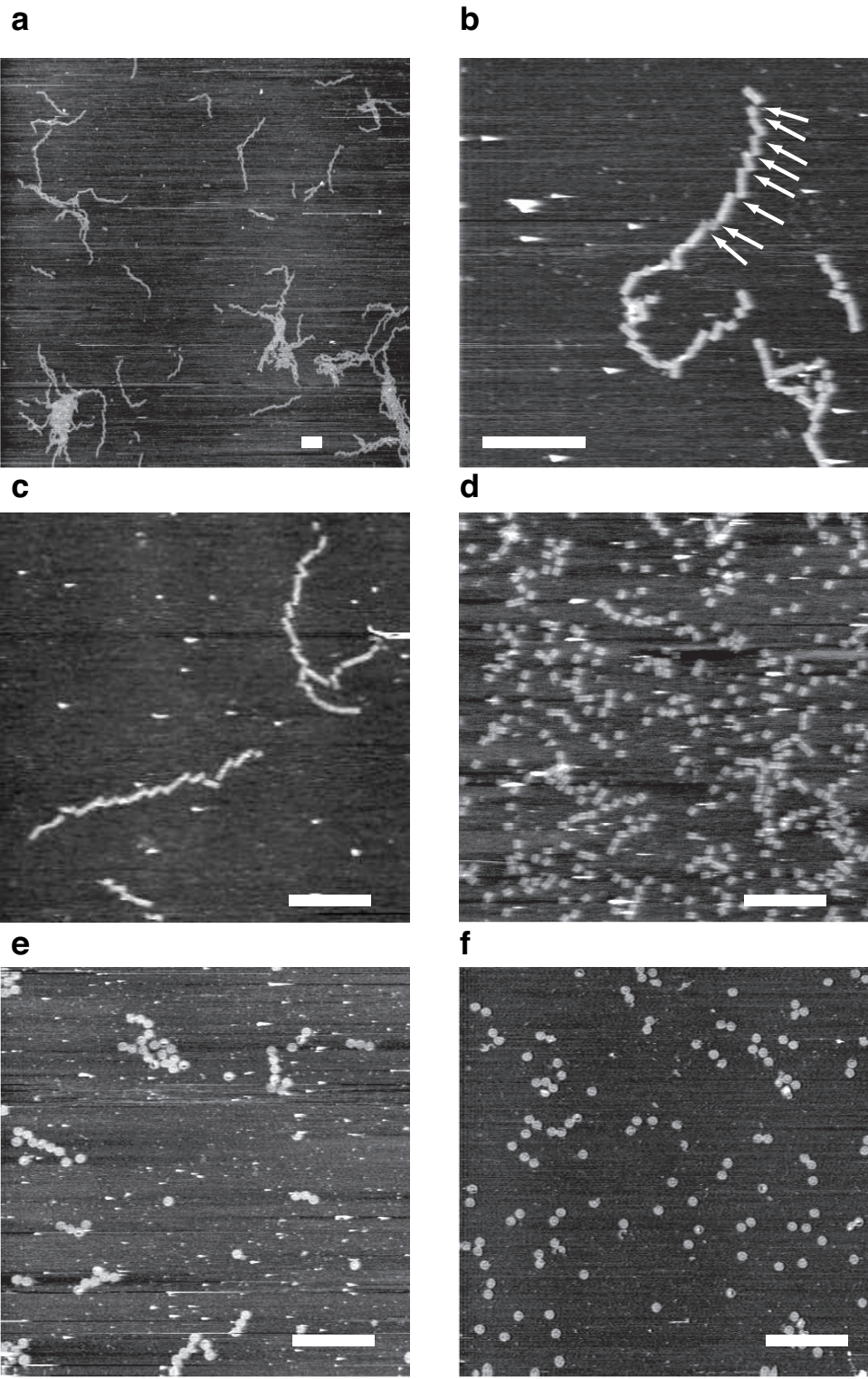
Unbridged seams in scaffolded origamis are those held together only by stacking interactions. Sometimes such seams dislocate; this is best observed in patterned rectangles because the two distinct halves of a rectangle can be unambiguously identified, as snowflake patterns in Supplementary Note S6 show. Supplementary Fig. S53d shows a small dislocations along an unbridged seam. Large dislocations at unbridged seams are also common. Supplementary Fig. S53c has white arrows that point to dislocations in which the two halves of the origami are completely separated.

## **Supplementary Note S5.7: Prevention of stacking**

Stacking interactions based on blunt-ended helices can be quite strong; rectangles which have many parallel blunt-ends along their left and right edges stack so strongly that they may form long chains over 5 microns in length (Supplementary Fig. S45a–c). As deposited on mica, such chains exhibit frequent  $\sim$ 75 nm dislocations, every few rectangles along the chain (arrows, Supplementary Fig. S45b). I hypothesize that in solution rectangles in such chains are completely stacked and no such offsets occur.

To avoid aggregation based on stacking interactions, several methods can be employed. First, the staple strands along the edges of a shape may be simply left out, and the scaffold left unstructured along these edges. Supplementary Fig. S45d shows rectangles that have been disaggregated in this way. Simply omitting staple strands out leaves unstructured scaffold at the edges of the rectangle and decreases the size of the potential pixel array by two columns. Thus a second, more aesthetically pleasing, method is that employed in Fig. 3e: the addition of 4T hairpin loops to staple strands on the edges of a shape. (The use of 4T hairpin loops to disaggregate DNA nanostructures was first demonstrated by Rebecca Schulman for her “zig-zag boundaries”.) A third very similar method is to add 4T tails to staple strands that have ends on the edge of the shape. Supplementary Fig. S45e shows the normal amount of aggregation for 3-hole disks. Supplementary Fig. S45f shows that the addition of just a small number (12) of 4T tails to the 3-hole disks causes almost complete disaggregation.

These experiments show that, when it is desirable to do so, stacking and the aggregation it induces can be almost entirely suppressed.



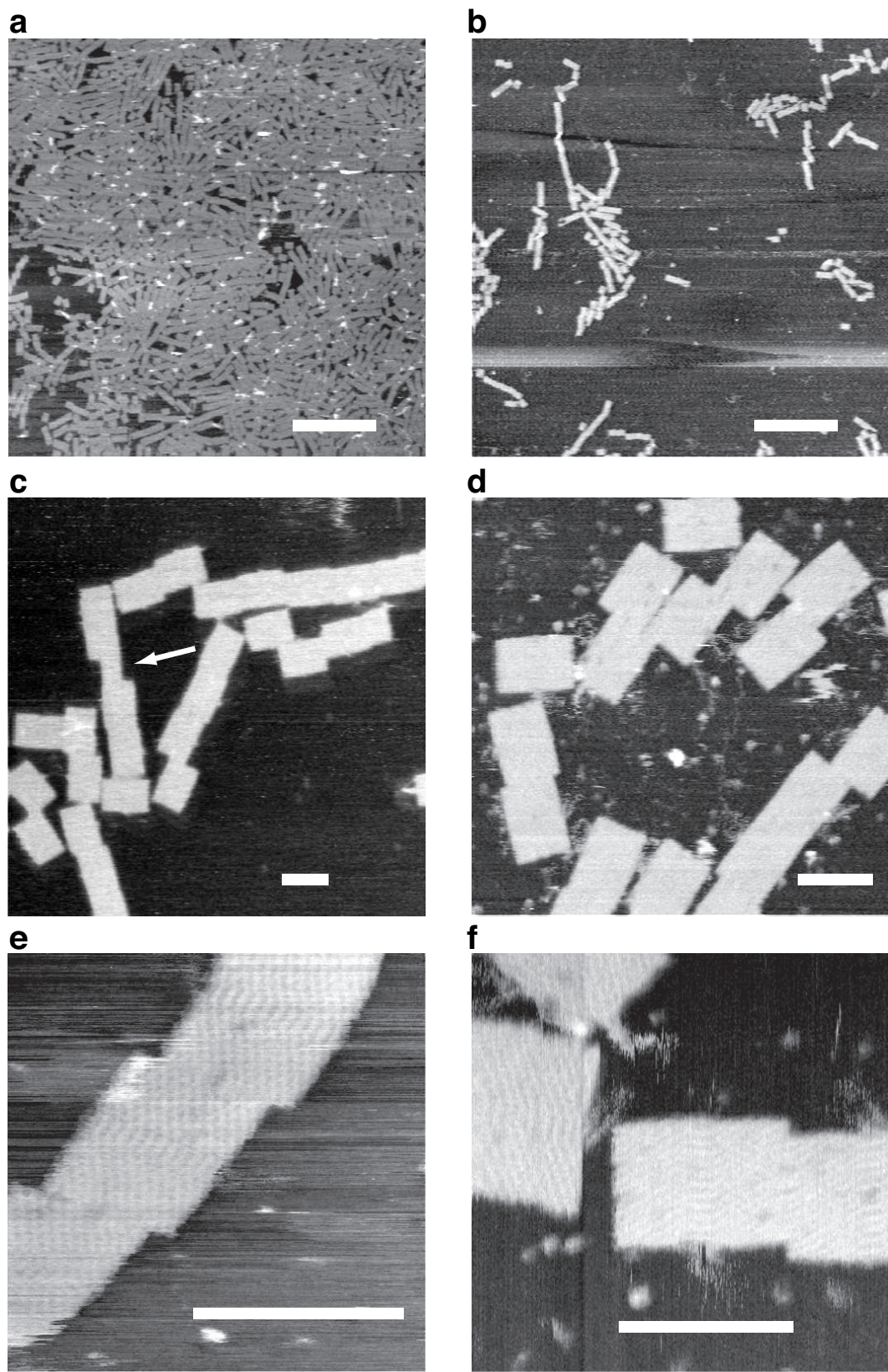
Supplementary Figure S45: Methods to discourage stacking of DNA origami. **a–c** In addition to large aggregates, rectangles often form very long stacked chains. Arrows indicate dislocations of rectangles by a single rectangle width (roughly 75 nm). **d** Stacking (and aggregation) are almost completely inhibited by omitting staples on the left and right edges of the rectangle. **e** Normal 3-hole disks aggregate strongly; almost no 3-hole disks occur as singlettons. **f** The simple addition of 4T-tails to the 6 blunt-end helices its left and right edges of the 3-hole disks almost completely abolishes stacking and aggregation. Scale bars, 1 micron.

### **Supplementary Note S5.8: A different M13mp18 clone**

While all viruses labelled M13mp18 are supposed to have identical DNA sequences, in practice this does not appear to be the case. The originally deposited sequence for M13mp18 in Genbank (accession X02513, 7249 bases long,<sup>36</sup>) appears to have an error that was corrected by adding a 'T' at position 900 (accession M77815, 7250 bases long). Amersham Biosciences gives the sequence of M13mp18 (evidently their clone) as a 7249 sequence that differs from X02513 by a pair of compensatory frame shifts (bounding the region from 977 to 1556) and 3 point mutations outside of the frameshift. New England Biolabs gives a 7249 sequence (Supplementary Fig. 39) for their clone (resequenced in 2002) that differs from the Amersham sequence by a pair of compensatory frameshifts (bounding the region 900-977) and 23 point mutations outside of the frameshift.

The staple strands given in this paper were created using the New England Biolab's sequence and all experiments save those described here were performed with New England Biolab's M13mp18 single-stranded DNA (Catalog number: N4040S). To test whether small differences in sequence could be detected by AFM, staples for the rectangle were used to fold a sample of M13mp18 DNA from Bayou Biolabs (which reports that their sequence is the same as that of Amersham, although it has not been recently resequenced). Thus the staple strands should have had mismatches with the scaffold at 23 positions and a 78 base section should have been shifted by 1 base with respect to the scaffold. Qualitatively, no differences were observed between rectangles created with Bayou Biolabs M13mp18 DNA and New England Biolabs M13mp18 DNA (Supplementary Fig. S46).

While this seems to suggest that small sequence differences do not matter, I am uncomfortable suggesting that the staple sequences described in this paper be used for M13mp18 DNA with a sequence that is known to be different. Thus I suggest either generating new staple strand sequences, or using New England Biolabs M13mp18. Given that the difference (in point mutations) between the New England Biolabs sequence and Amersham sequence is 0.32% of the M13mp18 genome, and that the sequencing error rate in both these sequences could easily be 1%, this suggestion is probably based in irrational fear.

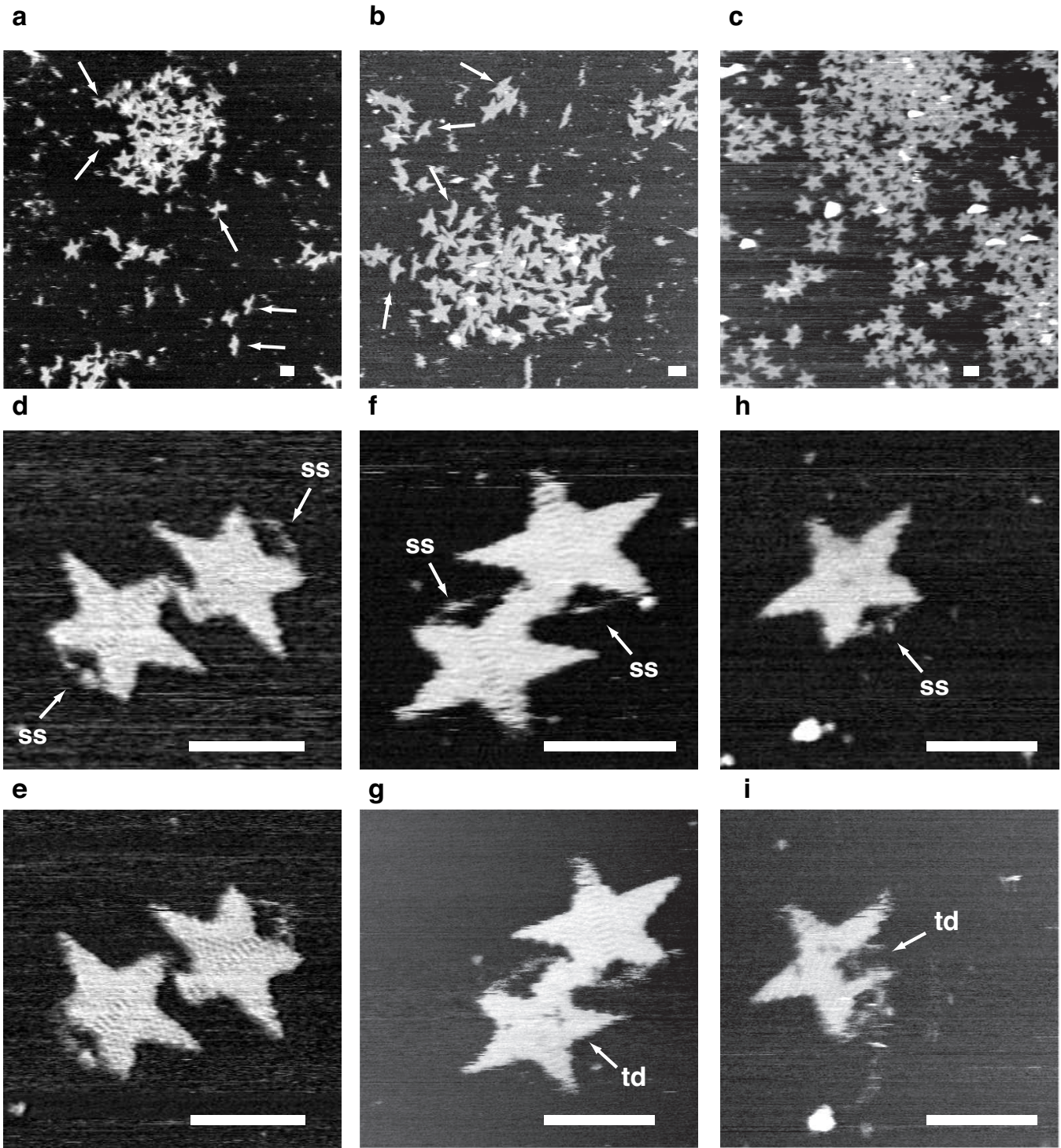


Supplementary Figure S46: Rectangles created using Bayou Biolabs M13mp18 DNA.

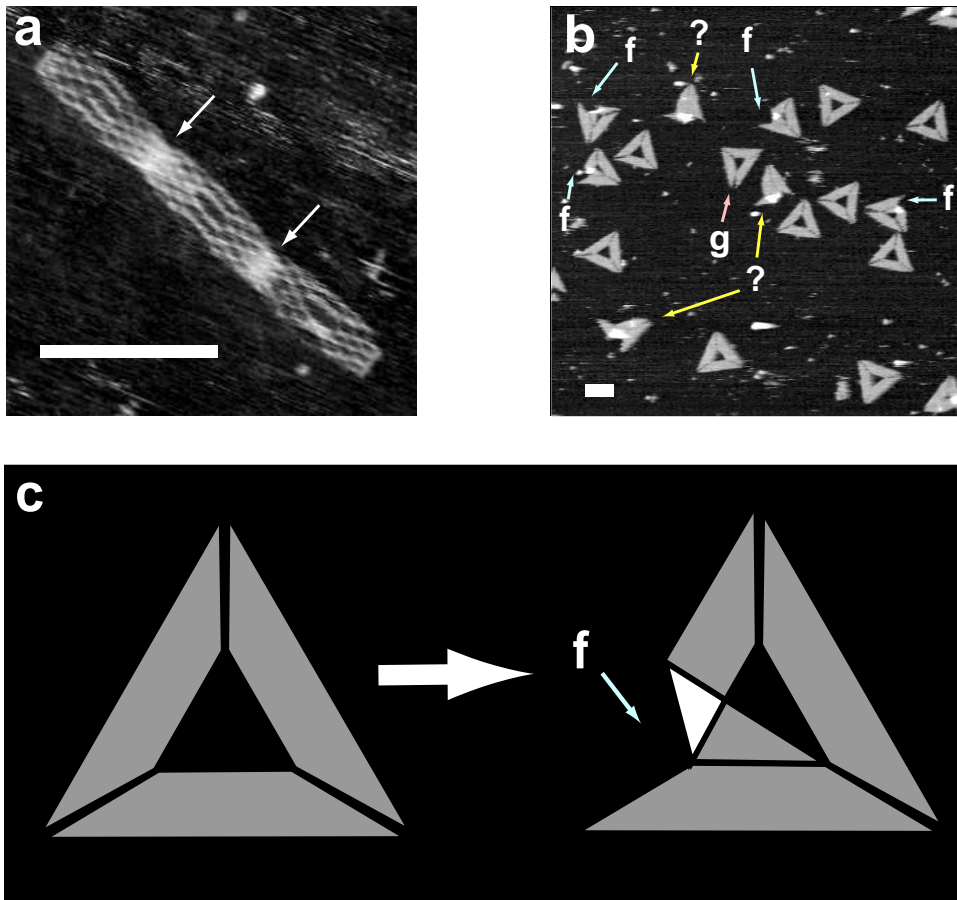
### **Supplementary Note S5.9: Use of circular scaffold for Stars**

Use of circular scaffold with stars (Supplementary Fig. S47c–i) appears to give better results than with linear scaffold (Supplementary Fig. S47a,b). Fewer structures appear to be fragments of stars (arrows in Supplementary Fig. S47a,b). However, it is difficult to tell whether the lower two points of the star, which the circular scaffold bridges and often image poorly, are well-formed. The circular scaffold that bridges the two lower points is easily visualized, however, as a single, somewhat diffuse, arc (labelled as ‘ss’ in Supplementary Fig. S47d,f, and h). The fact that circular scaffold appeared to give better results may be attributed to the high purity of the circular scaffolds. After linearization, the quality of linear scaffold, in terms of the percentage of strands that were full length, was not assessed and a large percentage of the strands may have not been full length.

Of incidental interest, Supplementary Fig. S47d–i show the range of outcomes that is observed when a structure is imaged more than once in an attempt to get higher resolution images. (In an attempt to get higher resolution, the tip-sample interaction is increased by increasing the tapping amplitude or decreasing the amplitude setpoint.) Sometimes a structure (Supplementary Fig. S47d) is imaged with higher resolution (Supplementary Fig. S47e.) Sometimes a structure (Supplementary Fig. S47f) sustains a small amount of damage from the tip (labelled ‘td’ for “tip-damage” in Supplementary Fig. S47g). Sometimes a structure (Supplementary Fig. S47h) sustains severe damage (Supplementary Fig. S47i).



Supplementary Figure S47: The difference between stars created using a circular scaffold and those created using a linear scaffold. **a,b** Stars created using a linear scaffold. Arrows indicate example fragments; not all fragments are labelled. **c–i** Stars created using a circular scaffold strand.



Supplementary Figure S48: Deformation of triangles. **a** Triangles made from rectangle domains sometimes break and form 3-domain rectangles based on stacking interactions (white arrows). **b** Sharp triangles made from trapezoidal domains but without bridges. ‘g’ and a pink arrow mark a gap between trapezoids in an non-equiangular triangle. ‘f’ and green arrows mark places where tips of trapezoids have have folded into the interior of sharp triangles. ‘?’ and yellow arrows mark structures for which no sensible interpretation has been made. **c** Interpretation of the sharp triangles with folded trapezoids from **b**. Gray indicates a single thickness of DNA structure, white a region of double thickness. Scale bars, 100 nm.

#### **Supplementary Note S5.10: Deformation of triangles and unbridged sharp triangles**

In experiments designed to create triangles from three rectangular domains, 88% of structures (of 199 structures observed) had roughly triangular shapes but < 1% (a single structure) were equiangular. The remaining 12% of structures took a variety of forms but, strikingly, 3% of structures took the form of three-domain rectangles held together by stacking interactions (Supplementary Fig. S48a). This suggests that the scaffold may break preferentially at the vertices of the triangle.

A large percentage (55%) of sharp triangles (created from trapezoidal domains) remain well-formed when bridges are not used along the seams between trapezoidal domains (Supplementary Fig. S48b). Typical defects take the form of trapezoids that fold back away from seams (‘f’ labels) into the interior of the triangle. Some structures cannot easily be interpreted (‘?’ labels).

## Supplementary Note S6: Hairpins for creating patterns

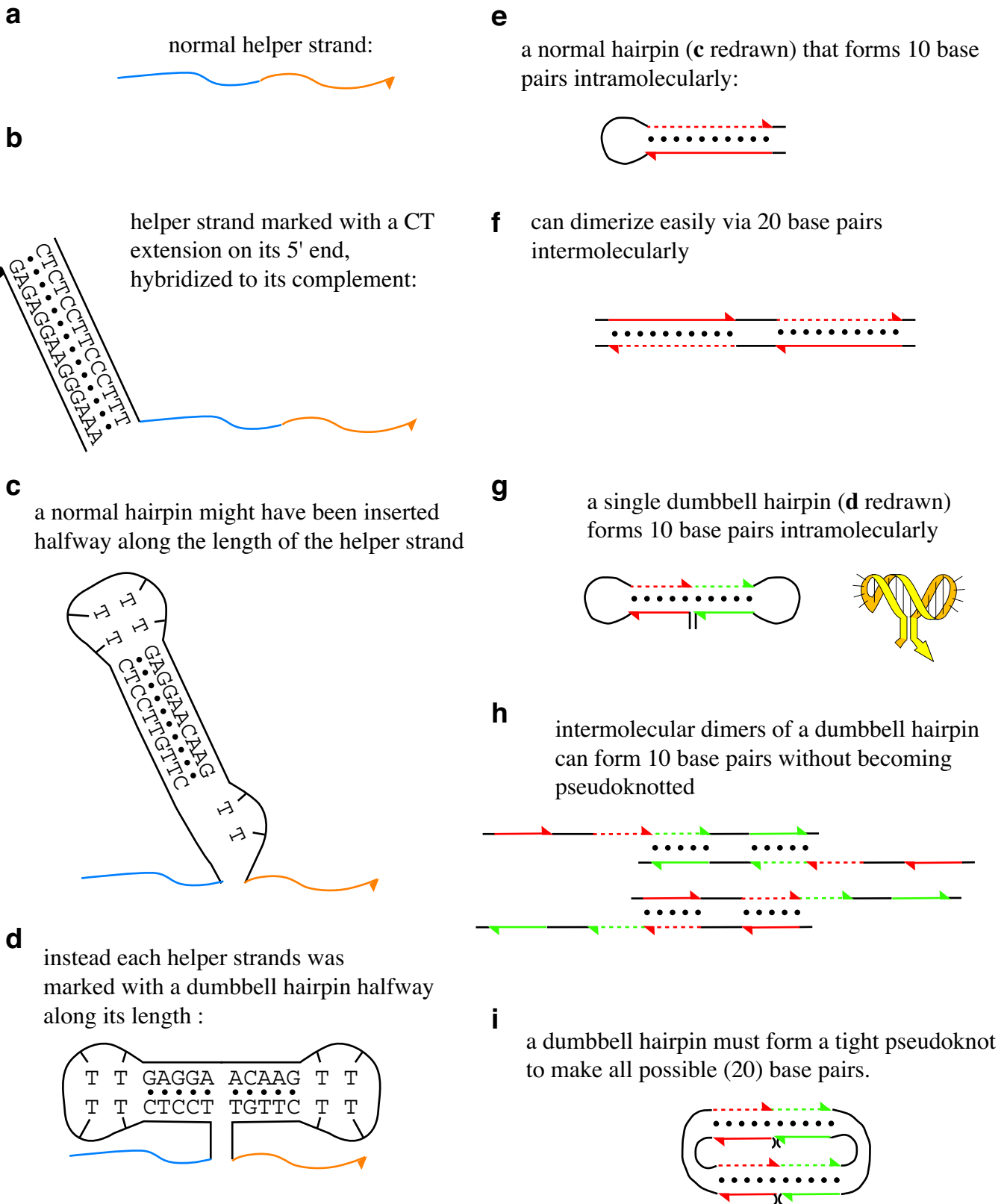
To label a DNA nanostructure, DNA hairpins are often added to increase the height of the nanostructure at a desired location. DNA hairpins have a tendency to dimerize, and, at the high concentrations at which they occur (up to 40 uM if all positions were labelled by the same hairpin) might inhibit formation of the shapes. Thus a new type of hairpin, a *dumbbell* hairpin was designed (Supplementary Fig. S49d) that, in order to dimerize, must form a presumably strained pseudoknotted structure (Supplementary Fig. S49i). Dumbbell hairpins were inserted between nt. 16 and 17, for all 32-mers in the rectangle design *except* strands r9t0f and r-9t24e which had the hairpins inserted between nt. 8 and 9. Note that (1) no normal hairpins were tested, they might have worked without difficulty and (2) the idea that dumbbell hairpins to form fewer dimers has not yet been tested (by say gel electrophoresis comparing normal and dumbbell hairpins at high concentration).

In an attempt to allow post-labelling of the shapes after formation a second type of marker was explored (Supplementary Fig. S49b): a 14 base mixed C and T tail was added to the 5' end of each staple strand. The idea was that this polypyrimidine addition would not hybridize with any staple strands or to itself. After formation of a shape, the corresponding 14 base polypurine strand was added to create duplex at desired positions, which it was assumed would yield good AFM height contrast. Instead the duplex markers imaged very poorly in a manner that was highly scan angle dependent. Multiple scans from multiple angles suggest that the poly-CT tails do in fact get labelled by poly-AG complements but imaging was very difficult (data not shown). The duplex markers, because they are attached to the origami by only one covalent bond, appear to be flexible. Thus such a method may be useful for attaching gold balls or other materials to the shapes but serves as a warning that verification of the correct structure by AFM may be difficult.

Despite the apparent complexity of the patterns, physically selecting and mixing strands was relatively simple. Because the set of '0' strands and set of '1' strands (bearing dumbbell hairpins) are complementary, and '0' and '1' strands are stored in characteristic positions of matched 96 well plates, two complementary pipette tip boxes are easily constructed, one for selecting the '0' strands and the other for selecting '1' strands. This is accomplished by taking a full tip box, and, for each position of a desired '1', moving that tip to the same position in an empty tip box. The originally full tip box becomes a box for selecting the '0' strands, and the originally empty tip box a box for selecting the '1' strands. A multichannel pipettor or robotic workstation can then be used to apply the tip boxes to the 96 well plates. The pipettor gets a tip if and only if the corresponding position in the tip box has a tip, and thus performs only the desired pipetting operations. This idea is diagrammed in Supplementary Fig. S50 and a worksheet for creating the snowflake design is given in Supplementary Fig. S51.

To give a better feeling for the range of structures that were observed in the pattern experiments, I give a page of images for each structure that was observed and include some zoom-outs of the images used in the paper (Supplementary Fig. S52, 53, and 54). Note the presence of flipped structures with hairpins down that image poorly. Note also that the "DNA" and "snowflake" patterns were rendered on a rectangle with 18×12 pixels and that the "Map" was rendered on a completely different rectangle with 14×16 pixels.

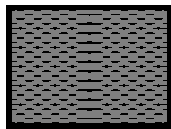
The resolution of patterns was measured directly from staggered patterns. Distances measured between pairs of '1' pixels in alternating columns (two pixel widths:  $11.5 \pm .9$  nm s.d.,  $n = 26$ ) and adjacent rows (one pixel height:  $6.6 \pm .5$  nm s.d.,  $n = 24$ ) are consistent with an expected pixel size of  $5.4$  nm  $\times$   $6$  nm. I note that the measured pixel width is exactly that expected given the measured width of the rectangle. The measured width was 104.14 nm and the theoretical width 97.92 nm. Assuming that the scale is off (by 6.36%) and that the latter value is correct, then the width of two columns of pixels is  $10.8 \pm .85$  nm, spot on. The same holds true for the measured pixel height. The measured height was 77.08 nm and from our estimation of the gap (based on many experiments we would expect a height of 71 nm. Assuming the latter was actually correct the scale is off (by 8.56%) then one pixel height is  $6.1 \pm .46$ , very close to the expected value.



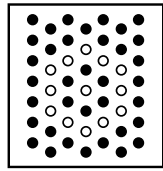
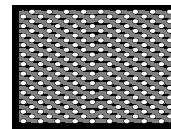
Supplementary Figure S49: Markers for AFM contrast, possible unintended interactions.

## Creating arbitrary patterns

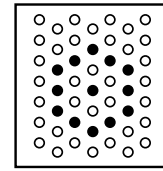
original shape strands



new strands with hairpin labels

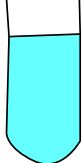


From a full box (left) the desired pattern of tips (black dots) to an empty box (right) so that the boxes hold complementary patterns of tips.

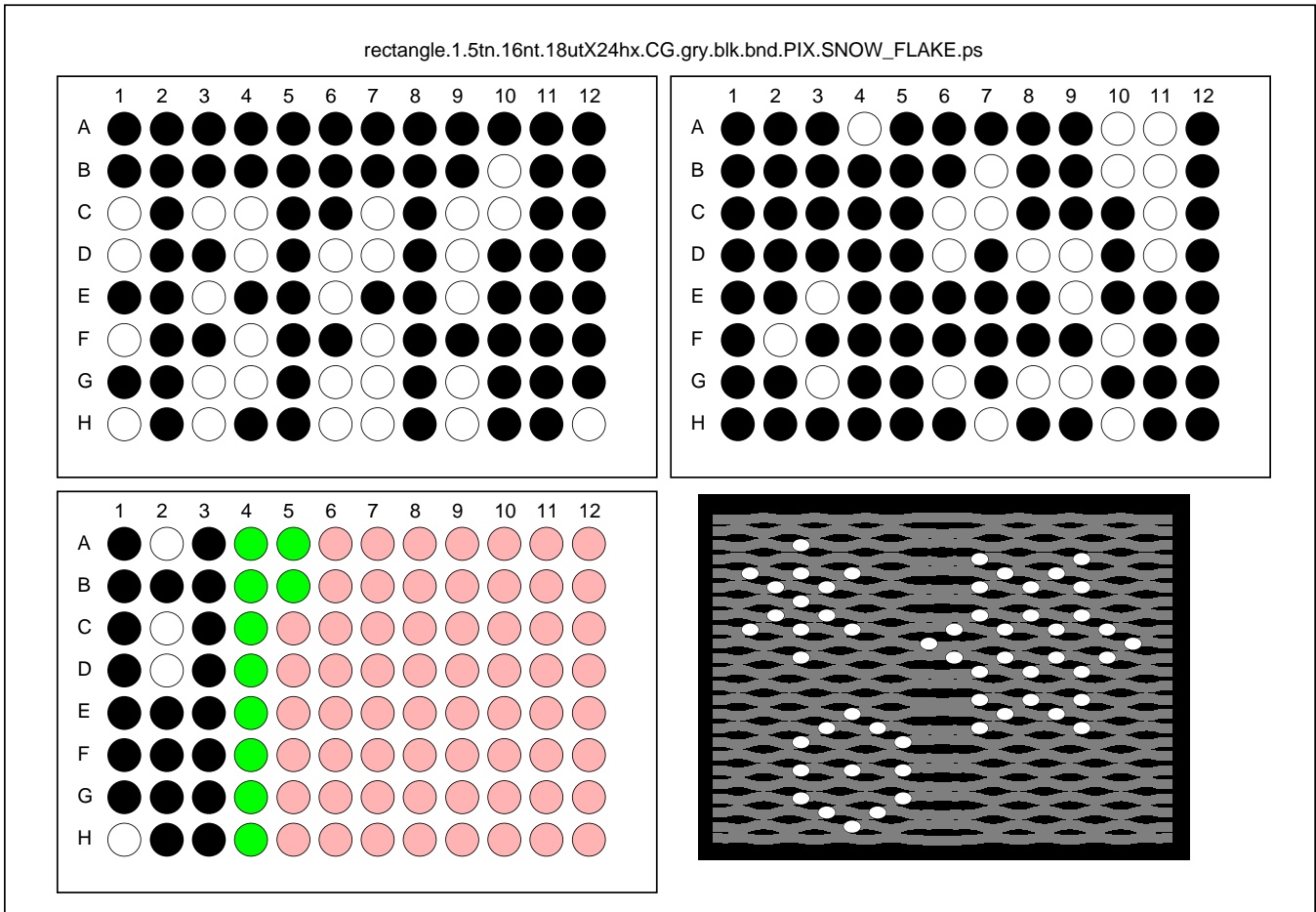


The formerly full box is used to draw from plates holding the original strands.

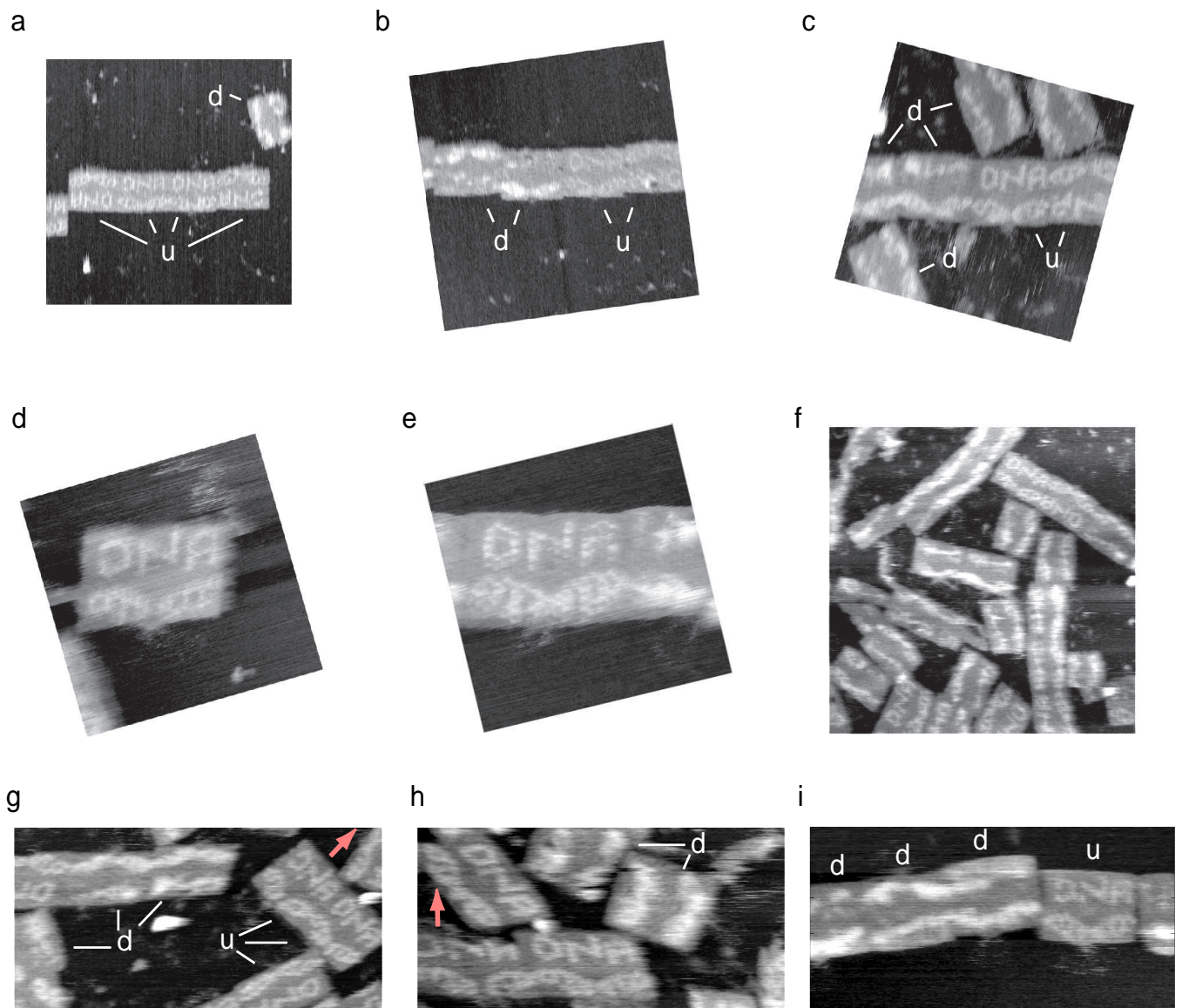
The formerly empty box is used to draw from plates holding the new strands with hairpins.



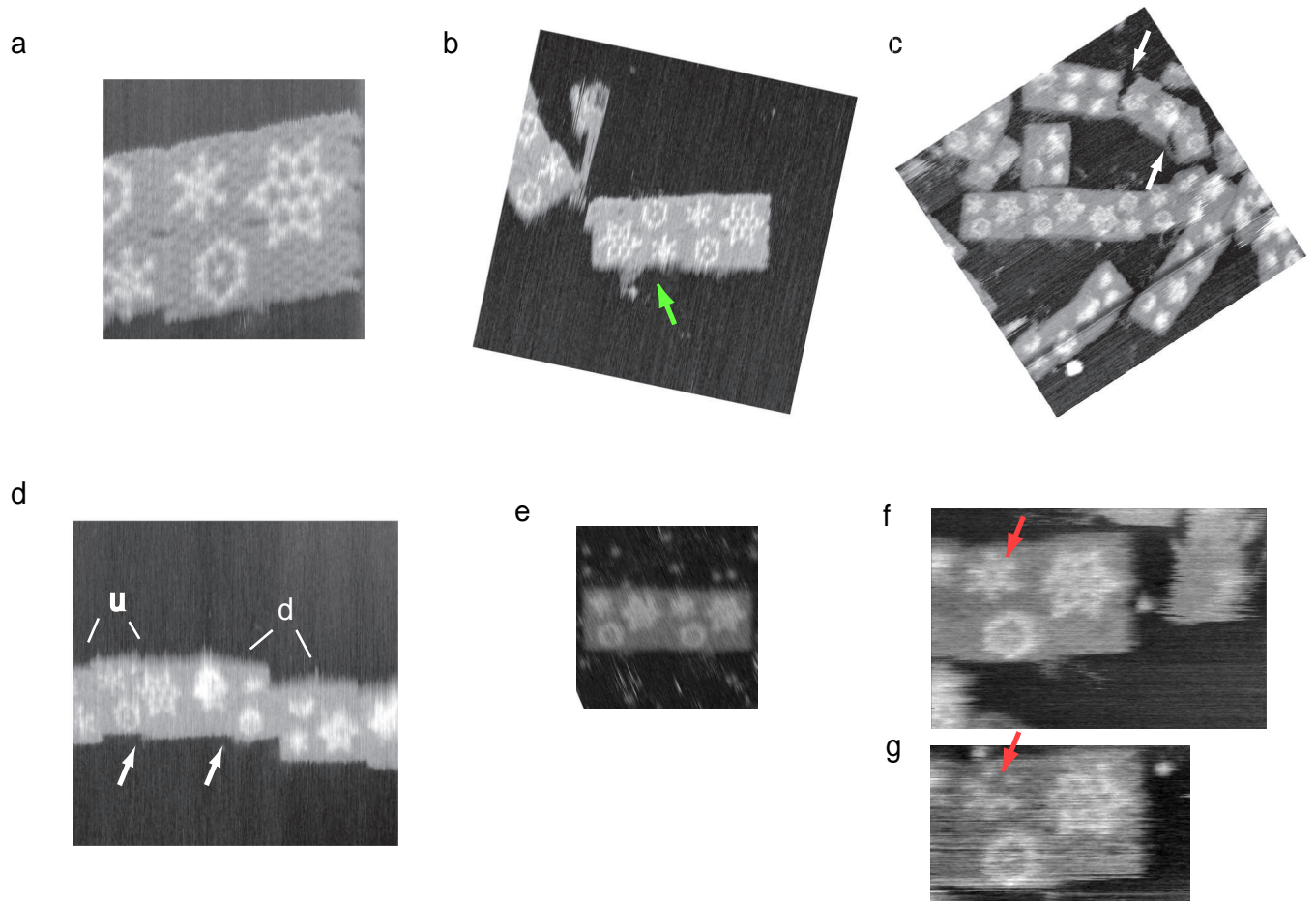
Supplementary Figure S50: Making a pattern on DNA origami.



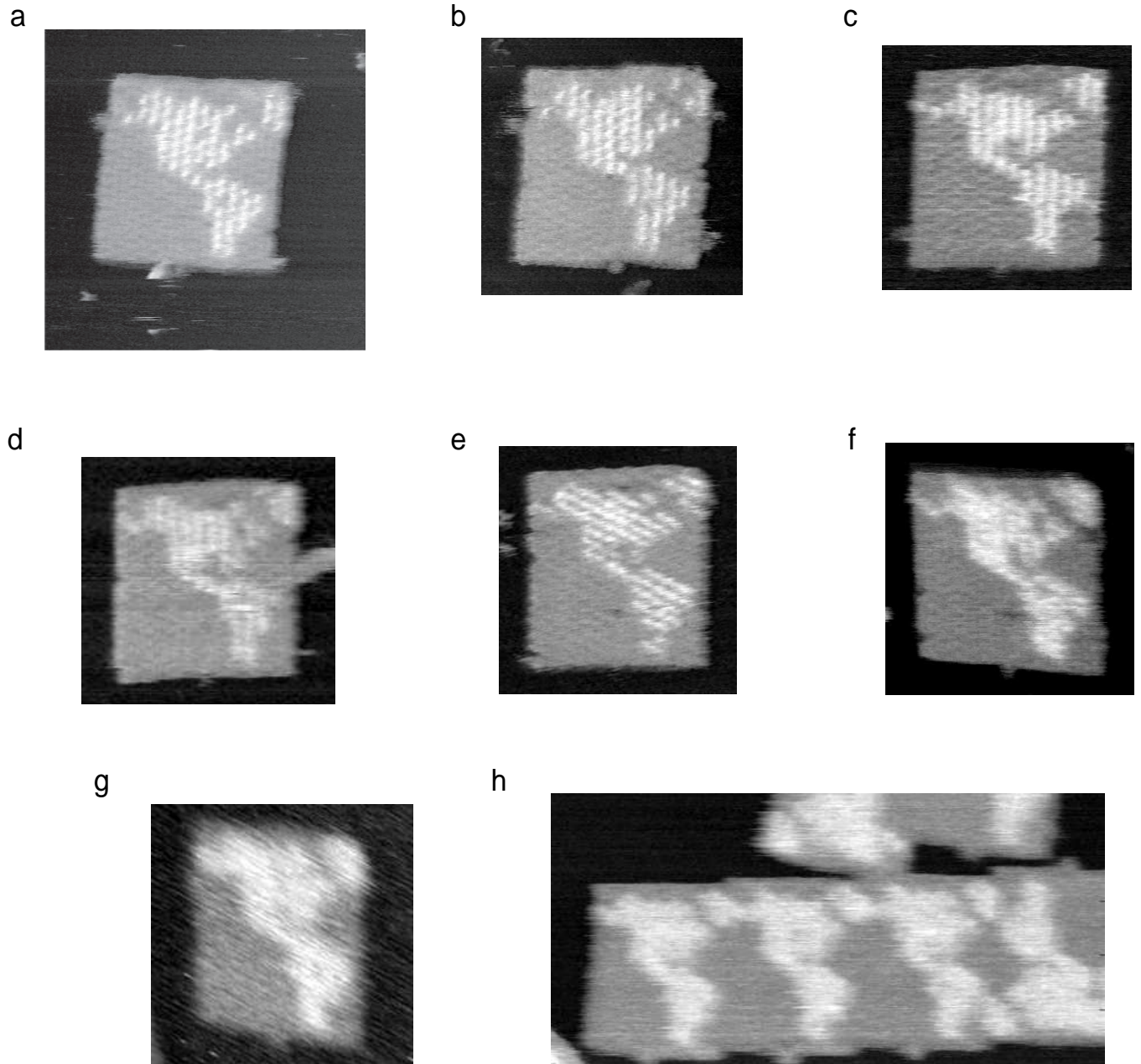
Supplementary Figure S51: A worksheet that allows easy preparation of a DNA pattern. Three 96 well plates are represented. Black circles mark wells that should be sampled from a set of 3 plates with unlabelled staple strands. White circles mark wells that should be sampled from a set of 3 homologous plates with dumbbell hairpin labels. Green circles represent the remainder strands that should be drawn independent of what pattern is being created. The pattern created using this mix of strands is diagrammed in the fourth quadrant.



Supplementary Figure S52: Extra images of 'DNA' pattern. **a** Enlarged view of Fig. 3b. **b-i** Other relatively high resolution images. 'u' indicates a rectangle with hairpins facing up; 'd' a rectangle with hairpins facing down. 42% ( $S = 55$ ) of rectangles with the 'DNA' pattern were face-up. Pink arrow indicates the position and orientation of the same position in two images (**g** and **h**).



Supplementary Figure S53: Extra images of ‘snowflake’ pattern. **a** An uncorrected version (unsheared and unstretched) of Fig. 3d; this original was heavily distorted by AFM drift. **b** An uncorrected zoom out (none was required) of the structures from Fig. 3d showing surrounds. Green arrow indicates an area of damage in a neighboring structure, probably caused by the tip. **c–g** Extra relatively high resolution images. ‘u’ indicates hairpins are facing up; ‘d’ that hairpins are facing down. Rectangles in all these images have unbridged seams that occasionally dislocate slightly (white arrows, **d**) or grossly (white arrows, **c**). Sometimes a hairpin irreversibly disappears, see pink arrows in **f**, **g**.



Supplementary Figure S54: Extra images of the ‘Map’ pattern. **a** An uncorrected version (unsheared and unstretched) version of Fig. 3f; this original was distorted by AFM drift. **b-f** Other high resolution maps for comparison. Observe that there is no correlation between missing pixels. Depending on the batch of AFM tips used (Veeco NP-S, oxide sharpened), only 1 tip in 5 to 1 tip in 30 provides such resolution. **g,h** More typical (but still good) resolution.

## Supplementary Note S7: Composition of shapes

To give sharp triangles specific binding interactions, staple strands along their edges were cut and pasted to yield two new types of staple strands: (1) extended staple strands that project 8 bases from the edge of the triangle which served as ‘donors’ and (2) truncated staple strands that left an 8 base section of the scaffold single-stranded available as an ‘acceptor site’. Given a sharp triangle as drawn in the design (with a particular face of the triangle facing up out of the page), extended staple strands were always positioned on the righthand half of the sharp triangle’s edge and truncated staple strands were always positioned on the lefthand half the sharp triangle’s edge. In this way, whenever the edges of two triangles met (with the faces of the triangle pointing in the same direction) the position of extended staple strands on one edge matched up with the position of the truncated staple strands on the other edge (and vice versa). If the sequences of the 8-base donor sections of the extended staple strands complemented the single-stranded acceptor portions of the scaffold, then the two edges could bind. Sequences are given in Supplementary Fig. S55.

The composition of sharp triangles into hexagons and lattices was only of limited success. While the interactions between sharp triangles were specific and as designed, the formation of hexagons and lattices were not quantitative. Several factors are likely to influence yields: (1) the stoichiometry of extended staple strands (2) the formation temperature of sharp triangles relative to the formation of inter-triangle bonds (3) the flexibility of inter-triangle bonds. There is much room for the optimization of these factors and quantitative composition of origami shapes into larger structures remains an open problem.

Because extended staple strands are not like normal staple strands in that they do not bind exclusively to a single scaffold strand, the stoichiometry of the extended staple strands immediately becomes important. For example, if a full 100-fold excess of extended staple strands were used, then excess staple strands could fill up all of the available single-stranded vacancies left by truncated staple strands. Ideally, there would be exactly 1 copy of each extended staple strand for each scaffold strand. Practically, because the stoichiometries of staple strands were uncertain, I used a range of extended staple:scaffold ratios (approximately 100, 20, 4 and 1) and retained the normal 100-fold excess for the rest of the staple strands. As expected, at a high relative excess of extended staple strands (100-fold) few triangles associated into hexagons. At a somewhat lower excess (20-fold) some hexagons formed. No matter what the ratio of extended staples to scaffold the yield of hexagons was low (Supplementary Fig. S56); the best results were obtained with a ratio of 4.

The formation temperature of sharp triangles relative to the formation of inter-triangle bonds is probably very important to the correct composition of triangles. Ideally, over the course of annealing, sharp triangles would form completely at a high temperature, and then only at a much lower temperature would weak inter-triangle bonds be strong enough to bring triangles together. If the bonds between triangles are too strong, then they will form at a temperature near that at which the sharp triangles themselves form and the sharp triangles may still be partially melted, disordered and floppy. This would seem to result in poorly formed structures.

The strength of inter-triangle interactions can be tuned by the number of extended staple strands that are used. I tried variations in which 2, 4, 8, and 16 staple strand bridges should have formed between sharp triangle edges (using subsets of the sequences in Supplementary Fig. S55). Hexagons and lattices formed with 4 and 8 staple strand bridges between edges but not for 2 and 16 staple strands. The experiments suggest that 2 bridges are too weak, and 16 bridges are too strong, for proper composition of triangles. These experiments are preliminary, however. Given the poor stoichiometry in the experiments, it is possible that on average 2 acceptor sites per edge were filled with excess extended staple strands. If this were true then it would explain why in 2-bridge experiments, few triangles bound each other. Further, the 16-bridge experiments are not really comparable with the others. In the 16-bridge experiments, the acceptor (left side) of a sharp triangle is left almost completely single-stranded and floppy because 8 truncated staple strands are occur in a single row. This is in sharp contrast to the 4 and 8 bridge experiments in which truncated staple strands alternate with normal staple strands on the acceptor side of the edge; the normal staple strands potentially make the edge more rigid.

Finally, I note that the hexagon of triangles may, at 30 megadaltons, hold the record for the largest man-made molecular complex. It has  $6 \times (7249 + 7156 + 980) = 92310$  nt (counting scaffold, staples and 35 hairpins/triangle at 28 bases each, not counting remainder strands) for a total molecular weight of 30.46 megadaltons (counting 330 daltons per nt). Individual unpatterned origami are all  $\sim 4.7$  megadaltons. For comparison, the molecular weight of the eukaryotic ribosome is 4.2 megadaltons.

Truncated versions of the right hand side bottom row strands. To make lattices of sharp triangles, or hexagons these strands are used to create acceptor sites. Potentially all of them might be used for a lattice (since acceptors must be placed on 3 sides) but only 2/3 of them might be used for hexagons (since acceptors must be placed on 2 sides). The actual number depends on the number of donor/acceptor pairs desired. Here, the name of the strand indicates the position in the sharp triangle plates that it is meant to replace.

t1s10g-TR-P1-B2, A5, ATTAACACTCGGAATAAGTTTATTCCAGCGCC  
 t1s20g-TR-P1-G2, B5, CATTCACTTAAGAGGAAGCCGATCAAAGCG  
 t1s30g-TR-P1-E3, C5, CACGTACTGAAATGATTATTTAATAAAAG  
 t3s10g-TR-P1-E5, D5, GTAAATTGATGCCAACATAAAAAGCGATTGAG  
 t3s18g-TR-P1-H5, E5, AACCTCCAAGATTGCATCAAAAAGATAATGAG  
 t3s20g-TR-P1-A6, F5, GGAAATTACAGTCAGAAGCAAAGGGCAGGTGAG  
 t3s28g-TR-P1-D6, G5, AGAGATAGTTGACGCTCAATCGTAGCTGCTT  
 t3s30g-TR-P1-E6, H5, AGCGGGGAGATGGAATACCTTACATAACCCCTTC  
 t3s8g-TR-P1-H6, A6, CATTCAACAAACGCAAAAGCACCCAGAACACC  
 t5s10g-TR-P1-E8, B6, ACAAGAATGTTAGCAACCGTAGAAAAATTATT  
 t5s18g-TR-P1-H8, C6, TAATTGCTTACCCCTGACTTATATGAGGCATA  
 t5s20g-TR-P1-A9, D6, CATAACCCATCAAAATCAGGCTCTTGTGA  
 t5s28g-TR-P1-D9, E6, GAATACGTAAACAGGAAAACGCTCTAAACAG  
 t5s30g-TR-P1-E9, F6, ATTATAGATACCGCCAGGCAATGCGGCACAGA  
 t5s8g-TR-P1-H9, G6, TTGACGGAAATACATACATAAAAGGGCCTAAT  
 t7s10g-TR-P1-B11, H6, AAGAAACATGGCATGATTAAGACTCCGACTTG  
 t7s20g-TR-P1-F11, A7, CCAAAATTAACAGTCAGAAATTAGAGCT  
 t7s18g-TR-P1-E11, B7, CGGATGGCACAGGAATGACCAATAATCGTTAC  
 t7s28g-TR-P1-A12, C7, CTATTAGTATACTCGAACAAATCAGGAACG  
 t7s30g-TR-P1-B12, D7, AGAAGTGTATCGGCTTGTGGTACTTTAATG  
 t7s8g-TR-P1-E12, E7, CACCGTACCCCTTATACCGCATATTGAGTTAA  
 t9s10h-TR-P2-D1, F7, CGAACCCCCAAACCAATAAACGAAAATCAGCAG  
 t9s18g-TR-P2-F1, G7, TGCTGTAGATCCCCCTCAAATGCTGGAGAGG  
 t9s20h-TR-P2-G1, H7, TTGGCCAGCATATAATTATCATGACTCAACATGTT  
 t9s28g-TR-P2-A2, A8, TAAACATTAGAAGAACTCAAACCTTTTATAA  
 t9s30h-TR-P2-B2, B8, GTAAAAGAACATCACTTGCGCTGAGGCCCATTTAA  
 t9s8g-TR-P2-D2, C8, GAGCCAGCGAATACCCAAAGAACATGAAATA

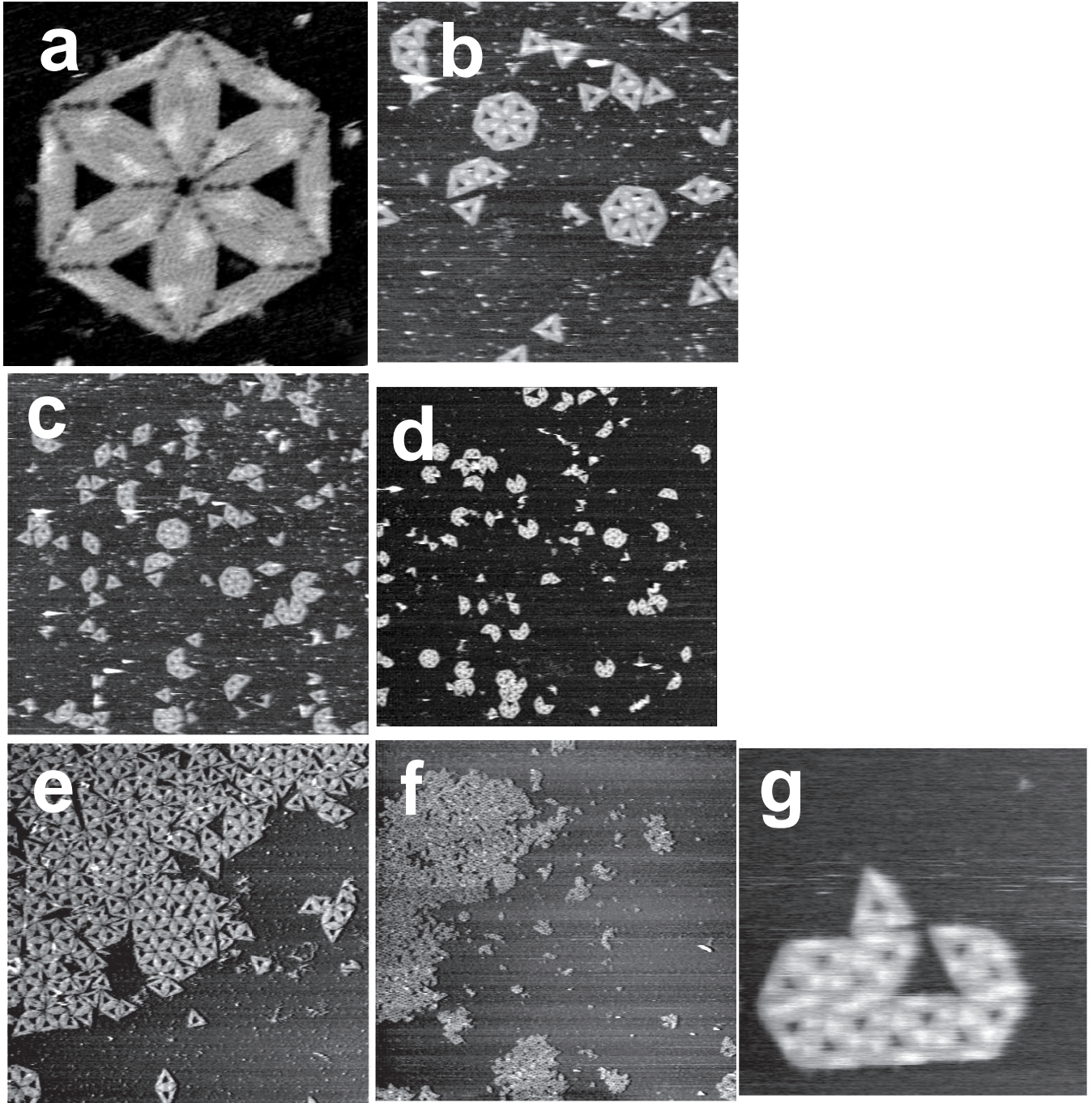
These strands have been extended to provide donors that make triangular lattice.  
 Here again the name of the strand gives its provenance.

t-10s17h-LT-P2-E2, A1, ACCAACCTAAAAAAATCAACGTAACAAATAATTGGGCTTGAGAAAAAGT  
 t-10s27h-LT-P2-F2, B1, AACCTCACATTATGAGTGTGTTCCAGAACCGCTTACAGGGCCACCGA  
 t-10s7h-LT-P2-G2, C1, ACGACAATAAACCGACTTGCAGGAGATCTGAACTTACCATATCTTAC  
 t-1s18g-LT-P2-D4, D1, CGAACCTGGCTCAATCATAAAGGAAAGCGAACACATTATGAACATCA  
 t-1s28g-LT-P2-D5, E1, TTTCACAGCCTGAGGAGAACGGCCGAAACGGTTGACGAG  
 t-1s8g-LT-P2-D6, F1, TTCCCTAGACCATCGAGAACAAATAGCAGCCTTACAGGACGGAG  
 \* t-3s18g-LT-P2-E6, G1, TGAACACAAAGCTCAAATAAGGAAAGCAACGGTTTATGAAACCAA  
 t-3s18g-LT-P2-E8, H1, TATCATCGTGAAGAGGAGCATGGAGAAGAAAATCTAGGCCAAAA  
 \* t-3s18g-LT-P2-F8, A2, ATACATAATAAAGGAACTACCCGACTGACCAACTCTGTATAA  
 t-3s28g-LT-P2-A9, B2, GTTGTGCTCACGGTGTGCCCCAACGGGCCCCGATTAGAATCAG  
 \* t-3s30g-LT-P2-B9, C2, TCCCTGTTAGACGGTGTGACGGGGAGTGTGACAGCAAGCGGTCTATTGGCG  
 \* t-3s8g-LT-P2-E9, D2, AGCATGATTTCTCGTAGGAACTAACGATTTTTGTGACAGG  
 \* t-5s10g-LT-P2-B11, E2, ATACAGACATCCAAATCAAAGGATTACCGCCCAATAATAATAT  
 t-5s18g-LT-P2-E11, F2, CCAAGCCAGGGCATAGGCTGGCAGAACCTGGCTATTATAACACT  
 \* t-5s20g-LT-P2-B2, G2, GTAAGAGCACAGTCAGGACGGTGAAGCGTACAGCGGAAACAAA  
 t-5s28g-LT-P2-A12, H2, TTAATGAAGTTGATGGTGGTCCAGGGTGGCTAACGATTAAAGGG  
 \* t-5s30g-LT-P2-C12, A3, GAGGCCGCAACTAACGGAACCTAACGAGGAAACCTGGGCCA  
 t-5s8g-LT-P2-E12, B3, ACAAGAAAGCAACAAATCAGAACGCTATTATTTAGATAACCC  
 \* t-7s10g-LT-P3-G1, C3, GCCCAATAAGCGACTTAAACAAATAAGAGCTTATCCGGTTATCAAC  
 \* t-7s18g-LT-P3-A2, D3, AAAACACTTAATCTGACAAAGAATTATCTGTGAATTGATAAAAA  
 \* t-7s20g-LT-P3-B2, E3, CAGACGACACCTTATCGCATTTTGACCTTCATCAAGGACATCTTG  
 t-7s28g-LT-P3-D2, F3, TTCCAGTCTTAATAAAAGGAAAGGACCCATACCGGAAATTAACACT  
 \* t-7s30g-LT-P3-E2, G3, GTACCGCACAGTTTTGGGGTCAAGGAAACCTGGAAATTCAGGAAAC  
 t-7s8g-LT-P3-G2, H3, GCGGCTGTATTCTAAGAACGCCATTCAGGCTTAATTATAAGAGC  
 \* t-9s10g-LT-P3-F3, A4, GCAATACAGCGCTAACGGGCTCTGGCTTTACGGAACCCAACTAT  
 \* t-9s20g-LT-P3-H3, B4, CTTTTGCGATGGTTAATTCTAACCTCGGATATTCAACCCAGAAAGA  
 \* t-9s30g-LT-P3-B4, C4, TCAGTGAGCGATGGGCCACTACGATAGCCGAGATAGGGATTGCGT

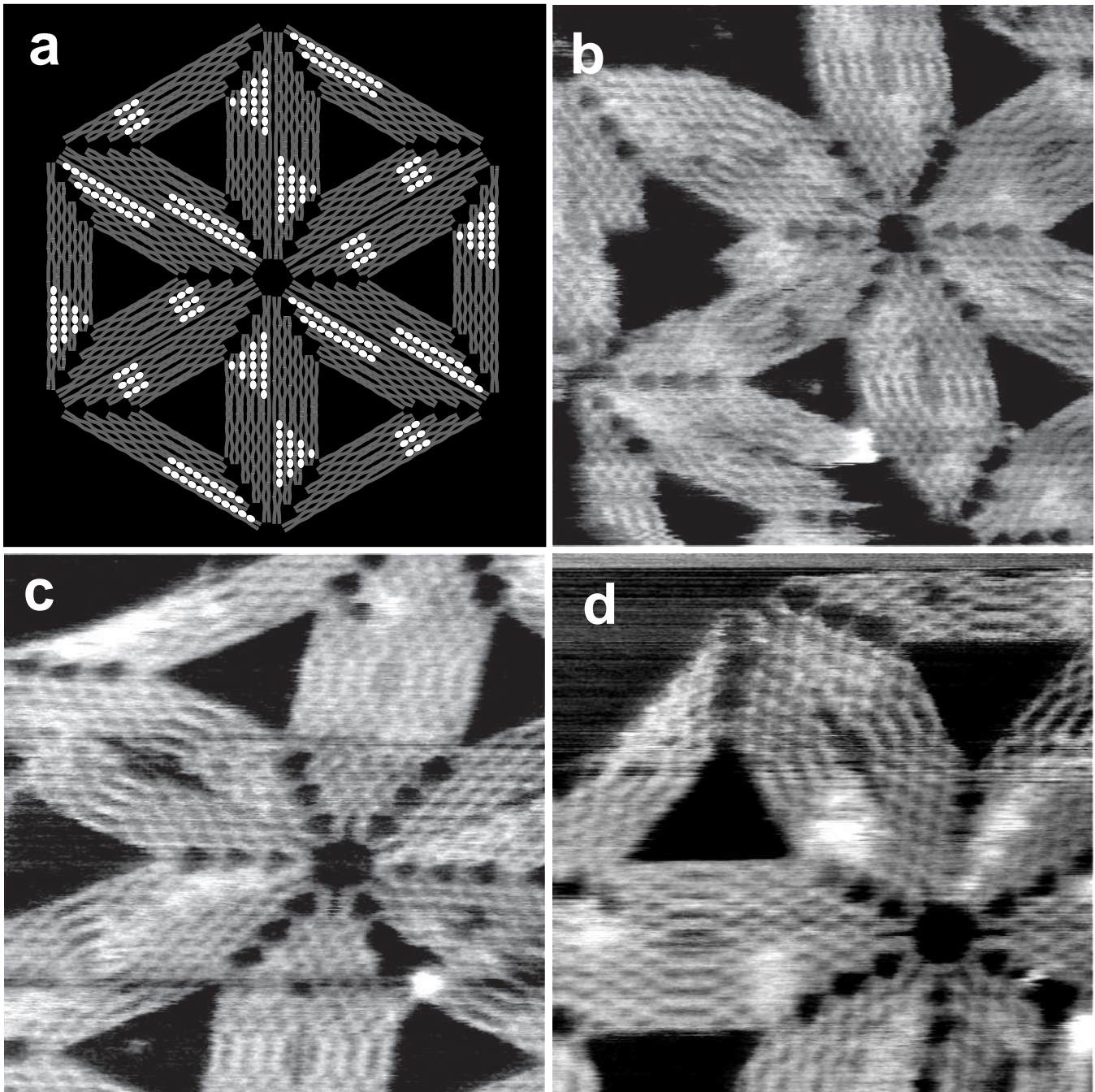
Supplementary Figure S55: Staple strand variants for creating hexagons and lattices from triangles. Truncations provide acceptor sites, extended versions, donor sites. Stars (\*) indicate extended staples that were used for the 8-bridge hexagons (8 starred strands) and 8-bridge lattices (12 starred strands) described in this paper. Four extended staples per side were used. Corresponding truncated strands were also used, and may be derived from the design.

These strands have been extended to provide donors that make hexagons.

t-10s17h-HX-P2-E2, A6, ACCAACCTAAAAAAATCAACGTAACAAATAATTGGGCTTGAGATATCTAC  
 t-10s7h-HX-P2-G2, B6, ACGACAATAAACCGACTTGCAGGAGATCTGAACTTACCAAAGAAGT  
 t-1s18g-HX-P2-D4, C6, CGAACCTGGCTCAATCTAAAGGAAACGGAAACACATTATGACGGGAG  
 t-1s8g-HX-P2-D6, D6, TTCCCTAGACCATCGAGAACAAATAGCAGCCTTACAGGAATACCA  
 \* t-3s10g-HX-P2-B8, E6, ATACATAAAACGCTAAAATGAAAGAACGAAAGCCGTTTTATGAAACCAA  
 t-3s18g-HX-P2-E8, F6, TATCATCGTGAAGAGGAGCATGGAGAAGAAAATCTACGGTCAGAGG  
 \* t-3s20g-HX-P2-F8, G6, TGAACAAATAAAACGAACTAACCGAACACTGACCAACTCTGTATAA  
 \* t-3s8g-HX-P2-E9, H6, AGCATGATTTCTCGTAGGAACTAACGATTTTTGTGCGGAAAA  
 \* t-5s10g-HX-P2-B11, A7, GTAAAGGCTCCAAATCAAATAAGATTACCGGCCAAATAAATAT  
 t-5s18g-HX-P2-E11, B7, CCAAGCCAGGGCATAGGCTGGCAGAACTGGCTCATTATGATAACCC  
 \* t-5s20g-HX-P2-F11, C7, ATCAGAGACCCAGTCAGGACCTTGTGACCGTGTACAGCGGAAACAAA  
 t-5s8g-HX-P2-E12, D7, ACAAGAAAGCAACAAATCAGATAACGCCATTATTTAACACTAT  
 \* t-3s8g-HX-P3-G1, E7, CAGACGACCCAGTCAACAAATAAGAAGGCTTATCCGGTTATCAAC  
 t-7s18g-HX-P3-A2, F7, AAAACACTTAATCTGACAAAGACTTATCTGTGAATTATAAGAGC  
 \* t-7s20g-HX-P3-B2, G7, GCCCCAATAACCCCTATGCGATTTTATGACCTTCATCAAGAGCATTITG  
 t-7s8g-HX-P3-G2, A8, GCGCCTGTATTCTAAGAACGCCATTCAGGCTTAATTGATAAAAA  
 \* t-9s10g-HX-P3-F3, B8, CTTTTGCAACCGTAAACGCGCTGGCTTTAGCGGAAACCCACATGT  
 \* t-9s20g-HX-P3-H3, C8, GCATACTGGTTAATTCAACTCGGATATTCAACCCAGAAAGA



Supplementary Figure S56: Extra images of the composition of triangles into hexagons and lattices. All structures shown here use 4 donor and 4 acceptor sites per edge (as depicted in Fig. 3n and o), for a total of 8 staple strand bridges between each pair of edges; all structures also use a 100-fold excess of normal staple strands. **a** Higher resolution image of hexagon from Fig. 3q. The tip-sample interaction force has been increased and hairpins marking the hexagon are less visible (but finer details appear.) **b** and **c**, Zoom-outs of Fig. 3q show that the fraction of hexagons formed is quite low < 2%; the excess of extended staples is about 20-fold. **d** Another sample with a lower concentration of extended staples (about 4-fold excess) has fewer free triangles but no greater a number complete hexagons. **e** and **f**, Zoom-out of Fig. 3t shows large aggregates of triangles with only small well-ordered domains; the extended staple:scaffold ratio was roughly 1:1. **g** A well-formed 13-triangle aggregate at low resolution; the resolution is barely sufficient to show that the matching rules are correct in this structure. The extended staple excess was about 4-fold.



Supplementary Figure S57: High resolution images of the composition of triangles into lattices. Compare the fine structure of the model to AFM images. **a** Six triangles arranged in the bonding pattern used for the lattice. **NOTE:** this is **not** the hexagon, it is the inner segment of Fig. 3r rotated by 30 degrees. **b** a reproduction of Fig. 3u, only larger. **c** and **d** two more high resolution views. While damaged and suffering from AFM scan artifacts, these images show fine structure associated with crossovers well.

## Supplementary Note S8: M13mp18 scaffold and staple strand secondary structure

Repetition of sequences (and their complements) in the scaffold and staple strands may cause them to have undesired binding to each other or to themselves (secondary structure). How much repetition can be tolerated is an interesting question. Clearly a poly-A scaffold cannot work, but could scaffolds limited to an AT alphabet fold robustly? Understanding such limits will require solving difficult combinatorial and thermodynamic problems. Here, I give examples of secondary structure and other undesired binding interactions in the M13mp18 scaffold and the staple strands, structure that was not too difficult to overcome. I argue that, for its length and base composition, M13mp18's sequence is not special in this regard—it is not a particularly "lucky" sequence with little secondary structure.

To get a feeling for M13mp18 secondary structure, I used Michael Zuker's DNA Mfold<sup>37</sup>

<http://www.bioinfo.rpi.edu/applications/mfold/old/>

to obtain predicted foldings for 6000 base sections of M13mp18 sequence, as well as predicted foldings of 6000 base random sequences of similar base composition. All folds were computed at 20°C, 40 mM Na<sup>+</sup> and 12 mM Mg<sup>2+</sup>. Rather than use the M13mp18 sequence reported in Genbank, I used the sequence found by New England Biolabs (NEB) the last time their M13mp18 clone was resequenced, (F.J. Stewart, NEB, 5/28/02).

Lowest energy folds for seven 6000 base segments of the M13mp18 sequence (using a sliding window, starting at  $n = 1, 1001, 2001, 3001, 4001, 5001, 6001$  and 7001) were obtained. (I would have folded all 7249 bases at once, but 6000 is the Mfold server's limit). The strongest structure ( $n=4001, -1003$  kcal/mole) and weakest structure ( $n = 6001, -904$  kcal/mole) are shown in Supp. Fig. S58 and Supp. Fig. S59. I noticed strong secondary structure around base 5500. This structure, a series of several strong hairpins, is well-known structure of biological significance and occurs in the intergenic region (5500-6000) of M13<sup>38</sup>. Of particular interest is a strong 20 base hairpin, [A], that has been enlarged in the inset of Supp. Fig. S58.

To get a quantitative measure of the predicted secondary structure I averaged free energies of folding (for the lowest energy structures). For the seven sections examined the average is  $-965 \pm 37$  kcal/mole. The large variation in energy is due to the fact that these 6000 base segments can be classed into two types. (1) Those that span the intergenic region ( $n = 1001, 2001, 3001, 4001, 5001$ ) with its strong, biologically relevant secondary structure; they have an average energy of  $-990 \pm 12$  kcal/mole. (2) Those that don't span the intergenic region completely ( $n = 1, n=6001, n=7001$ ) which have an average energy of  $-924 \pm 24$ .

To evaluate whether M13mp18's sequence has unusually strong or weak secondary structure, ten random 6000 base sequences were generated to have a base composition similar to the M13mp18 sequence (24.4% A 21.1% C 21.2% G 33.4% T, fixed at 1462 A's, 1266 C's, 1270 G's, 2002 T's). Supp. Fig. S60 shows the lowest energy fold for one of these sequences; visually it appears that the M13mp18 sequence (Supp. Fig. S58 and 59) has secondary structure similar to that of a random sequence of similar length. However, the average calculated energy for random sequences is significantly less than that for M13mp18's sequence,  $-867 \pm 13$  kcal/mol. Thus it seems that M13mp18's sequence has somewhat stronger secondary structure than would be expected.

The secondary structure of M13mp18 DNA does appear to be less strong than that predicted for sequences of even base composition. For comparison, ten 6000 base sequences of composition A=G=C=T=1500 have an average calculated free energy of  $-1080 \pm 21$ . To explore the strong effect that base composition has on secondary structure, I looked at two more examples. For A=G=T=2000 and C=0 the predicted average energy is  $-157 \pm 13$ . And for A=C=T=2000 and G=0 the predicted average energy is  $-93 \pm 6$ . In the event that secondary structure becomes a limiting factor in the creation of DNA origami, such skewed base compositions might be used but at the cost of specificity in staple-scaffold binding.

Of all the potential secondary structure that the M13mp18 sequence has, only the [A] loop was deemed worrisome enough to be avoided. Mfold predicts the structure of loop [A] as a hairpin, (20 nt stem, 4 G-T mispairs,  $\Delta G = -14.4$  kcal/mole) at positions 5515-5557. The sequence at these positions is:

GGCGGGTGTGGTGGTTACGCGCAGCGTGACCGCTACACTTGCCAGCGCCCTAGCGCCCGCTCCTTCGCTTTC

In designing DNA origami, I decided to avoid the entire 73 base section (5515-5587).

GGCGGGTGTGGTGGTTACGCGCAGCGTGACCGCTACACTTGCCAGCGCCCTAGCGCCCGCTCCTTCGCTTTC

This allowed me to linearize M13mp18 DNA by incubating with the complement of bases (5558-5587)

GAAAGCGAAAGGAGCGGGCGCTAGGGCGCT

and cutting with BsrB I between positions 5573 and 5574. (BsrB I has recognition sequence, CCGCTC at 5571-5576; it leaves a blunt end between bases 3 and 4.) Because I did not purify the linearized DNA away from the complement used to linearize it, in all designs I avoided the entire 73 base section. I don't know if this is necessary.

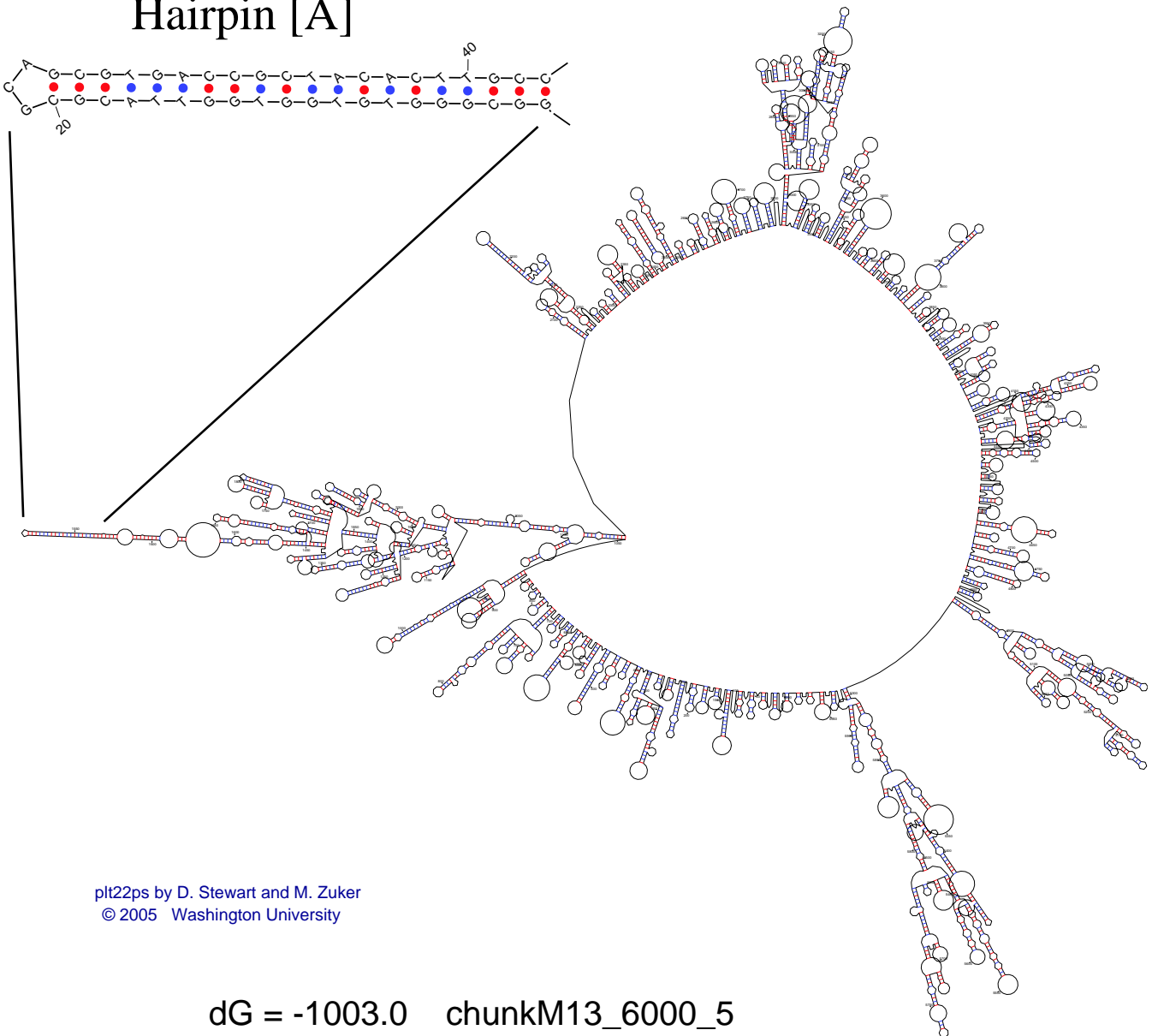
Other less strong but well known secondary structure in the scaffold did not seem to cause problems. For example, the hairpin [C] GGGTGATGGTTCACGTAGTGGGCCATCGCCC has a 14 base-pair stem. Occurring at bases 5704-5734, this sequence is 116 nucleotides into the origami structures. It occurs, for example in the rectangle on the bottom edge of the lower left corner, a position that suffers no apparent defects.

Finally, I note that staple strands themselves may have unintended secondary structure or binding interactions. By concatenating the sequences of staple strands with 'NNNN' linkers between them and folding the resulting sequence with Mfold, I was able to find a couple potential bindings between different staple strands (with lengths of 10 and 11 nucleotides and having single G-T mispairs) as well as some secondary structure within single staple strands. For example, the rectangle staple strand r7t22e, GCCAACAGTCACCTTGCTGAACCTGTTGGCAA can form an 8 base hairpin:

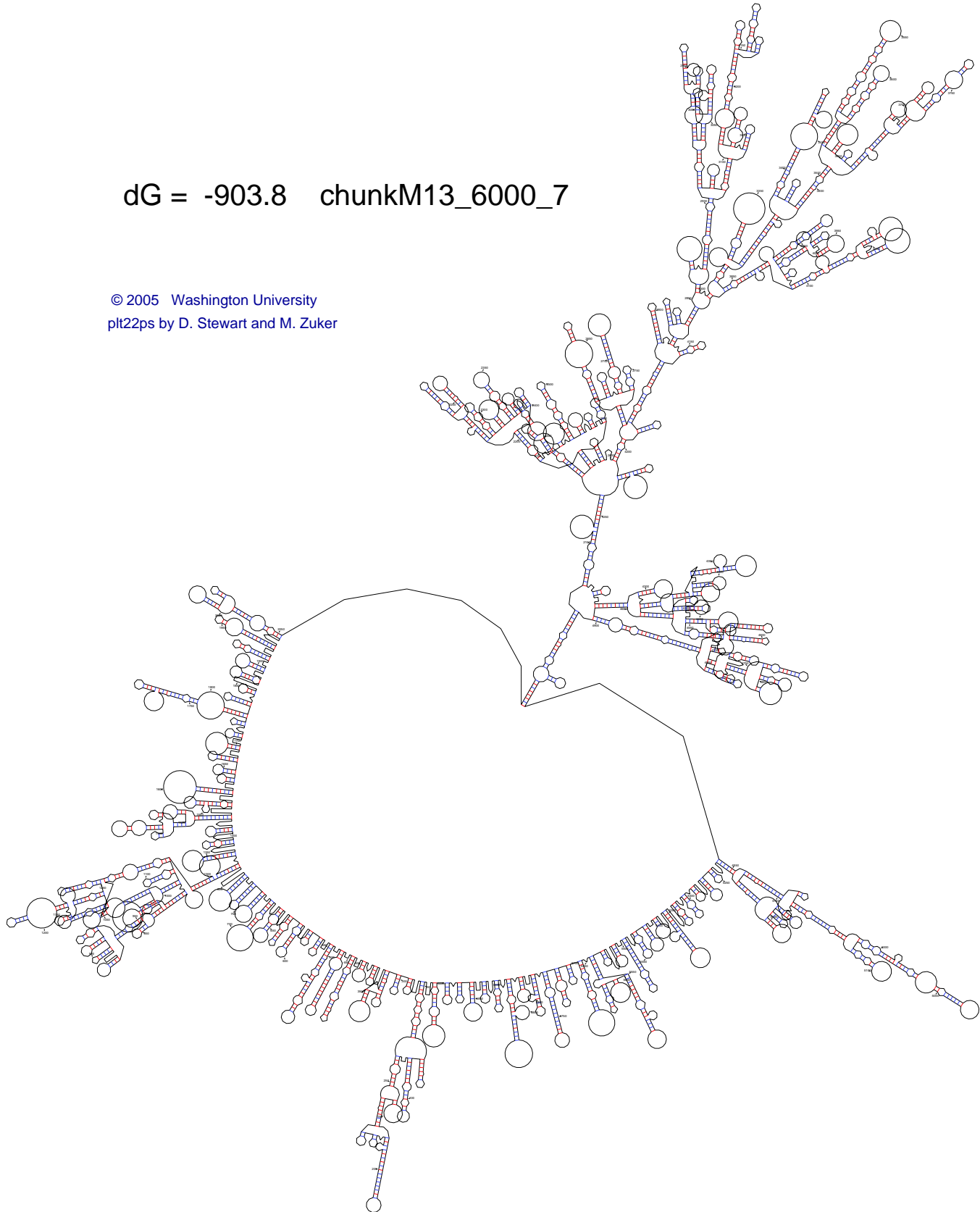
```
GCCAACAGTCACCTT\  
||||||| |  
AACGGTTGTCCAAGTCG/
```

Such secondary structure would normally be considered unacceptable in the design a DNA nanostructure. The next section explores reasons for why scaffold and staple secondary structure might not cause problems for the formation of scaffolded DNA origami.

## Hairpin [A]



Supplementary Figure S58: A 6000 base chunk of M13mp18 sequence spanning the intergenic region.



Supplementary Figure S59: A 6000 base chunk of M13mp18 sequence that skips the intergenic region.

$$dG = -858.4$$

rand\_M13A\_6000\_2

plt22ps by D. Stewart and M. Zuker  
© 2005 Washington University



Supplementary Figure S60: A 6000 base random sequence with the same base composition as M13mp18's sequence.

## Supplementary Note S9: Why does scaffolded DNA origami work?

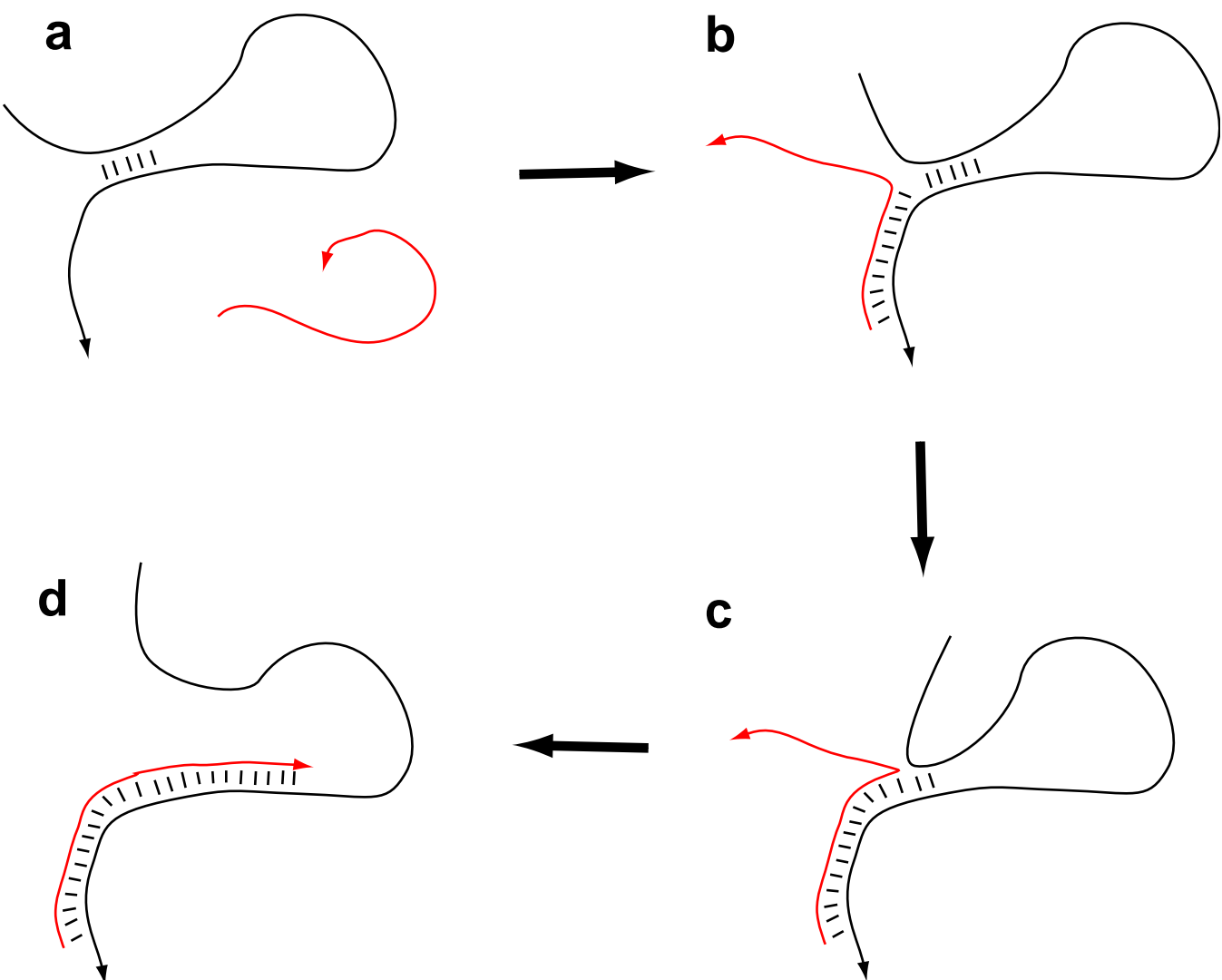
Consider any secondary structure that the scaffold might assume. It is unlikely that this secondary structure perfectly blocks the binding sites for all the staple strands that should bind its sequence. Thus staple strands may bind by partial matches at first (to gain a ‘toehold’), and then participate in a branch migration that displaces the secondary structure (Supplementary Fig. S61). A longer region of complementarity between the staple and the scaffold stabilizes the staple-scaffold interaction over the scaffold secondary structure. The excess of staple strands may help drive this process. Explicit use of strand displacement to actuate nanomachines appears in<sup>39, 40, 41, 42</sup>. (It was Bernie Yurke’s work on DNA motors that convinced me that strand invasion might make scaffolded DNA origami possible.)

Another factor that may work against scaffold secondary structure is the role of staple strands as intramolecular bridges. Each successful addition of a staple strand organizes the scaffold for subsequent binding of adjacent staple strands and constrains the scaffold in a way that precludes a large set of undesired secondary structures. Thus one might expect the binding of staple strands to be highly cooperative. To see why intramolecular interactions may be important, consider cutting a scaffolded shape into a multi-stranded structure based on unique tiles (for which the minimum free energy state should be the scaffolded shape, just with more backbone nicks). For such a system the addition of a tile at any one position does not significantly constrain the global structure.

Next consider the interactions of staple strands with themselves. Many strong complexes exist between them; none is a perfect match, however. The scaffold can displace such structure and gain a required staple strand.

Now consider purity. A truncated staple strand might bind to the scaffold. However, because of the excess of staple strands, there exist many full length length staple strands that can bind and displace the truncated strand. This means that only the purity of the scaffold matters; because the scaffold is derived from a biological source, it is very pure.

In a similar way, because staple strands do not bind to each other, the relative stoichiometry between the staple strands does not matter. With staple strands in excess over the scaffold, the remaining relevant concentration is the effective local concentration of scaffold in intramolecular events. Here the intramolecular nature of scaffold folding enforces a kind of equimolarity—any two sections of the scaffold that are brought together by a staple strand are by definition, equimolar. Again, such could not be said for the same sections if the scaffolded structure were cut into multi-stranded unique tiles. This highlights a crucial difference between the scaffolded method shown here and that previously proposed<sup>17,18</sup>. In the latter scheme the scaffold runs through every other helix; the structure is held together by interactions between multi-stranded tiles and so the staple strands must bind to each other. For such schemes precise equimolarity is likely important.



Supplementary Figure S61: Opening of scaffold secondary structure by strand displacement. **a** Five bases of undesired secondary structure in the scaffold occur in the middle of the binding site for the red staple. **b** The red staple strand can still bind by 10 bases adjacent to the hairpin stem and gain a ‘toehold’. **c** A random walk at the junction between the staple and hairpin allows the staple strand to gain three more basepairs. **d** Eventually the random walk results in the hairpin opening, which allows the rest of the staple to bind.

## **Supplementary Note S10: Cost**

The going rate for oligonucleotides synthesized unpurified, in plates, at the 100 nmole scale is between \$.18 and \$.25 per nucleotide (USD). Thus a 32-mer oligonucleotide costs about \$7 for about 80 nmol of material. (Additional PAGE purification costs \$40-80 per oligonucleotide and yields, on average, 10 nmol of material. Thus per nmol, purified oligonucleotides are about 50× as expensive as unpurified ones.) The total cost then, for about 80 nmol of each staple strand to complement the 7249 base pair M13mp18 scaffold is \$1500; staples thus cost about \$19/nmol. Four picomoles (10 micrograms) of scaffold was purchased from New England Biolabs for \$30; scaffold thus cost \$7500/nmol. Using a 100-fold excess of staple strands, the cost of DNA origami (of the current size) would be \$7500 + \$1900 = \$9400 per nmol of which the scaffold strand is 80% of the cost.

Recent controls have shown two things: 1) results using only a 10-fold excess of staple strands are indistinguishable from those with a 100-fold excess and 2) results using a 10-fold cheaper source of M13mp18 DNA (Bayou Biolabs) yield results indistinguishable from those with New England Biolabs. The net result of these observations is that, if these two modifications to the protocol were implemented, the cost of DNA origami would be closer to \$1000 per nmol but that the scaffold strand would still be 80% of the cost of the origami.

In sum, the price of synthetic oligonucleotides does not, as one might expect, dominate the cost of DNA origami. In principle excess staple strands might be recycled—removed from the reaction after folding of the scaffold is complete—further decreasing their contribution to the cost of origami.

## Supplementary Note S11: Additional references

- [24] LaBean, T., Yan, H., Kopatsch, J., Liu, F., Winfree, E., Reif, J., and Seeman, N. Construction, analysis, ligation, and self-assembly of DNA triple crossover complexes. *J. Am. Chem. Soc.* **122**, 1848–1860 (2000).
- [25] Winfree, E., Liu, F., Wenzler, L., and Seeman, N. Design and self-assembly of two-dimensional DNA crystals. *Nature* **394**, 539–544 (1998).
- [26] Wang, J. C. Helical repeat of DNA in solution. *Proc. Nat. Acad. Sci. USA* **76**, 200–203 (1979).
- [27] Rhodes, D. and Klug, A. Helical periodicity of DNA determined by enzyme digestion. *Nature* **286**, 573–578 (1980).
- [28] Kallenbach, N., Ma, R.-I., and Seeman, N. An immobile nucleic-acid junction constructed from oligonucleotides. *Nature* **305**, 829–831 (1983).
- [29] Murchie, A., Clegg, R., von Kitzing, E., Duckett, D., Diekmann, S., and Lilley, D. Fluorescence energy transfer shows that the four-way DNA junction is a right-handed cross of antiparallel molecules. *Nature* **341**, 763–766 (1989).
- [30] Duckett, D., Murchie, A., Diekmann, S., von Kitzing, E., Kemper, B., and Lilley, D. The structure of the Holliday junction, and its resolution. *Cell* **55**, 79–89 (1988).
- [31] Sha, R., Liu, F., and Seeman, N. Direct evidence for spontaneous branch migration in antiparallel DNA Holliday junctions. *Biochemistry* **39**, 11514–11522 (2000).
- [32] von Kitzing, E., Lilley, D., , and Diekmann, S. The stereochemistry of a four-way dna junction: a theoretical study. *Nucleic Acids Research* **18**(9), 2671–2683 (1990).
- [33] Eis, P. and Millar, D. Conformational distributions of a four-way junction revealed by time-resolved fluorescence resonance energy transfer. *Biochemistry* **32**(50), 13852–13860 (1993).
- [34] Jr., M. R., Anderson, C., and Lohman, T. Thermodynamic analysis of ion effects on the binding and conformational equilibria of protein and nucleic acids: the roles of ion association or release, screening, and ion effects on water activity. *Quarterly Reviews of Biophysics* **11**, 103–178 (1978).
- [35] Puglisi, J. and I. Tinoco, J. Absorbance melting curves of RNA. In Methods in Enzymology: RNA Processing, Dahlberg, J. and Abelson, J., editors, volume 180, 304–325 (Academic Press, New York, 1989).
- [36] Yanisch-Perron, C., Vieira, J., and Messing, J. Improved M13 phage cloning vectors and host strains: nucleotide sequences of the M13mp18 and pUC19 vectors. *Gene* **33**(1), 103–119 (1985).
- [37] Zuker, M. Mfold web server for nucleic acid folding and hybridization prediction. *Nucleic Acids Research* **31**(13), 3406–3415 (2003).
- [38] Zinder, N. and Horiuchi, K. Multiregulatory element of filamentous bacteriophages. *Microbiological Reviews* **49**(2), 101–106 (1985).
- [39] Yurke, B., Turberfield, A., Mills, Jr., A., Simmel, F., and Neumann, J. A DNA-fuelled molecular machine made of DNA. *Nature* **406**, 605–608 (2000).
- [40] Simmel, F. and Yurke, B. Using DNA to construct and power a nanoactuator. *Physical Review E* **63**, 041913–1–5 (2001).
- [41] Yan, H., Zhang, X., Shen, Z., and Seeman, N. A robust DNA mechanical device controlled by hybridization topology. *Nature* **415**, 62–65 (2002).
- [42] Turberfield, A., Mitchell, J., Yurke, B., Mills, Jr., A., Blakey, M., and Simmel, F. C. DNA fuel for free-running nanomachines. *Physical Review Letters* **90**(11), 118102–1–4 (2003).